R98-5.103.0007-4

The Effect of Processing on the Interface, Microstructure, and Properties of Coated Fiber Reinforced Glass-Ceramic Matrix Composites

Final Report

Prepared for:
U.S. Air Force
Air Force Office of Scientific Research
Bolling AFB, DC 20332

Under Contract No. F49620-95-C-0021

John J. Brennan

May 15, 1998

United Technologies

Research Center

AFRL-SR-BL-TR-98-
0482

REPORT DOCUMENTATION PAGE

/188

1. AGENCY USE ONLY *(Leave blank)*	2. REPORT DATE	3. REPORT TYPE AND DATES COVERED
	15-May-98	Final Report 01 Mar 95 - 31 Mar 98

4. TITLE AND SUBTITLE

THE EFFECT OF PROCESSING ON THE INTERFACE MICROSTRUCTURE AND PROPERTIES OF COATED FIBER REINFORCED GLASS-CERAMIC MATRIX COMPOSITES

5. FUNDING NUMBERS

F49620-95-C-0021

6. AUTHOR(S)

John J. Brennan

7. PERFORMING ORGANIZATION NAME(S) AND ADDRESS(ES)

United Technologies Corporation
United Technologies Research Center
411 Silver Lane
East Hartford, CT 06108

8. PERFORMING ORGANIZATION REPORT NUMBER

R98-5.103.0007-4

9. SPONSORING/MONITORING AGENCY NAME(S) AND ADDRESS(ES)

Dr. Alexander Pechenik
Air Force Office of Scientific Research
Directorate of Aerospace and Materials Sciences
110 Duncan Avenue
Bolling AFB DC 20332-8050

NA

10. SPONSORING/MONITORING AGENCY REPORT NUMBER

11. SUPPLEMENTARY NOTES

12a. DISTRIBUTION / AVAILABILITY STATEMENT

Approved for public release; distribution unlimited.

12b. DISTRIBUTION CODE

13. ABSTRACT *(Maximum 200 words)*

The primary objective of this program was to study the processing of coated fiber reinforced glass-ceramic matrix composites that will result in reproducible, reliable fiber coatings and the composites that incorporate them, for use to 1200C in advanced gas turbine engine applications. The primary glass-ceramic system was a barium magnesium aluminosilicate (BMAS), while the fibers were Ceramic Grade Nicalon Si-C-O and Nextel 720 aluminosilicate fibers, as well as new advanced high temperature SiC based fibers. The primary fiber coating system was layered BN(+C) for the Nicalon fiber composites, and BN, monazite ($LaPO_4$), and fugitive carbon for the Nextel 720 fiber composites.

The layered 3M BN(+C) coatings on Nicalon fibers produced very strong and "tough" BMAS glass-ceramic matrix composites, due to the limited matrix element diffusion through the coating and matrix crack deviation within the layered coating structure. These composites exhibited excellent tensile fatigue and stress-rupture properties, although oxidation of the layered BN coatings at intermediate temperatures (700-900C) under conditions of high fatigue stress (138 MPa) may potentially limit the stress at which these composites can be utilized for structural applications. Alternate BN and Si-doped BN coatings from other vendors did not perform as well, with excessive BN crystallization occurring during composite fabrication. Nextel 720 aluminosilicate fibers with either BN, fugitive carbon, or $C/Al_2O_3/C$ coatings did not result in strong or "tough" BMAS matrix composites for a variety of reasons, but primarily because of coating debonding leading to fiber/matrix interactions. Monazite ($LaPO_4$) coated Nextel 720 fibers reacted excessively with the BMAS matrix during composite fabrication. The crystalline SiC fibers from the U. of Fla., especially with the *in-situ* BN coatings, appear to offer future promise for high temperature CMC reinforcement.

14. SUBJECT TERMS

ceramic composite interfaces, coated fiber/glass-ceramic composites, BMAS glass-ceramic matrix/coated Nicalon fiber composites, layered BN(+C) fiber coatings, Si doped BN, in-situ coated SiC fibers

15. NUMBER OF PAGES

100

16. PRICE CODE

17. SECURITY CLASSIFICATION OF REPORT	18. SECURITY CLASSIFICATION OF THIS PAGE	19. SECURITY CLASSIFICATION OF ABSTRACT	20. LIMITATION OF ABSTRACT
Unclassified	Unclassified	Unclassified	SAR

NSN 7540-01-280-5500

Standard Form 298 (Rev. 2-89)
Prescribed by ANSI Std. Z39-18
298-102

United Technologies

Research Center

R98-5.103.0007-4

The Effect of Processing on the Interface, Microstructure, and Properties of Coated Fiber Reinforced Glass-Ceramic Matrix Composites

Final Report

Contract F49620-95-C-0021

Reported by: John J. Brennan

Approved by: William K. Tredway

DATE: May 15, 1998

TABLE OF CONTENTS

THE EFFECT OF PROCESSING ON THE INTERFACE, MICROSTRUCTURE, AND PROPERTIES OF COATED FIBER REINFORCED GLASS-CERAMIC MATRIX COMPOSITES

I. INTRODUCTION AND BACKGROUND

Fiber-reinforced glass-ceramic matrix composites are prospective materials for high-temperature, lightweight, structural applications.[1] In the last decade, research in this type of ceramic matrix composite has concentrated on the fiber/matrix interface and the relationship of the interfacial microstructure, chemistry, and bonding to the resultant composite mechanical properties and interface stability.[2-4] As discussed in Ref. 2, polymer derived SiC type fibers such as Nicalon (Nippon Carbon Co.), that contain excess carbon and oxygen over stoichiometric SiC, form a thin (20-50nm) carbon rich fiber/matrix interfacial layer when incorporated into glass-ceramic matrices at elevated temperatures. The formation of this weak interfacial carbon layer is responsible for the high toughness and strength observed in these composites, but is also responsible for composite embrittlement and concurrent strength and toughness degradation when either stressed at elevated temperatures in an oxidizing environment, or thermally aged in an unstressed condition in oxidizing environments. This embrittlement and strength degradation is a result of oxidation of the carbon layer and its replacement by a glassy oxide layer that is bonded strongly to both the fiber and matrix, thus inhibiting matrix crack deflection at the fiber/matrix interface.

It is imperative that the fiber/matrix interface in fiber-reinforced ceramic matrix composites be controlled, or "engineered", so that relatively weak interfacial bonding exists for matrix crack deflection while maintaining oxidative stability. One approach to accomplish this is to utilize coatings on the fiber surfaces that are applied before composite processing. Not only must these interfacial coatings be relatively weak and oxidatively stable, they must also be resistant to matrix and/or fiber interdiffusion so that interfacial reactions do not occur.

At UTRC, research into coated fiber-reinforced ceramic matrix composites has concentrated on BN and SiC/BN coated Nicalon SiC fibers in a barium-magnesium aluminosilicate (BMAS) glass-ceramic matrix. Previous research, both at UTRC and at other institutions, dealt primarily with either low temperature CVD BN deposited utilizing a BCl_3 precursor (usually containing excess B and O),[5] or a higher temperature deposited BN that yielded a uniform microstructure with a composition of ~42at%B, 42%N, and 15%C.[6-10] For these types of BN, a CVD SiC overcoat was found to be necessary to prevent matrix element diffusion into and crystallization of the turbostratic BN layer, as well as to prevent boron diffusion from the BN into the BMAS matrix. The

current studies at UTRC on nano-structured layered BN based coatings with carbon additions have shown improved resistance to matrix interdiffusion, potentially eliminating the need for the SiC overcoat.[11] These composites have been shown to possess high strength and good fracture toughness to temperatures of 1200°C. From tensile creep, tensile fatigue, and long-time tensile stress-rupture tests, it was found that if the coating chemistry and microstructure are controlled, this composite system can withstand high temperature stressed oxidative exposure at stress levels significantly above the proportional limit, or matrix microcrack stress, which is key to the utilization of ceramic matrix composites for high temperature structural components.

Other issues the current program has addressed deal with the characterization and testing of BMAS matrix composites with BN coated woven Nicalon fiber construction, silicon doped BN coated Nicalon fiber/BMAS matrix composites for enhanced moisture resistance, the characterization and testing of potentially lower cost Nextel 720 aluminosilicate fiber/BMAS matrix composites, utilizing interfaces of BN, C/Al_2O_3/C, carbon (fugitive), and lanthanum phosphate ($LaPO_4$), and the characterization of crystalline SiC fibers from the Univ. of Fla., with and without *in-situ* BN coatings.

II. TECHNICAL DISCUSSION

As discussed in the Introduction, the majority of effort on this program during the past three years was concentrated on BMAS matrix/BN coated Nicalon fiber composites, where the BN interfacial coating was deposited by 3M in a layered structure with alternate layers of low carbon content (~15at%C) and high carbon content (~50at%C) BN. This system was characterized thoroughly by SEM, TEM, and scanning Auger analyses, and subjected to a variety of mechanical property tests, including fast-fracture flexural and tensile testing from RT to 1200°C, tensile stepped stress-rupture, tensile creep, and tensile fatigue testing at both intermediate (500-900°C) and high temperatures (1100°C) in air, as well as tensile stepped stress-rupture testing in inert environment.

In addition, in response to the decision by 3M in late 1996 to stop providing fiber coatings to outside customers, alternate sources of BN coated Nicalon fiber were evaluated. These sources, primarily Advanced Ceramics Corp. (ACC), and (BFG), both utilized a batch process with the boron source being BCl_3, to deposit BN coatings on woven cloth preforms. ACC also provided some samples of silicon doped BN coated fiber for the evaluation of moisture resistance.

In order to evaluate potentially less expensive fibers and fiber coatings for glass-ceramic matrix composites, a number of experiments were performed utilizing coated Nextel 720 aluminosilicate fibers, provided by AFML. The coatings consisted of sol-gel derived $LaPO_4$ (monazite) and $C/Al_2O_3/C$, and CVD carbon coatings that were then oxidized to form "fugitive" interfaces.

Finally, a considerable amount of effort was expended in the analysis of new crystalline SiC fibers from the University of Florida (UF), both with and without *in-situ* BN surface coatings.

A. 3M Multilayer BN(+C) Coated Nicalon Fiber Composites

1. Composite Processing

The glass-ceramic matrix utilized for this study was a barium-magnesium aluminosilicate (BMAS), formulated to yield the barium osumilite phase ($BaMg_2Al_3(Si_9Al_3O_{30})$) on crystallization. The reinforcement was a polycarbosilane derived Si-C-O fiber (Nicalon NLM 202) with a BN or dual layer SiC over BN coating. The BN and SiC coatings discussed in this paper were deposited continuously by 3M on fiber tows by atmospheric chemical vapor deposition (CVD) at a temperature of ~1000°C, with BN and SiC coating thicknesses of ~300-400 and 200nm, respectively. The BN was deposited using a proprietary precursor chosen to yield a layered structure consisting of alternate layers of ~42at%B, 42%N, and 15%C and a very carbon rich (~50%C, 25%B, and 25%N) BN. From scanning Auger analysis, the oxygen content of

both the BN and SiC layers was less than 2%. The measured tensile strength of the coated Nicalon fibers of >2 GPa indicated essentially no loss in fiber strength during coating.

The layered BN(+C)/Nicalon fiber composites (10cm x 10cm) were fabricated by hot-pressing a lay-up of 0/90° oriented unidirectional fiber plus matrix powder plies at a maximum temperature of ~1450°C for 5 minutes under 6.9 MPa pressure, yielding an essentially fully dense matrix with a fiber volume of ~45%. After hot-pressing, the composite panels were machined into flexural samples (~5mm width) and reduced cross-section tensile samples, most of which had an ~40mm gage length and 6.3mm gage width, and then heat-treated ("ceramed") in argon at 1200°C for 24 hrs to crystallize the BMAS matrix to the barium osumilite phase.

A variety of mechanical property measurements were done, including flexural testing from RT to 1200°C, fast fracture tensile, tensile creep, tensile fatigue, and stress-rupture to 1100°C. All testing was conducted in air, except some tensile fatigue tests performed at the University of S. California in inert environment.

After composite fabrication, the composite microstructures were characterized by transmission electron microscopy (TEM) of polished composite cross-section replicas and ion beam thinned foil sections. After composite testing, the fracture surfaces were examined using scanning electron microscopy (SEM), and the changes to the microstructure examined by TEM analysis.

2. Microstructural Analysis and Flexural Testing

A typical microstructure of a BMAS matrix composite (0/90°) with 3M layered BN(+C) coated Nicalon fibers is shown in Figs. 1 and 2. The layered structure of the BN(+C) coatings is quite evident in Fig. 2. Two initial composites were fabricated with the layered BN, #3-95 with a SiC overcoat, and #7-95 without a SiC overcoat. The microstructures shown in Figs. 1 and 2 are of composite #7-95 in the ceramed, or matrix crystallized condition, and from the TEM micrograph the lathe-like structure of the barium osumilite grains, along with a small number of residual mullite grains, can be seen in the matrix. Flexural tests (3-pt) were performed on samples machined from composites #3-95 and #7-95, with the results being shown in Table I. From these results, it is apparent that the flexural strength and strain-to-failure of these composites is very high to temperatures of 1200°C, with the BN interface sample being stronger to 1100°C, and the SiC/BN retaining strength better to 1200°C. One interesting aspect of these tests is that the elastic modulus of the BN interface sample at elevated temperature is significantly higher than previous composites without a diffusion barrier SiC overcoat.[12] This indicates that the diffusion of boron into the BMAS matrix with subsequent glassy phase formation, is potentially less in the layered BN(+C) composites.

Indeed, from TEM thin foil microstructural analyses of the BMAS matrix composites fabricated with the multilayer BN(+C) fiber coatings, it was found that the

interdiffusion of matrix elements (Ba, Al, Mg, O, Si) into the BN(+C) coatings and diffusion of boron into the BMAS matrix were much reduced from previous BN coated Nicalon fiber composites. For a layered BN(+C) total thickness of ~275nm (six layers of low carbon content BN and five layers of high carbon content BN), as shown in Fig. 3, the BN is coarsened (crystallized) only through the first BN layer (~40nm), and there is very little evidence of any interaction between the BN and the Nicalon fiber. The first carbon rich layer nearest the matrix appears to act as a matrix element diffusion barrier. However, for a standard 3M BN layer with 15%C, the crystallization of the BN layer occurs to a depth of over 100nm, with subsequent carbon plus silica sublayers formed at the BN/Nicalon fiber interface. From EDS and scanning Auger analyses, a significant amount of matrix element (Si, A1, Mg, Ba, O) diffusion was found in the coarsened BN. These layers are formed by the carbon condensed oxidation of the Nicalon fibers, as initially described by Cooper and Chyung:[3]

$$SiC(s) + O_2(g) \rightarrow SiO_2(s) + C(s)$$

This reaction is enhanced by the diffusion of oxygen from the BMAS matrix through the deposited BN layer during composite fabrication.

Also shown in Fig. 3 is the scanning Auger depth profile for a layered BN(+C) coated Nicalon fiber. The alternate layers of carbon rich BN can be seen in the first 200nm of the coating. Further into the coating, the Auger analysis does not discriminate the individual layers due to the curved nature of the coated fiber surface.

From previous studies,[12] it was found that crystallization of the BN layer is caused by matrix element (Ba, Mg, Al, Si, O) diffusion into the BN during composite fabrication, and results in a composite with lower mechanical properties and reduced toughness, due to the crystallized BN being a less effective crack deflecting interfacial layer than the turbostratic BN. As shown in Fig. 4, the basal planes of the hexagonal BN in the crystallized layer tend to be randomly oriented, while those of the layered BN(+C) are essentially aligned parallel to the fiber surface, thus enhancing crack deflection within the BN(+C) layer. While the layered BN(+C) interface composite in Fig. 3 exhibited a 1200°C flexural strength of 522 MPa, modulus of 69 GPa, and a strain-to-failure of 1.26%, the standard BN composite of Fig. 3 exhibited a 1200°C flexural strength of 329 MPa, modulus of 57 GPa, and a strain-to-failure of 1.03%.

In addition, the layered structure of the BN(+C) interface causes matrix cracks that occur when the composite is stressed above the proportional limit stress to deviate within the layered BN structure, rather than at the BN/Nicalon fiber interface, Fig. 5. This keeps the fiber from degrading due to surface oxidation from ingress of the atmosphere through matrix cracks. This could be very important at intermediate temperatures (650°-900°C), where matrix crack sealing is not significant. These observations may eliminate the need for a SiC diffusion barrier overcoating, thus leading to reduced cost and complexity related to fiber coatings.

3. Tensile and Tensile Fatigue Testing

Two BMAS matrix composites (15.2x15.2cm) were fabricated with a layered BN(+C) interface (#29-95) and a layered BN(+C) interface with a SiC overcoating (#28-95), in order to perform fast fracture tensile testing and tensile fatigue testing. These composites were first tested in monotonic tension at 550° and 1100°C, with the results being shown in Table II. These composites had slightly higher fiber content (~50 vol%) compared to the previous ones shown in Table I (~45 vol%). The loading rate was 20 MPa/s, and the proportional limit (PL) stress (deviation from linearity), was measured utilizing a 0.005% offset strain. The stress-strain curves for these tests are shown in Fig. 6. In general, the BN(+C) coated Nicalon fiber composites exhibited higher ultimate strengths and strain-to-failures, and lower proportional limit stresses and elastic moduli at each temperature, compared to the SiC/BN(+C) coated Nicalon composites. The elastic modulus of the composites was lower at 1100°C than at 550°C, reflecting the softening of the residual glassy phase in the BMAS matrix. All composites exhibited very fibrous fracture surfaces.

Tensile fatigue (tension-tension, R=0.1) experiments were conducted on the two types of coated fiber composites at 550°C under a maximum stress of 104 MPa, and at 1100°C under maximum stresses of both 104 MPa and 138 MPa. Both of these stresses are at or above the proportional limit stress of the composites, as was shown in Table II. The frequency was 3 Hz, which resulted in a 106 cycle runout time of ~93 hours. All of the samples fatigued at both stress levels survived 10^6 cycles without failure, and were then tested to failure in monotonic tension at temperature (20 MPa/s loading rate). The temperature of 550°C (due to a miscommunication, the fatigue tests were actually run at 500°C) was chosen because previous studies indicated that this temperature was particularly severe for the oxidation of carbon interfaces, and thus there was concern that the carbon rich BN layered interfaces might suffer enhanced oxidation at this temperature. The temperature of 1100°C was chosen since this is near the planned use temperature for composites of this type.

The residual monotonic tensile properties of the composite samples after fatigue runout are shown in Table III. From the data shown in Table III, it can be seen that the residual tensile strengths of the samples fatigued at 104 MPa at both 550° and 1100°C, and with both BN and SiC/BN coatings, increased over that measured on as-fabricated composites. This increase may be due to straightening of the 0° plies during the fatigue testing. The strain-to-failure of the composites also tended to increase. At 1100°C and 138 MPa fatigue stress, the residual ultimate strength of the composites tended to decrease, as did the proportional limit stress. In the case of the SiC/BN coated Nicalon fiber composite fatigued at 138 MPa, the strain-to-failure also decreased substantially. The stress-strain behavior of the BN and SiC/BN coated Nicalon fiber composites at 550°C, as-processed and after 104 MPa fatigue, and at 1100°C, as-processed and after 104 MPa and 138 MPa fatigue, are shown in Figs. 7 and 8, respectively. From these figures, the increase in ultimate strength after 104 MPa fatigue is evident, as is the

degradation in properties of the SiC/BN coated Nicalon fiber composite after 138 MPa fatigue testing.

The fracture surfaces of all fatigued composites were very fibrous in nature, as shown in Figs. 9-13, except for a region of the SiC/BN coated Nicalon fiber composite that had experienced the 1100°C, 138 MPa fatigue, as shown in Fig. 14. From this figure, it can be seen that one of the edge regions on the fracture surface exhibited a very brittle and glazed appearance, indicating that a crack had formed during the fatigue test and propagated partially through the composite. Even though this crack formation was not enough to fail the composite during fatigue, it did cause a significant reduction in the residual 1100°C tensile strength and strain-to-failure. Interestingly, no such brittle region was evident on the fracture surface of the composite fatigued at 1100°C, 138 MPa that contained a BN coating only on the Nicalon fibers (Fig. 13), even though this stress level is significantly higher than the proportional limit, or matrix microcrack stress.

The difference in behavior of the BN(+C) vs SiC/BN(+C) coated Nicalon fiber composites in 1100°C, 138 MPa fatigue, may be associated with the somewhat different fracture path that matrix cracks take when propagating into the fiber coatings. The crack path in the dual layer composite with the SiC overcoat is usually found to be in the carbon rich layer nearest to the Nicalon fiber surface, whereas that in the BN(+C) coating is invariably between the crystallized BN layer and the first carbon rich layer nearest the matrix. Figure 15 shows a crack path (filled with mounting resin) in the BN(+C) composite (#29-95) that was fatigued at 1100°C, 138 MPa, after tensile testing to failure. The matrix crack can be seen to be diverted around the fibers near the surface of the BN(+C) layer.

Oxidation of the fibers during fatigue at stress levels significantly above the proportional limit stress, may be more severe when the crack path is closer to the fiber surface. Previous studies[9] with uniform turbostratic SiC/BN fiber coatings showed that when the interfacial cracks followed the BN/Nicalon fiber interface, limited oxygen access through the matrix cracks during 1100°C tensile fatigue led to oxidation of the surface of the Nicalon fibers to silica before significant oxidation of the BN, resulting in increased bonding of the fiber/matrix interfacial region.

While the oxidative stability of the carbon rich BN layers did not appear to be a problem at 500°C in fatigue, there was still concern over the oxidative stability of these coatings in the 700°C to 900°C range. Thus, an additional composite (#56-95) with SiC over BN(+C) fiber coatings was fabricated and tested in tensile fatigue at 700°C and 900°C. This composite had a somewhat lower fiber content (~42 vol%) than the previously fatigue tested composites #28-95 and 29-95, thus the fast fracture tensile properties were somewhat lower. The fracture surfaces were still quite fibrous in nature, however, as shown in Figs. 16 and 17.

As shown in Table IV, which also includes 550°C and 1100°C data from the previously tested SiC/BN(+C) interface composite #28-95, all of the tests at 104 MPa

stress exhibited 10^6 cycle runout at 700°C and 900°C, while at 138 MPa, the SiC/BN(+C) coated fiber composites tested at 700° and 900°C did not runout, but failed during fatigue testing at ~350,000 and 720,000 cycles, respectively. SEM examination of the fracture surfaces of the 104 MPa tested samples showed similar fracture behavior to the samples tested in fast fracture at 700°C and 900°C, as shown in Figs. 18 and 19. However, the 138 MPa tested samples that did not runout, showed significant oxidation of the BN layers near the sample edges and/or corners, as can be seen in Figs. 20-22. The central regions of the composites did not show any evidence of oxidation, with the BN layers remaining intact. From TEM microstructural analysis on these samples, and on a 650°C, 138 MPa, tensile stress-rupture sample that failed after 6,269 hrs, as will be discussed in the next section, it was found that the BN(+C) coatings were oxidizing at a faster rate than previously found for samples tested at 1100°C, due to lack of rapid crack plugging by oxide that does occur at 1100°C. TEM analysis conducted on those composites that did exhibit fatigue runout in the 700°C to 900°C range, showed that only very fine matrix cracks were generated during fatigue, and were blunted at the fiber/matrix interface, usually within the BN(+C) layer at one of the high carbon content multilayers.

A number of tensile and tensile fatigue tests were performed at the Univ. of S. California on BMAS matrix/Nicalon fiber composites with BN(+C) interfacial coatings. The results of these tests are reported in the Appendix.

4. Tensile Creep and Stress-Rupture Testing

A variety of tensile creep and stress-rupture testing was conducted on the layered BN(+C) interface composites, both with and without a SiC overcoat layer. Among these tests were stepped tensile stress-rupture in air at 550°C and 1100°C, where the stress is incrementally increased every 50 hrs until composite failure, a constant load (138 MPa) stress-rupture at 650°C that lasted for 6,269 hrs until failure, a 100 hr constant stress (104 MPa) tensile creep test at 1100°C, and a stepped temperature tensile creep test at a stress of 138 MPa for a time of 72 hrs.

a) Stepped Tensile Stress-Rupture

Four stepped stress-rupture tests in air were run on composites #7-95 and #3-95 with layered BN(+C) and SiC over layered BN(+C) interface coatings, respectively. One test each was run at 550°C and at 1100°C. The initial stress was set at ~70 MPa, which for these samples is slightly less than the tensile proportional limit stress (~12-14 MPa). The stress was then held at this level for ~50 hrs, and then uploaded in ~14 MPa increments, being held for ~50 hrs at each increment. The results of these tests are shown in Table V.

From the results shown in Table V, the samples tested at 550°C reached a maximum stress of 220 to 234 MPa, which corresponds to a time of 632 to 678 hrs, before failure occurred. The fracture surfaces of these two samples are shown in Figs. 23 and 24, and appear very similar to those shown earlier for fast fracture 550°C tensile

samples. No evidence of environmental attack of the layered BN(+C) interface can be seen. Figure 25 shows a light micro and TEM replica of a polished section right on the fracture surface of sample #7-95, and indicates that the layered BN(+C) interface is intact with matrix crack deflection occurring between the BMAS matrix and the layered BN(+C) coating. While not visible at the magnifications of Fig. 25, the crack deflection in these coatings is actually between the crystallized outer BN layer and the turbostratic inner BN layers, as shown previously, keeping the environment within the matrix cracks away from the fiber surface.

At 1100°C, the maximum stress reached in the stepped stress-rupture tests was 207 MPa for the layered BN(+C) sample #7-95, and 180 MPa for the SiC over layered BN(+C) sample #3-95, which corresponds to ~70% of their measured fast-fracture strengths at that temperature. The respective times to failure were 598 and 436 hrs. The fracture surfaces of these samples, shown in Figs. 26 and 27, were very fibrous with no evidence of oxidative embrittlement. Some glazing and oxidation can be seen on these fracture surfaces, due to oxidation of the BN exposed on the fracture surface after the sample has fractured, as has been seen on fast-fracture tensile samples when tested above ~900°C. The only oxidation seen for these samples was on the cut edges of the tensile gauge section, where the BN coatings and Nicalon fibers were attacked to a depth of ~50 microns, as shown in Fig. 28 for sample #7-95.

b) Tensile Stress-Rupture at 650°C

A sample of layered BN(+C) interface composite #15-95 was subjected to a constant 138 MPa stress-rupture test in air at 650°C, similar to a standard 3M SiC/BN interface sample tested a few years ago at 1100°C, which lasted over 14,000 hrs at a stress of 138 MPa without failing.[12] The stress of 138 MPa is well over the measured proportional limit, or matrix microcrack stress of these composites. At 650°C, the plugging of matrix cracks with silica that can occur at 1100°C is less likely. Even so, this sample lasted for 6,269 hrs at a stress of 138 MPa before fracturing. The fracture surface, as shown in Fig. 29, indicates that oxidation of the layered BN(+C) interface has progressed from the outside surfaces inward during the 6,000+ hr test. While the central region of the composite shows considerable fiber pullout and visible BN fiber coatings, the edge regions are quite brittle, with the BN apparently oxidized and replaced by a borosilicate glass that is well bonded to the fibers and matrix. This can be seen in Figure 30, which shows TEM replicas of 0° fibers on a polished section of the composite near the cut edge of the tensile sample. While the BN layer is intact on some of the fibers, it has been replaced by an oxide layer on others that presumably are connected to the surface by matrix cracks. Where the oxide layer is thicker, dissolution of the Nicalon fibers is evident. This obviously leads to weakening of the fibers as well as strong bonding between the fibers and matrix, and when it progresses into the composite far enough, composite failure will occur. This interfacial oxidation is obviously more pronounced at intermediate temperatures than at higher temperatures (1100-1200°C) where matrix crack sealing can more easily occur.

c) Tensile Creep Testing

In conjunction with the tensile fatigue testing discussed previously, two tensile creep tests were performed at 1100°C and 104 MPa stress. One sample (#29-95) had a layered BN(+C) interface while the other had a SiC over layered BN(+C) interface (#28-95). The results of these tests are graphically illustrated in Fig. 31, and are consistent with previous tensile creep results.[10] The measured steady-state creep rate for both samples was on the order of 10^{-9} s^{-1}, with the SiC overcoat interface sample creeping somewhat less that the BN(+C) interface sample. This result is probably a result of some slight diffusion of boron from the BN(+C) layer into the BMAS matrix leading to increased residual glass formation. The SiC overcoating would have prevented this from occurring. The residual tensile strength and strain-to-failure at 1100°C of the crept samples was higher than the fast-fracture results, but somewhat lower that the tensile fatigue results, as illustrated for the SiC/BN sample in Fig. 31. As was the case for the 1100°C, 104 MPa fatigue samples, the fracture surface of the composites remained very fibrous with no indication of oxidative attack, as shown in Fig. 32 for the crept sample from composite #28-95.

The final creep test performed on the layered BN(+C) interface composites was a stepped temperature tensile creep experiment performed at a stress of 138 MPa, with a temperature range of 430°C to 980°C. The results of this test are shown in Fig. 33, for both composite samples #28-95 (SiC over BN) and #29-95 (BN). As in the previous creep tests, the SiC overcoating appeared to result in a lower total creep strain for the composite. The crept composite surfaces both had a pattern of visible cracks, with the BN interface sample exhibiting a saturated crack pattern of relatively equally spaced cracks at intervals of ~232 microns, while the SiC/BN interface sample exhibited a pattern of discontinuous cracks. While discontinuous, the crack spacings were similar in both samples, indicating that, while the matrix creep rates were different, the interfacial shear strength of the composites were essentially identical. Polished sections of the gauge region showed that matrix cracks were again diverted away from the fiber surface in the first layer of the BN(+C) coating, for both the BN and SiC over BN coated samples (Fig. 34).

5. Summary

The layered 3M BN(+C) coatings on Nicalon fibers produced very strong and "tough" BMAS glass-ceramic matrix composites, due to the limited matrix element diffusion through the coating and matrix crack deviation within the layered coating structure. These composites exhibited excellent tensile fatigue and stress-rupture properties at stress levels significantly higher that the proportional limit, or matrix microcracking stress of the composite. The diffusional characteristics of the carbon rich layers within the BN(+C) fiber coatings may obviate the need for a SiC diffusion barrier overcoating, thus resulting in a simpler, lower cost composite system. However, oxidation of the layered BN coatings at intermediate temperatures (700°-900°C) under

conditions of high fatigue stress (138 MPa) may potentially limit the stress at which these composites can be utilized for structural applications.

B. Alternate BN Coated Nicalon Fiber Composites

Unfortunately, late in 1996, 3M made the decision to stop providing fiber coatings to outside customers. In light of this, a series of experiments were performed on alternate sources of BN coated Nicalon fiber. These sources, primarily Advanced Ceramics Corp. (ACC) and BF Goodrich (BFG), utilize a batch process with the boron source being BCl_3, to deposit BN coatings on woven cloth preforms. Previous BMAS matrix composites that utilized BN coated Nicalon fibers from Synterials, Inc., did not result in very high strength or high toughness composites. From scanning Auger studies, it was determined that these BN coatings were relatively high in oxygen, and at least part of the BN coating was very boron rich (Fig. 35). From TEM replica analysis of the composites made with these BN coated fibers, it was found that during BMAS matrix composite fabrication, the BN coating crystallized totally, as shown in Fig. 36. This BN crystallization is much more severe than that for the 3M layered BN(+C) coatings (Fig. 36), and leads to boron diffusion into the BMAS matrix as well as matrix element diffusion to the fiber surface, with subsequent fiber degradation. As pointed out earlier, the crystallized BN does not act as a good matrix crack deflector, thus limiting composite toughness.

BMAS matrix composites were fabricated utilizing both ACC and BFG BN coated satin weave Nicalon cloth lay-ups, with moderate success. Tables VI and VII list the composite flexural strengths vs temperature for the Advanced Ceramics and BFG BN coated Nicalon (and Hi-Nicalon) fiber composites, respectively. While the RT flexural strengths were quite high in most cases, the elevated temperature (900-1200°C) strengths were low. TEM studies have shown that, similar to the Synterials BN coatings, both the ACC and BFG BN coatings tended to crystallize during composite fabrication, as shown in Figs. 37 and 38. The enhanced boron diffusion into the matrix from the BN when this crystallization occurs, undoubtedly accounts for the poor high temperature properties, along with the formation of thin sub-layers of C/SiO_2 at the BN/Nicalon fiber interface, and diffusion of matrix elements through the BN into the Nicalon fiber surface, as was shown in Fig. 3. It was also found that the matrix crack path proceeded through the BN layer and was diverted at the BN/Nicalon interface, not within the BN layer as had been seen for the 3M layered BN(+C) coatings. This mode of crack diversion, which is enhanced by the carbon sublayer formation, can lead to environmental degradation of the Nicalon fiber surface due to oxide layer formation during high and intermediate temperature testing.

C. Silicon Doped BN Coated Fibers and Composites

One of the concerns related to the use of BN as an interfacial layer in CMC's is its stability in hot, moist environments such as might be encountered in certain sections of an

advanced gas turbine engine. Water vapor can react with the boria formed when BN oxidizes, forming volatile HBO species. Morscher, et.al, recently measured the recession of a variety of BN fiber coatings in a hot, moist environment.[13] Some of the results obtained are shown in Table VIII. While the 3M layered BN(+C) coatings were somewhat better than the standard BN in recession at 800°C, 90% water, higher temperature (1400 and 1800°C) deposited ACC BN coatings and silicon doped BN coatings (deposited at 1400°C) were significantly better. The higher temperature BN coatings were presumably better in moisture stability due to higher crystallinity over the standard and layered BN's, while the silicon doped BN was even better due to the formation of a high silica glass instead of boria. The formation of silica instead of a boria glass apparently sealed the interphase and thus resulted in minimal recession. All of these coatings were on SiC fibers surrounded by a CVI SiC matrix, except for the 3M layered BN(+C), which was in the UTRC BMAS matrix. Figures 39 and 40 show the BMAS matrix composite after the 800°C, 90% water exposure. The BN layer has been entirely replaced with a silica glassy layer down the length of the Nicalon fibers from the exposed cut edge of the composite.

It was decided to evaluate the ACC Si-doped BN coatings in a BMAS matrix composite. ACC deposited Si-doped BN on High-Nicalon fiber 8 harness satin weave cloth at 1400°C. A typical scanning Auger depth profile of one of these fibers is shown in Fig. 41. It can be seen that the average composition of the Si-doped BN coating is on the order of 51%N, 35%B, 12%Si, and 1-2% C with a trace of oxygen. While the sample subjected to Auger depth profiling had a Si-doped BN thickness of ~400nm, most of the fibers showed coating thicknesses of 100-200nm, as can be seen in the TEM replica of Fig. 42 and the TEM thin foil of Fig. 43. The high resolution TEM micrograph of the coating as shown in Fig. 44, indicates that the Si-doped BN has a randomly ordered microcrystalline hexagonal BN structure, with the measured d(0002) basal plane spacing being on the order of 3.60Å. This is much larger than the ideal interlayer spacing of highly crystalline BN of 3.33Å.

A BMAS matrix composite was fabricated utilizing six layers of the silicon-doped BN coated Hi-Nicalon 8HS cloth under the normal BMAS matrix composite processing conditions. The resultant composite (#24-97) was ceramed, and then machined into flexural specimens and tested in 3-pt flex from RT to 1200°C. The measured flexural strengths were between 170 and 220 MPa, with strain-to-failures of 0.1-0.2%. An example of the fracture surface of the RT tested sample is shown in Fig. 45. The mode of failure was essentially totally brittle, with very little evidence of fiber pullout. While some of the fibers showed the presence of a fiber coating, many did not. From TEM replica and thin foil analysis, as shown in Figs. 46, 47, and 48, it was apparent that many of the fibers in the composite did not have a trace of the Si-doped BN fiber coating, and for those that did, the coating was totally recrystallized. The very large, randomly oriented hexagonal BN grains, as shown in the HRTEM of Fig. 48, are surrounded by glassy BMAS matrix. This type of interface is definitely not optimum for matrix crack deflection parallel to the fiber surface. Scanning Auger depth profiling was also performed on a fiber surface and matrix trough on a longitudinal fracture surface of this

composite, as shown in Fig. 49, and clearly shows that significant interdiffusion of matrix elements (Al, Si, Ba, Mg, and O) have occurred into the Si-doped BN layer. It is apparent that Si-doped BN interfacial coatings, at least those with high Si content, are too reactive with the BMAS glass-ceramic matrix system to act as a viable interface coating concept. Perhaps with a SiC overcoat, the viability would be improved.

D. Coated Nextel 720 Fiber Composites

In order to investigate alternate, potentially less expensive, fibers for the reinforcement of glass-ceramic matrices, that might also lead to composites with interesting electrical properties such as lower dielectric constant, the recently developed 3M Nextel 720 aluminosilicate fibers were incorporated into BMAS matrices utilizing a variety of fiber coating concepts. Nextel 720 fibers consist of 85% Al_2O_3 and 15% SiO_2, with crystalline phases of alpha alumina plus mullite. The ~12 micron diameter fibers have a tensile strength of 300 ksi (2.07 GPa), modulus of 38 msi (262 GPa), thermal expansion of $6x10^{-6}$/°C, and a relatively low creep rate for an oxide fiber at temperatures to 1200°C.

1. BN and SiC over BN Coated Nextel 720 Fibers and Composites

Initial experiments utilized 3M BN and SiC/BN coated Nextel 720 fibers. These coatings were not the layered BN(+C) type discussed previously. Table IX shows the measured tensile properties of the coated Nextel 720 fibers. While the BN and SiC/BN coatings appear to degrade the UTS of the fibers somewhat, the loss in strength is not severe. BMAS composites were fabricated with these two types of coated Nextel 720 fibers, machined into flexural samples, and tested in 3-pt flex from RT to 1200°C. the results of these tests are shown in Table X. From this data, it can be seen that the flexural strengths and strain-to-failures of these composites are significantly lower than that measured for the layered BN(+C) coated Nicalon fiber composites (Table I). Table XI shows some of the electrical properties measured for these composites.

One of the reasons for the relatively low mechanical properties of these composites is that during composite fabrication, the coatings became detached from the fibers, leading to severe fiber/matrix reaction, especially in the case of the SiC/BN coatings, as shown in Figs. 50 and 51. Cracks in the matrix adjacent to the reacted fibers were also often observed. It is likely that the detachment of the coatings was due to thermal expansion mismatch stresses between the coatings and the Nextel 720 fibers. There may have been cracks in the coatings on cooling from the deposition temperature, that then caused them to detach during composite fabrication. The SiC overcoating, with its 33% lower thermal expansion coefficient than the Nextel 720 fibers, added to the coating detachment problem. The reaction between the BMAS matrix and the Nextel 720 fibers was not studied extensively, but was likely exaggerated grain growth of one or both of the fiber constituents due to glassy phase intrusion into the fibers from the BMAS

matrix during the ~1450°C hot-pressing step. Attempts to alleviate these reactivity problems by hot-pressing at lower temperatures were not successful.

2. Carbon Coated "Fugitive" Nextel 720 Fibers and Composites

Experiments were performed to evaluate the "fugitive" interface concept that has been described[14] as a potential mechanism for obtaining "tough" and strong oxide/oxide CMC composites. This mechanism relies on creating a gap at the fiber/matrix interface that will allow matrix crack diversion and fiber pullout to occur, thus creating a "tough" composite failure, while still retaining enough contact between the fibers and matrix for load transfer to occur, thus creating a strong composite. CVD Carbon coated Nextel 720 fibers were obtained from 3M via AFML that had two different thicknesses of carbon; a "thick" carbon of ~0.3 microns, and a "thin" carbon of ~0.1 microns. The flexural strength results of BMAS matrix composites fabricated with these carbon coated Nextel 720 aluminosilicate fibers are shown in Table XII. The carbon coated Nextel 720 fiber composites exhibited relatively low strengths and very low strain-to-failures, which did not improve when the carbon interface was oxidized away to create a "fugitive" interface composite. Some fiber/matrix reaction was seen in the as-pressed composites with the carbon layer in the unoxidized state, as well as some grain growth of the Nextel 720 fibers, as shown in Fig. 52 In unreacted areas, as shown in Fig. 53, the CVD carbon fiber coating can be seen to be layered, similar to that seen previously for the layered BN(+C) coatings on Nicalon fibers. TEM analysis showed that the carbon interface was removed completely by the 550°C oxidation treatment (Fig. 54), but the significant amount of reaction between fiber and matrix in this composite system (Fig. 55) did not allow the "fugitive" interface concept to lead to strong or "tough" composites, as was desired. This concept must be demonstrated in a CMC system that does not exhibit as much inherent reactivity between the fibers and matrix.

Experiments were also performed with multilayer $C/Al_2O_3/C$ coated Nextel 720 fibers, obtained from AFML, that would presumably lead to a non-reactive alumina layer between the fibers and matrix when the carbon interfaces were oxidized to form "fugitive" interfaces. It was found that the $C/Al_2O_3/C$ coatings were very non-uniform, and tended to spall off the fibers during composite fabrication. The composites fabricated with these coated fibers were extremely weak and brittle.

3. Monazite ($LaPO_4$) Coated Nextel Fibers and Composites

The results of BMAS matrix composites fabricated with $LaPO_4$ (monazite) coated Nextel 720 aluminosilicate fibers were also not promising. The sol-gel derived monazite coatings[15] were very non-uniform and "lumpy", as seen in the SEM and scanning Auger analyses shown in Fig. 56, and reacted severely with the BMAS matrix during composite fabrication (Fig. 57), leading to total fiber reaction and very brittle and weak material. The reactivity in this system appeared to be enhanced over that in uncoated Nextel 720 fiber/BMAS matrix composites fabricated under the identical conditions. Evidently, the La containing glassy phase that is produced on reaction of the monazite with the BMAS

glass matrix, causes severe grain growth in the Nextel 720 fibers. Again, attempts to alleviate these reactivity problems by hot-pressing at lower temperatures were not successful.

E. Crystalline BN Coated and Uncoated SiC Fibers

An interesting approach to applying fiber coatings has recently been studied by the University of Florida (UF), in concert with their fabrication of crystalline SiC fibers. These fibers are small diameter, polymer-derived, near-stoichiometric SiC with a slight amount of boron sintering additive, with a slightly carbon rich surface, that can be heat-treated at high temperatures in a nitrogen containing atmosphere to form an *in-situ* layer of BN on the fiber surface.[16] The coated and uncoated fiber tensile strengths are in the range of 2.7-2.9 GPa, with average fiber diameters of ~10μm. In a collaborative effort between UF and UTRC, uncoated and BN coated SiC fibers have been subjected to scanning Auger and TEM thin foil analysis. Auger and TEM analysis of the uncoated SiC fibers have shown them to be crystalline stoichiometric SiC with a very thin carbon rich surface, with minor amounts of boron (<3%), and no oxygen, as shown in the scanning Auger results and TEM thin foil analysis in Figs. 58 and 59. The β-SiC grain size ranges from 50-300nm, with some fine porosity that appears to be aligned along the fiber axis (Fig. 59).

The BN coated fibers exhibit relatively stoichiometric BN surface layers of from 50-200nm in thickness, as shown in the scanning Auger depth profiles in Figs. 60 and 61, depending on the fiber heat-treatment time and temperature. Some of the BN coated fibers showed an excess of carbon in the BN nearest the fiber surface. From TEM thin foil analyses, as shown in Figs. 62-64, certain observations can be made. From Fig. 62, the BN coating appears to be highly crystalline, and very uniform in thickness at ~150nm. It appears that the SiC grain size within 2-3 microns of the fiber surface has increased significantly as a result of the heat-treatment to form the *in-situ* BN layer, as shown in Fig. 63. The average grain size of the fiber surface region under the BN layer is now on the order of 300nm, compared to an average of ~120nm in the fiber central region. This increase in grain size did not appear to decrease the fiber tensile strength, however. From the HRTEM micrograph in Fig. 64, it can be seen that the BN coating has grown such that the hexagonal BN basal planes are oriented primarily perpendicular to the long axis of the fibers. The measured d(0002) lattice spacing of the BN is ~3.45Å, which is larger than the theoretical value of 3.33 Å.

There were insufficient Univ. of Fla. BN coated SiC fibers available to allow fabrication of even a very small BMAS matrix composite. Thus, the effectiveness of this type of quite thin BN coating for developing the weak fiber/matrix bonding that is necessary for matrix crack diversion in CMC's has not been evaluated. It is possible that the thickness of the coatings could be increased by utilizing SiC fibers with a higher initial boron content, however, the directionality of the BN basal planes perpendicular to the fiber axis does not appear to be optimum for interfacial crack diversion.

III. SUMMARY

In summary, the layered 3M BN(+C) coatings on Nicalon fibers produced very strong and "tough" BMAS glass-ceramic matrix composites, due to the limited matrix element diffusion through the coating and matrix crack deviation within the layered coating structure. These composites exhibited excellent tensile fatigue and stress-rupture properties, although oxidation of the layered BN coatings at intermediate temperatures (700°-900°C) under conditions of high fatigue stress (138 MPa) may potentially limit the stress at which these composites can be utilized for structural applications. Alternate BN and Si-doped BN coatings from other vendors did not perform as well, with excessive BN crystallization occurring during composite fabrication. Nextel 720 aluminosilicate fibers with either BN, fugitive carbon, or C/Al_2O_3/C coatings did not result in strong or "tough" BMAS matrix composites for a variety of reasons, but primarily because of coating debonding leading to fiber/matrix interactions. Monazite ($LaPO_4$) coated Nextel 720 fibers reacted excessively with the BMAS matrix during composite fabrication. The crystalline SiC fibers from the Univ. of Fla., especially with the *in-situ* BN coatings, appear to offer future promise for high temperature CMC reinforcement.

IV. ACKNOWLEDGEMENTS

The author would like to thank Dr. Chris Griffin of 3M for coordinating the coating of the layered BN(+C) coatings on the Nicalon fiber, Dr. Bruce Laube of UTRC for the scanning Auger analyses, Mr. Gerald McCarthy of UTRC for the TEM replica and thin foil analyses, Mr. David Murphy of P&W, Prof. Steven Nutt of USC, and Dr. John Holmes of Composite Testing and Analysis (CTA) for the composite mechanical testing, and Ms. Laura Austin, Mr. Paul Lasewicz and Mr. Mark Hermann of UTRC for the fabrication of the coated fiber composites, and to Dr. Alexander Pechenik of AFOSR for his sponsorship of this program.

Papers published to date under full or partial AFOSR support include:

1. "SiC-Whisker-Reinforced Glass-Ceramic Composites: Interfaces and Properties", John J. Brennan and Steven R. Nutt, J. Am. Ceram. Soc. 75, [5] 1205-16 (1992).

2. "Interfacial Studies of Fiber Reinforced Glass-Ceramic Matrix Composites", John J. Brennan, Symposium on High Temperature Ceramic Matrix Composites, 6th European Conference on Composite Materials, Sept. 20-24, 1993, Bordeaux, France, pp 269-283, Woodhead Publishing Ltd, Abington Cambridge, England.

3. "Evolution of Interface Microstructure in a Dual-Coated Silicon Carbide Fiber-Reinforced BMAS Glass-Ceramic Composite", Ellen Y. Sun, Steven R. Nutt, and John J. Brennan, Proceedings of the American Ceramic Society '93 Annual Meeting Symposium on Advances in Ceramic Matrix Composites, pp 199-210, Oct. 1993

4. "Interfacial Microstructure and Chemistry of SiC/BN Dual Coated Nicalon Fiber Reinforced Glass-Ceramic Matrix Composites", Ellen Y. Sun, Steven R. Nutt, and John J. Brennan, J. Am. Ceram. Soc. 77, [5] 1329-39 (1994)

5. "FIexural Creep and Creep-Rupture Behavior of SiC/BN Dual Coated Nicalon Fiber Reinforced Glass-Ceramic Matrix Composites, Ellen Y. Sun, Steven R. Nutt, and John J. Brennan, Cer. Engr. & Sci. Proc., Vol. 15, No. 4, 57-64 (1994).

6. "Interfacial Diffusion and Reaction Mechanisms in Coated Fiber Reinforced Glass-Ceramic Composites", Ellen Y. Sun, Steven R. Nutt, and John J. Brennan, Cer. Engr. & Sci. Proc., Vol. 15, No. 5, 943-950 (1994).

7. "Interfaces in BN Coated Fiber Reinforced Glass-Ceramic Matrix Composites", John J. Brennan, Scripta Metallurgica et Materialia, Vol. 31, No. 8, pp. 959-964, 1994.

8. "Microscopic Failure Mechanisms in SiC Fiber-Reinforced Glass-CeramComposites", Ellen Y. Sun, Steven R. Nutt, and John J. Brennan, Proceedings of the 1994 TMS

Spring Meeting (Symposium on Control of Interfaces in Metal and Ceramic Composites)

9. "Flexural Creep of Coated SiC-Fiber-Reinforced Glass-Ceramic Composites", Ellen Y. Sun, Steven R. Nutt, and John J. Brennan, J. Am. Cer. Soc., 78, [5] 1233-39 (1995).

10. "Interfacial Microstructure and Stability of BN-Coated Nicalon Fiber/Glass-Ceramic Matrix Composites", John J. Brennan, Steven R. Nutt, and Ellen Y. Sun, Ceramic Transactions, Vol. 58, "High-Temperature Ceramic-Matrix Composites II", Proceedings of the Second International Conference on High-Temperature Ceramic-Matrix Composites, August 21-24, 1995, Santa Barbara, CA, edited by A. G. Evans and R. Naslain, published by the Am. Cer. Soc. (1995).

11. "Oxidation of BN-Coated SiC Fibers in Ceramic Matrix Composites", Brian W. Sheldon, Ellen Y. Sun, Steven R. Nutt, and John J. Brennan, J. Am. Cer. Soc., 79, [2] 539-43 (1996).

12. "High-Temperature Tensile Behavior of a Boron-Nitride-Coated Silicon Carbide-Fiber Glass-Ceramic Composite", Ellen Y. Sun, Steven R. Nutt, and John J. Brennan, J. Am. Cer. Soc., 79, [6] 1521-29 (1996).

13. "Fiber Coatings for SiC-Fiber-Reinforced BMAS Glass-Ceramic Composites", Ellen Y. Sun, Steven R. Nutt, and John J. Brennan, J. Am. Cer. Soc., 80, [1] 264-66 (1997).

14. "Intermediate-Temperature Environmental Effects on Boron Nitride-Coated-Silicon Carbide-Fiber-Reinforced Glass-Ceramic Composites", Ellen Y. Sun, Hua-Tay Lin, and John J. Brennan, J. Am. Cer. Soc., 80, [3] 609-14 (1997).

15. "High-Temperature Load Transfer in Nicalon/BMAS Glass-Ceramic Matrix Composites", Sujanto Widjaja, Karl Jakus, John E. Ritter, Edgar Lara-Curzio, Ellen Y. Sun, Thomas R. Watkins, and John J. Brennan, Cer. Engr. & Sci. Proc., Vol. 18, Issue 3, 681-88, 1997.

16. "Processing and Properties of Glass-Ceramic Matrix/Nicalon Fiber Composites", Proceedings of the Fourth International Conference on Composites Engineering (ICCE/4), July 6-12, 1997, Kohala Coast, Hawaii, Edited by David Hui, Univ. of New Orleans, pp. 181-82.

Papers submitted for publication to date include:

1. "Interfacial Design and Properties of Layered BN(+C) Coated Nicalon Fiber-Reinforced Glass-Ceramic Matrix Composites", John J. Brennan, Invited paper at

Ceramic Microstructures '96, Berkeley, CA, June 24-27, 1996, to be published by Plenum Press.

2. "Creep-Induced Residual Stress Strengthening in Fiber-Reinforced Glass-Ceramic Composites", Sujanto Widjaja, Karl Jakus, John E. Ritter, Edgar Lara-Curzio, Ellen Y. Sun, and John J. Brennan, submitted to J. Am. Cer. Soc., June, 1997.

3. "Polymer-Derived SiC-Based Fibers with High Tensile Strength and Improved Creep Resistance", Michael D. Sacks, Gary W. Scheiffele, Lan Zang, Yunpeng Yang, and John J. Brennan, to be published in Cer. Engr. & Sci. Proc., 1998.

Papers presented at meetings to date and not submitted for publication include:

1. "Interfacial Reaction in BN Coated HPZ Fiber Reinforced Glass-Ceramic Matrix Composites", J. J. Brennan, presented at the 17th Annual Conf. on Composites, Materials, and Structures, Cocoa Beach, Fla. Jan. 10-15, 1993 (paper #140).

2. "Glass and Glass-Ceramic Matrix Composites", J. J. Brennan, presented at the 95th Annual Meeting of the Am. Cer. Soc, Cincinnati, OH, April 19-22, 1993 (Invited Paper #SII-81-93).

3. "Environmental Stability of Nicalon Fiber Reinforced Glass-Ceramic Matrix Composites", presented at the 20th Annual Conf. on Composites, Advanced Ceramics, Materials and Structures, Cocoa Beach, Fla. Jan. 7-11, 1996 (paper #C-141-96F).

V. REFERENCES

1. K.M. Prewo, J.J. Brennan, and G.K. Layden, "Fiber reinforced glasses and glass-ceramics for high performance applications," Am. Cer. Soc. Bull., 65 [2] 305 (1986).

2. J.J. Brennan, "Interfacial characterization of glass and glass-ceramic matrix/Nicalon SiC fiber composites," Materials Science Research, Vol. 20, Plenum Press, New York, 549 (1986).

3. R.F. Cooper and K. Chyung, "Structure and chemistry of fiber-matrix interfaces in SiC fibre-reinforced glass-ceramic composites: An electron microscopy study," J. Mater. Sci., 22, 3148 (1987).

4. C. Ponthieu, M. Lancin, J. Thibault-Desseaux, and S. Vignesoult, "Microstructure of interfaces in SiC/glass composites of different tenacity", Journal de Physique, 51, Cl-1021, (1990).

5. R.W. Rice: "BN coating of ceramic fibers for ceramic fiber composites", US Patent 4,642,271, Feb. 10, 1987.

6. J. Brennan: "Interfacial studies of fiber reinforced glass-ceramic matrix composites," High Temperature Ceramic Matrix Composites, HT-CMC-I, Editors: R. Naslain, J. Lamon, and D. Doumeingts, Woodhead Publishing, Ltd, Abington Cambridge, England, 269 (1993)

7. E. Sun, S. Nutt, and J. Brennan: "Interfacial microstructure and chemistry of SiC/BN dual coated Nicalon fiber reinforced glass-ceramic matrix composites", J. Am. Ceram. Soc. 77, [5] 1329 (1994)

8. J. Brennan, S Nutt, and E. Sun: "Interfacial microstructure and stability of BN coated Nicalon fiber/glass-ceramic matrix composites", High Temperature Ceramic Matrix Composites II: Manufacturing and Materials Development, Editors: A. Evans and R. Naslain, Ceramic Transactions,[58] 53 (1995).

9. B.W. Sheldon, E.Y. Sun, S.R. Nutt, and J.J. Brennan: "Oxidation of BN-coated SiC fibers in ceramic matrix composites", J. Am. Ceram. Soc. 79, [2] 539 (1996)

10. E.Y. Sun, S.R. Nutt, and J.J. Brennan: "High-temperature tensile behavior of a boron nitride-coated silicon carbide-fiber glass-ceramic composite", J. Am. Ceram. Soc. 79, [6] 1521 (1996)

11. J. J. Brennan: "Interfacial Design and Properties of Layered BN(+C) Coated Nicalon Fiber-Reinforced Glass-Ceramic Matrix Composites", Ceramic Microstructures '96, Berkeley, CA, June 24-27, 1996, to be published by Plenum Press.

12. J. Brennan, S. Nutt, and E. Sun: "Interfacial Studies of Coated Fiber-Reinforced Glass-Ceramic Matrix Composites", Final Report R94-970150-3 on AFOSR Contract F49620-92-C-0001, Dec. 31, 1994.

13. G.N. Morscher, D.R. Bryant, and R.E. Tressler: "Environmental Durability of BN-Based Interphases (For SiC_f/SiC_m Composites) in H_2O Containing Atmospheres at Intermediate Temperatures", Cer. Engr. & Sci. Proc., Volume 18, Issue 3, 525-33 (1997).

14. R.J. Kerans: "Control of Fiber-Matrix Interface Properties in Ceramic Composites", HT-CMC-I, Editors: R. Naslain, J. Lamon, and D. Doumeingts, Woodhead Publishing, Ltd, Abington Cambridge, England, 301 (1993)

15. R. S. Hay, E. Boakye, and D. M. Petry: "Sol-Derived Dense and Porous Monazite Fiber Coating", 21st A. Cer. S. Conference on Composites, Advanced Ceramics, Materials and Structures, Cocoa Beach, Fla., Jan. 12-16, 1997 (paper C-0042-97F).

16. M.D. Sacks, G.W. Scheiffle, L. Zhang, Y. Yang, and J.J. Brennan: "Polymer-Derived SiC-Based Fibers with High Tensile Strength and Improved Creep Resistance", 22nd A. Cer. S. Conference on Composites, Advanced Ceramics, Materials and Structures, Cocoa Beach, Fla., Jan. 20-24, 1998 (paper C-132-98).

Table I

Flexural Properties in Air for BMAS Matrix/Nicalon Fiber Composites (0/90°) with 3M Layered BN(+C) Fiber Coatings

(45 vol% fiber)

- **#3-95 (SiC/BN Coated Fiber)**

Temperature (°C)	σ-ksi (MPa)	E-msi (GPa)	ε_f - %
RT	66 (454)	18.6 (128)	0.45
1100	74 (512)	11.8 (81)	0.80
1200	90 (622)	10.7 (74)	1.11

- **#7-95 (BN Coated Fiber)**

Temperature (°C)	σ-ksi (MPa)	E-msi (GPa)	ε_f - %
RT	93 (640)	16.7 (115)	0.85
1100	85 (583)	11.3 (78)	1.08
1200	76 (522)	10.0 (69)	1.26

Table II

Tensile Properties in Air for BMAS Matrix/Nicalon Fiber Composites (0/90°) with 3M Layered BN(+C) Fiber Coatings

(50 vol% fiber)

- **#28-95 (SiC/BN Coated Fiber)**

Temperature (°C)	UTS-ksi (MPa)	PL-ksi (Mpa)	E-msi (GPa)	ε_f - %
550	48.7 (336)	12.9 (89)	18.4 (127)	0.73
1100	43.6 (301)	15.2 (105)	10.6 (73)	0.79

- **#29-95 (BN Coated Fiber)**

Temperature (°C)	UTS-ksi (MPa)	PL-ksi (MPa	E-msi (GPa)	ε_f - %
550	53.8 (371)	9.4 (65)	17.3 (119)	0.83
1100	53.5 (370)	10.7 (74)	9.6 (66)	0.98

Table III

BMAS Matrix/BN & SiC/BN Coated Nicalon Fiber Composite (0/90°) Tensile Durability

Tensile Fatigue

[R=0.1, 3 Hz, 10^6 cycle runout (~93hrs)]

Comp. #	Coating	Temp	Max. Str.-ksi(MPa)	UTS-ksi(MPa)	Res. UTS-ksi(MPa)
#29-95	BN	500°C	15 (104)	53.8 (371)* PL=9.4 (65)	66.2 (457)* PL=16.0 (110)
"	"	1100°C	15 (104)	53.5 (370) PL=10.7 (74)	57.7 (398) PL=15.2 (105)
"	"	1100°C	20 (138)	"	47.0 (323) PL=9.0 (62)
#28-95	SiC/BN	500°C	15 (104)	48.7 (336)* PL=12.9 (89)	55.6 (384)* PL=15.5 (107)
"	"	1100°C	15 (104)	43.6 (301) PL=15.2 (105)	54.0 (372) PL=15.5 (106)
"	"	1100°C	20 (138)	"	41.2 (284) PL=8.0 (55)

* Fast fracture conducted at 550°C

Table IV

BMAS Matrix SiC/BN Coated Nicalon Fiber Composite (0/90°) Tensile Fatigue Results

[R=0.1, 3 Hz, 10^6 cycle runout (~93hrs)]

Comp. #	Temp	UTS-ksi(MPa)	Stress-ksi(MPa)	# Cycles	Res.UTS-ksi(MPa)
#28-95 (50% fiber)	550°C	48.7 (336) PL=12.9 (89)	15 (104)	10^6	55.6 (384)* PL=15.5 (107)
#56-95 (42% fiber)	700°C	39.9 (275) PL=15.0 (104)	15 (104)	10^6	39.0 (269) PL=14.8 (102)
"	700°C	"	20 (138)	349,216	-
"	900°C	37.8 (260) PL=14.7 (101)	15 (104)	10^6	41.4 (285) PL=20.3 (140)
"	900°C	"	20 (138)	719,710	-
#28-95	1100°C	43.6 (301) PL=15.2 (105)	15 (104)	10^6	54.0 (372) PL=15.5 (106)
"	1100°C	"	20 (138)	10^6	41.2 (284) PL=8.0 (55)

Table V

BMAS Matrix/BN & SiC/BN Coated Nicalon Fiber Composite (0/90°) Tensile Durability

Stepped Tensile Stress-Rupture

(~50hrs at each 2 ksi (14 MPa) stress level, starting at 10 ksi (70 MPa)

Comp. #	Coating	Temp-°C	UTS-ksi(MPa)	Max. Str.-ksi(MPa)	Hrs to Failure
#7-95	BN	550°	-	34 (234)	678
"	"	1100°	41 (283) PL=12 (83)	30 (207)	598
#3-95	SiC/BN	550°	-	32 (220)	632
"	"	1100°	38 (262) PL=14 (97)	26 (180)	436

Table VI

Flexural Properties (4-pt) in Air for BMAS Matrix/Advanced Ceramics BN Coated Woven Nicalon Fiber Composites (0/90°)

#36-96 (Run #960467, 8HS CG Nicalon, 36% fiber)

Temperature (°C)	σ-ksi (MPa)	E-msi (GPa)	ε_f - %
RT	66.8 (460)	17.5 (121)	0.82
RT*	60.5 (417)	15.9 (110)	0.56
900	47.4 (327)	17.9 (123)	0.49
1000	35.5 (245)	14.7 (102)	0.43
1100	36.0 (248)	12.3 (85)	0.50

#37-96 (Run #960467, 8HS Carbon Coated CG Nicalon, 36% fiber)

Temperature (°C)	σ-ksi (MPa)	E-msi (GPa)	ε_f - %
RT	79.5 (548)	18.3 (126)	0.86
RT*	72.7 (501)	16.5 (114)	0.56
900	41.6 (287)	15.1 (104)	0.46
1000	36.8 (254)	13.3 (92)	0.38
1100	33.5 (231)	13.2 (91)	0.46

* (30 ksi pre-stress, 95%RH, 140°F, 150 hrs)

Table VII

Flexural Properties (3-pt) in Air for BMAS Matrix/BFG BN Coated Nicalon Fiber Composites (0/90°)

#26-96 (Run #42-1180, 8HS CG Nicalon)

Temperature (°C)	σ-ksi (MPa)	E-msi (GPa)	ε_f - %
RT	44.0 (303)	14.4 (99)	0.55
1000	36.3 (250)	9.5 (65)	0.62
1100	38.7 (267)	8.2 (56)	0.83
1200	23.8 (164)	6.8 (47)	1.17

#30-96 (Run #1179, 5HS Hi-Nicalon)

Temperature (°C)	σ-ksi (MPa)	E-msi (GPa)	ε_f - %
RT	71.5 (492)	21.3 (147)	0.46
1000	77.2 (532)	13.9 (96)	0.72
1100	50.0 (345)	9.6 (66)	0.68
1200	51.8 (357)	8.0 (55)	0.78

Table VIII

Recession of BN Fiber Coatings in Moist Environments*

(800C, 90% H_2O, 88 hrs)

Type of BN Coating/CMC	Recession Distance - microns
Standard BN/SiC	1500
3M BN(+C)/BMAS	1300
ACC 1400° BN/SiC	150
ACC 1800° BN/SiC	125
ACC Si-doped BN/SiC	<10

*Greg Morscher - NASA

Table IX

RT Tensile Properties of 3M BN and SiC/BN Coated Nextel 720 (85/15) Aluminosilicate Fibers
(Average of 15 fiber tests)

Fiber Coating	UTS - ksi (GPa)	E - msi (GPa)
none*	300 (2.07)	38 (262)
BN	254 (1.75)	40 (276)
SiC/BN	230 (1.59)	36 (248)

* 3M Data

Table X

Flexural Properties in Air for BMAS Matrix-SiC/BN and BN Coated Nextel 720 Fiber Composites (0/90°)

#145-94 (BN Coated Fiber)

Temperature (°C)	σ-ksi (MPa)	E-msi (GPa)	ε_f - %
RT	48 (332)	22 (152)	0.34
800	57 (391)	20 (138)	0.26
900	36 (249)	12 (80)	0.34
1000	30 (207)	11 (75)	0.32
1100	33 (229)	11 (75)	0.32
1200	19 (131)	7 (48)	0.49

#146-94 (SiC/BN Coated Fiber)

Temperature (°C)	σ-ksi (MPa)	E-msi (GPa)	ε_f - %
RT	41 (282)	22 (104)	0.37
800	33 (226)	15 (138)	0.22
900	31 (212)	13 (88)	0.26
1000	31 (212)	11 (75)	0.32
1100	31 (212)	11 (75)	0.32
1200	27 (187)	9 (62)	0.39

Table XI

Dielectric Properties of BMAS Matrix-SiC/BN and BN Coated Nextel 720 Fiber Composites (10 GHz)

Composite	Dielectric Constant	Loss Tangent
BMAS/BN/Nextel 720	7.1	0.098
BMAS/SiC/BN/Nextel 720	9.6	1.464

Table XII

Flexural Properties (3-pt) in Air for BMAS Matrix-3M Carbon Coated Nextel 720 Fiber Composites (0/90°)

#31-96 (Lot #105285-51-1, thick carbon coating)

Temperature (°C)	Treatment	σ-ksi (MPa)	E-msi (GPa)	ε_f - %
RT	none	33.0 (228)	21.1 (145)	0.19
"	550°C, 100hrs, O_2	26.2 (181)	17.9 (123)	0.15
1000	none	21.2 (146)	20.9 (144)	0.13
"	550°C, 100hrs, O_2	33.6 (232)	16.0 (110)	0.24

#32-96 (Lot #105285-50-1, thin carbon coating)

Temperature (°C)	Treatment	σ-ksi (MPa)	E-msi (GPa)	ε_f - %
RT	none	38.0 (260)	21.9 (151)	0.19
"	550°C, 100hrs, O_2	37.2 (256)	23.4 (161)	0.17
1000	none	31.6 (218)	20.1 (139)	0.17
"	550°C, 100hrs, O_2			

OPTICAL/TEM CHARACTERIZATION OF 3M BMAS BN-COATED NICALON
(0/90)FIBER COMPOSITE - #7-95-6 (As-ceramed) RTσ = 93KSI (640MPa)

100X

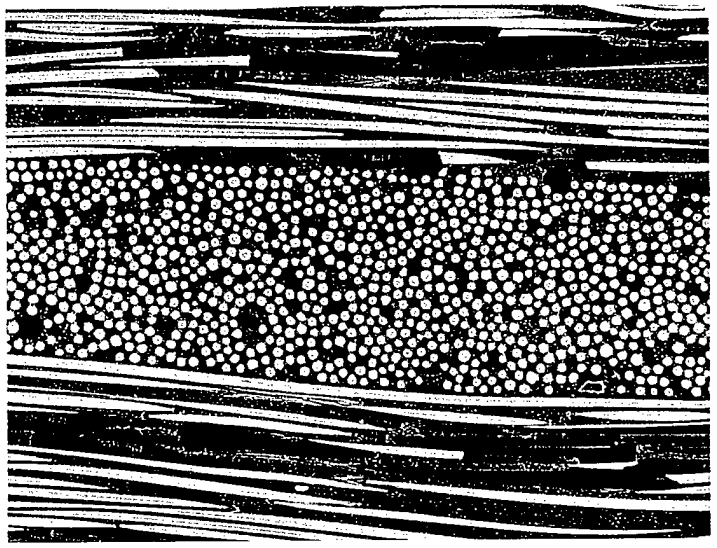

1000X

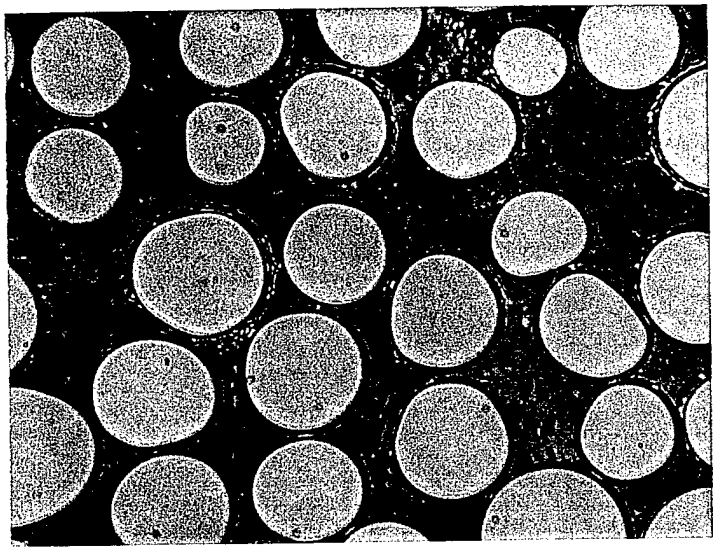

Mid-tow 5400X

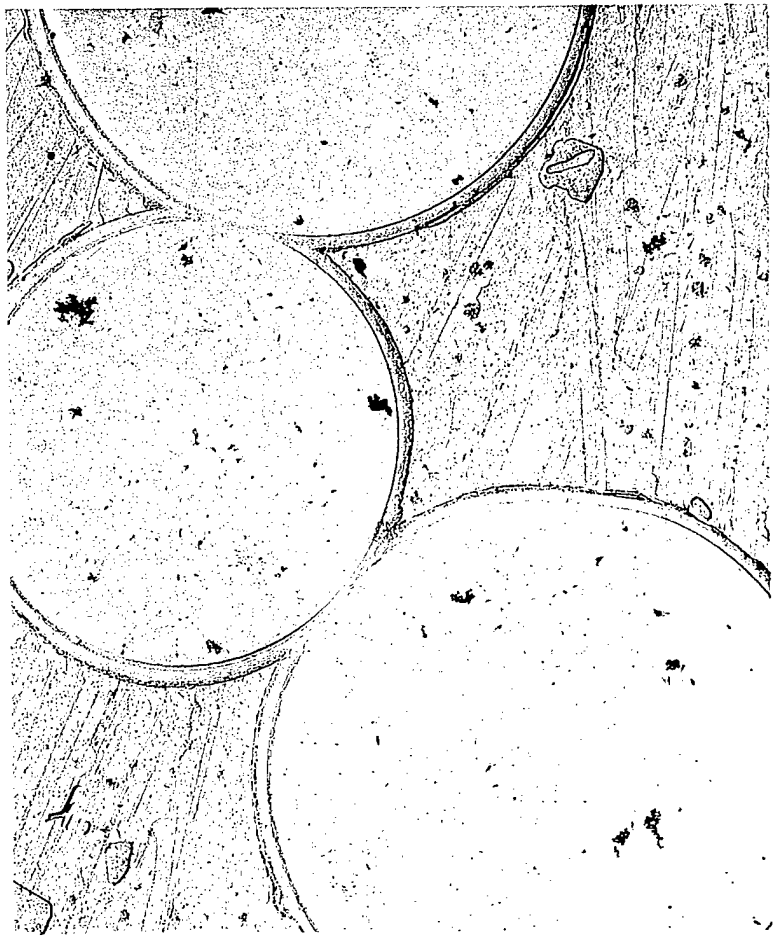

3.0μ

Fig. 1

UNITED TECHNOLOGIES RESEARCH CENTER

TRANSMISSION ELECTRON MICROSCOPE LABORATORY

TEM CHARACTERIZATION OF 3M BMAS BN-COATED NICALON (0/90)FIBER COMPOSITE - #7-95-6 (As-ceramed) RT σ = 93KSI (640MPa)

35000X

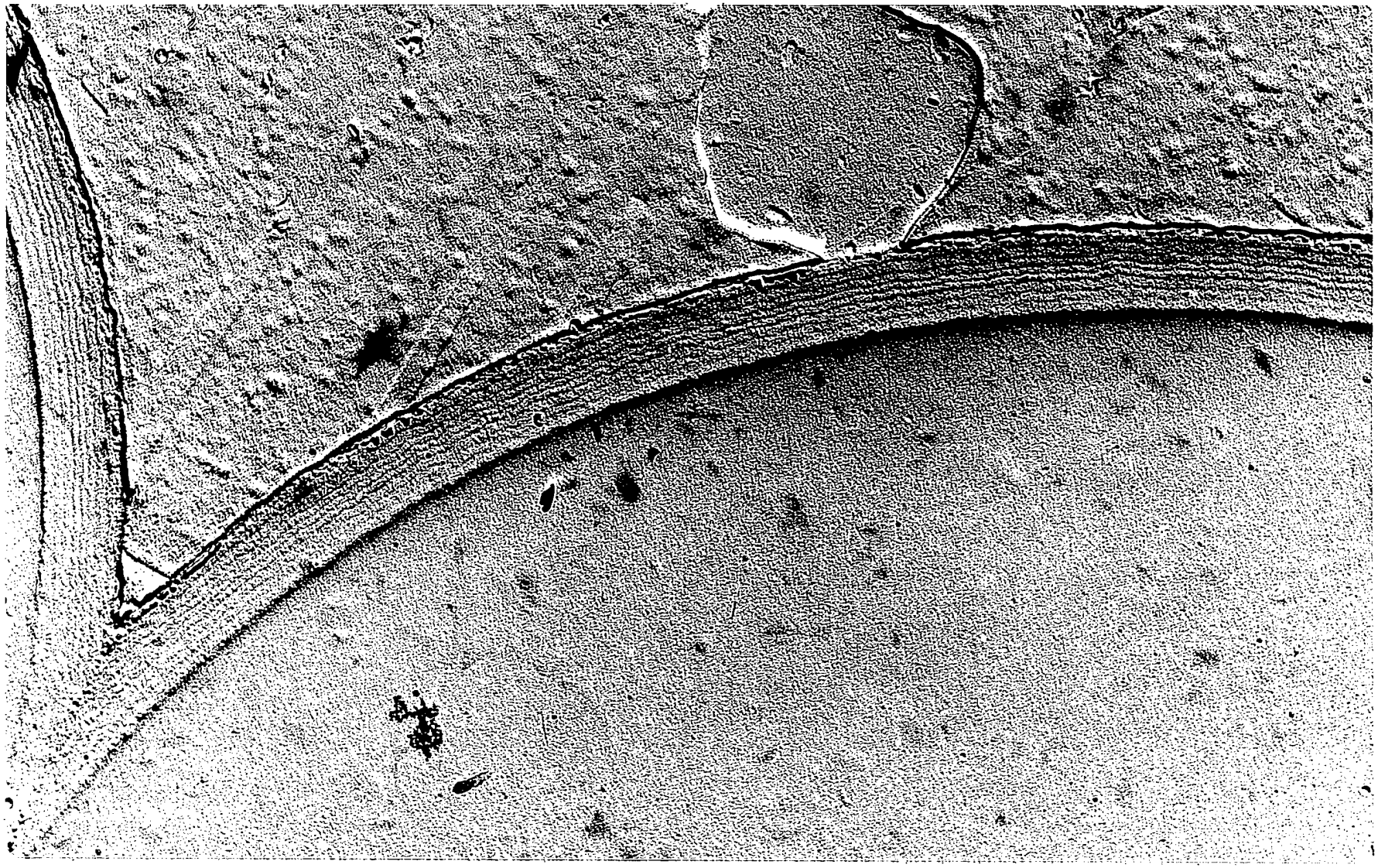

BN THICKNESS = 400nm

0.5μ

UNITED TECHNOLOGIES RESEARCH CENTER

TRANSMISSION ELECTRON MICROSCOPE LABORATORY

MMI 34421

Fig. 2

Increased Carbon Levels in 3M BN Coating and Layering of C/BN Decrease Matrix Diffusion and BN Crystallization During Composite Fabrication

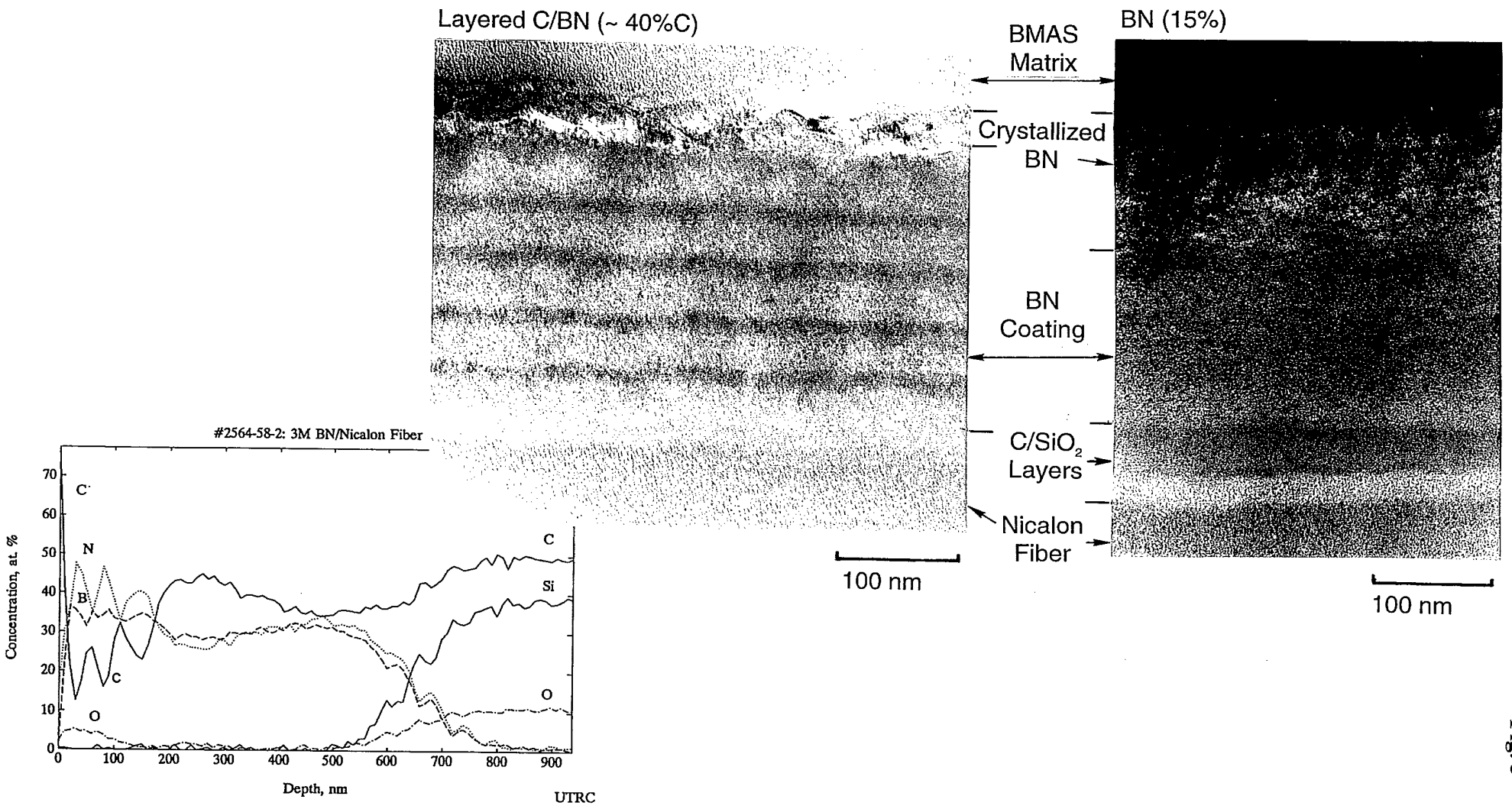

Fig. 3

HRTEM Thin Foil Characterization of BMAS Matrix/3M BN Coated Nicalon Fiber Composite (#7-95)

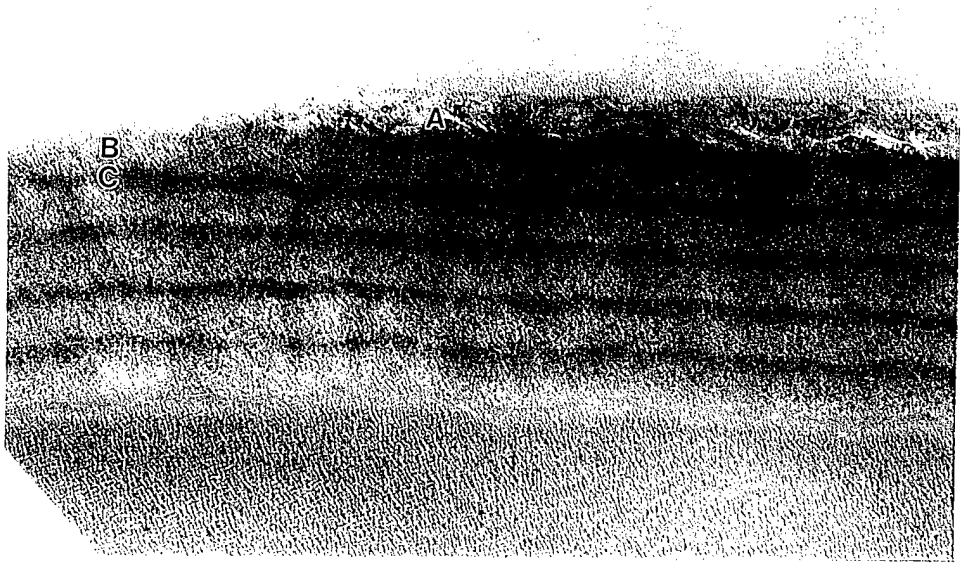

Overall view of multilayered BN-coating

0.2μ

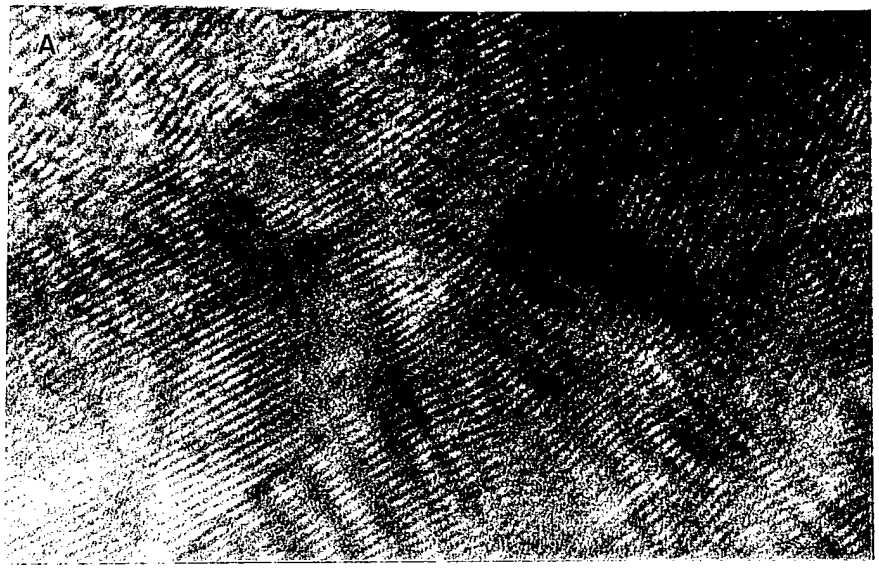

Enlarged view of recrystallized top layer of BN-coating

5nm

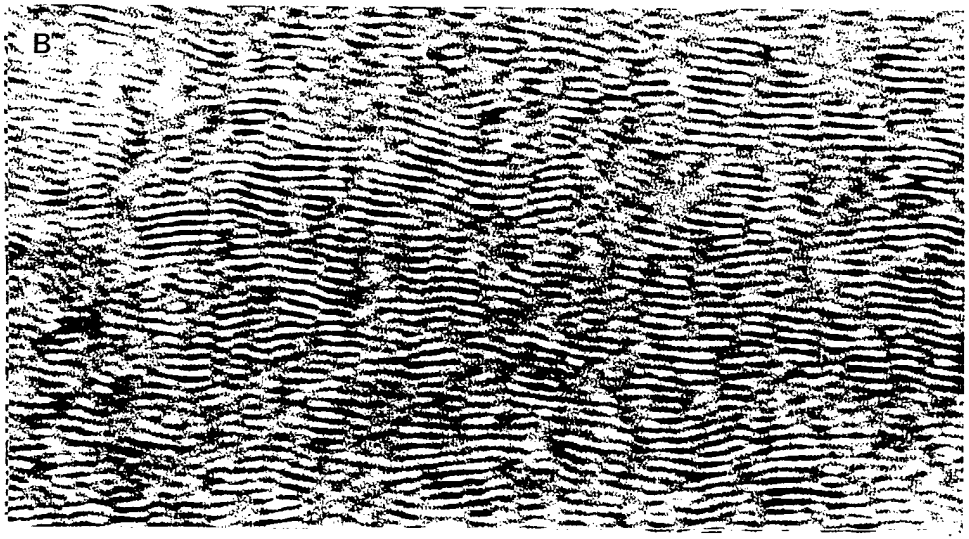

Turbostratic BN-coating (light band)

5nm

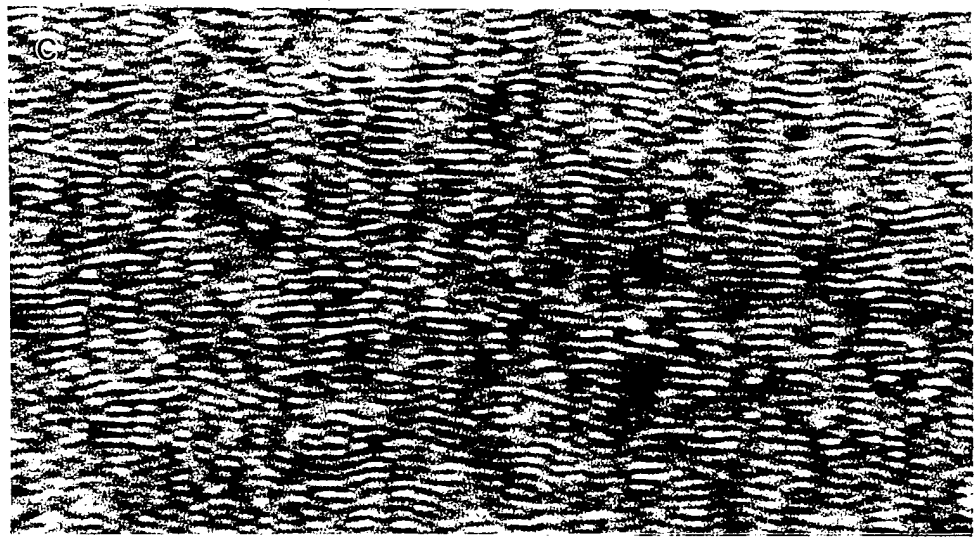

Turbostratic BN + C-coating (dark band)

5nm

Fig. 4

Crack Propagation Paths in Layered BN(+C) Coated Nicalon Fiber/BMAS Glass-Ceramic Matrix Composites

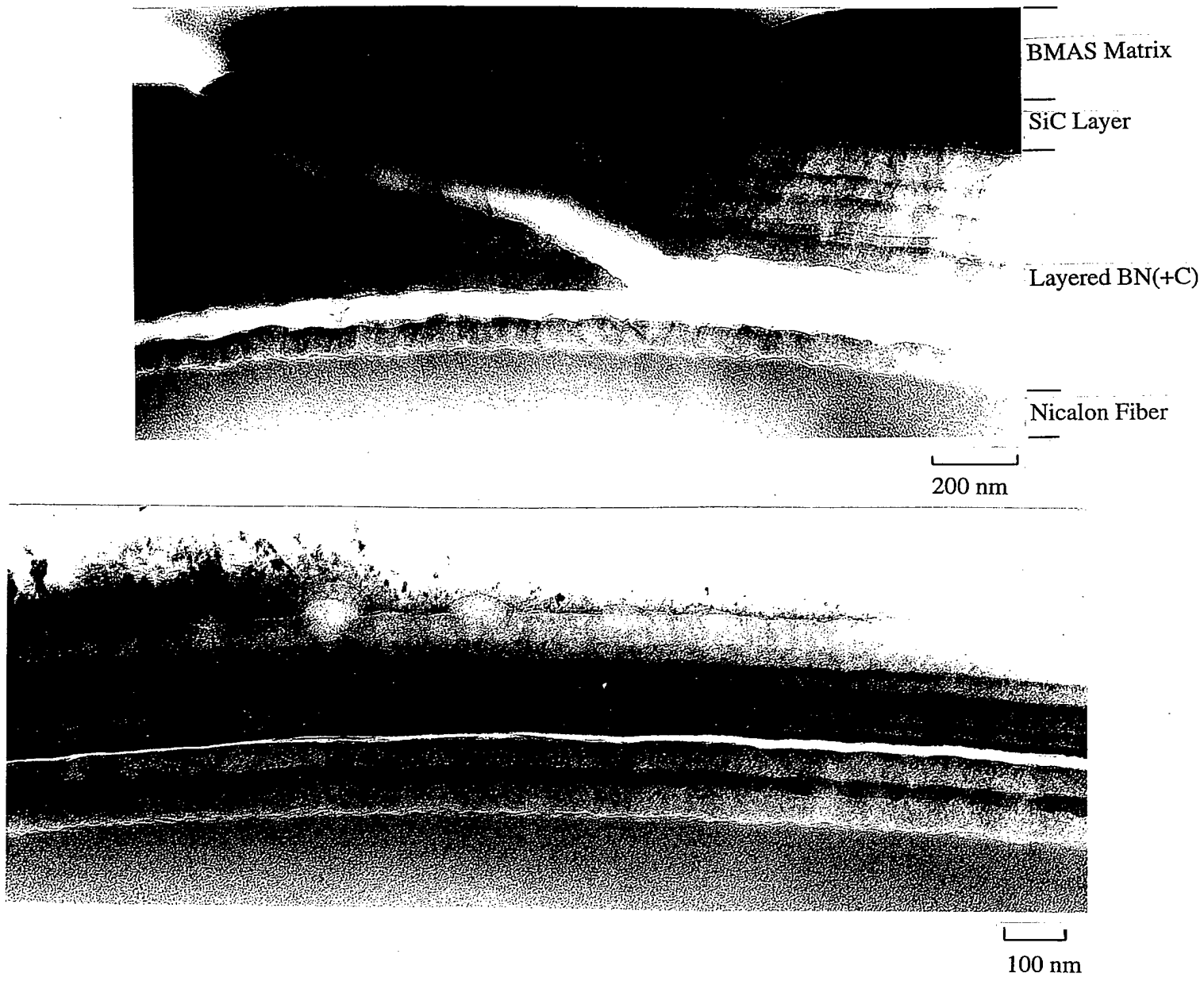

Fig. 5

BMAS Matrix/BN & SiC/BN Coated Nicalon Fiber Composite (0/90°) Tensile Testing at 550°C and 1100°C

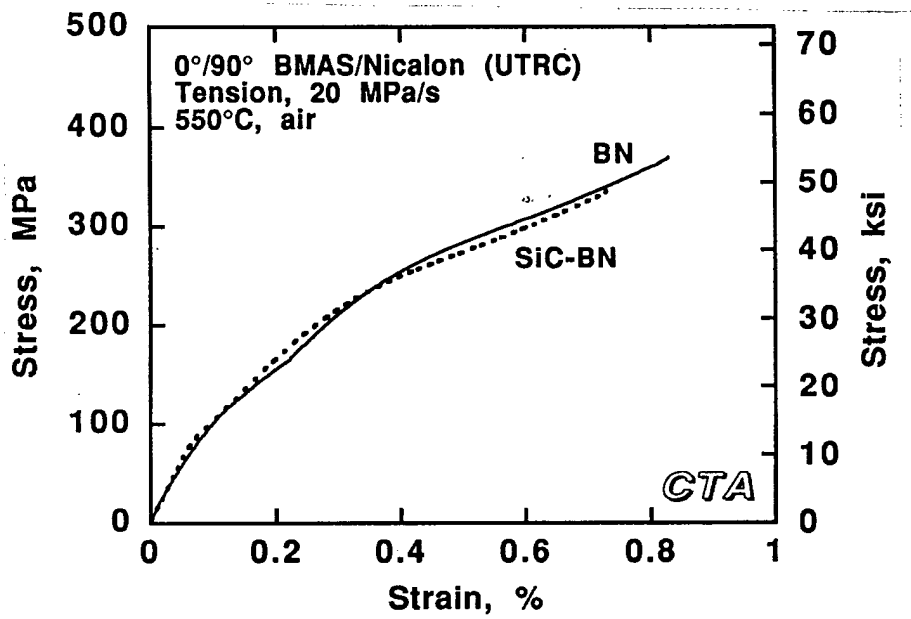

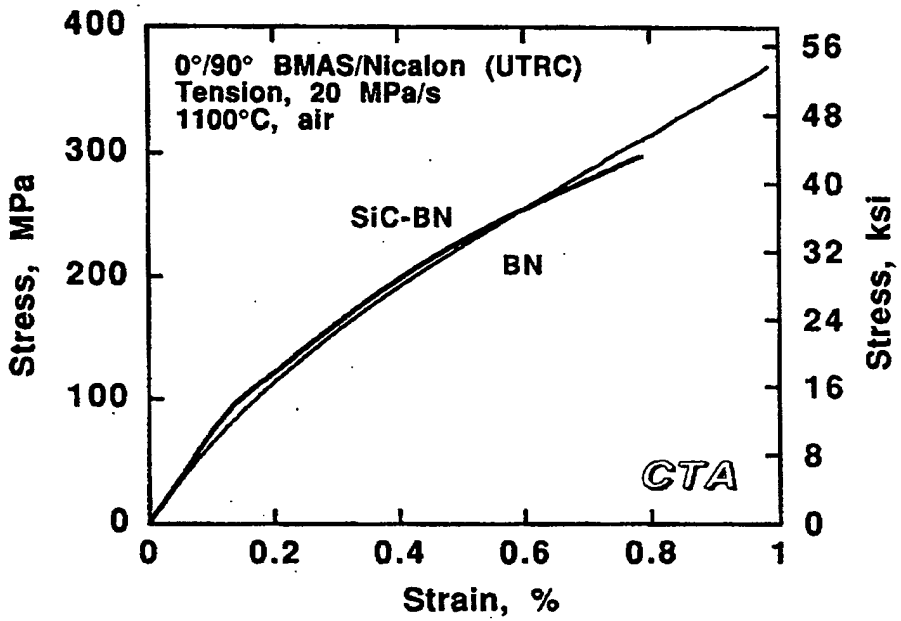

Fig. 6

BMAS Matrix/BN & SiC/BN Coated Nicalon Fiber Composite (0/90°) 550°C Tensile Results After 500°C Fatigue

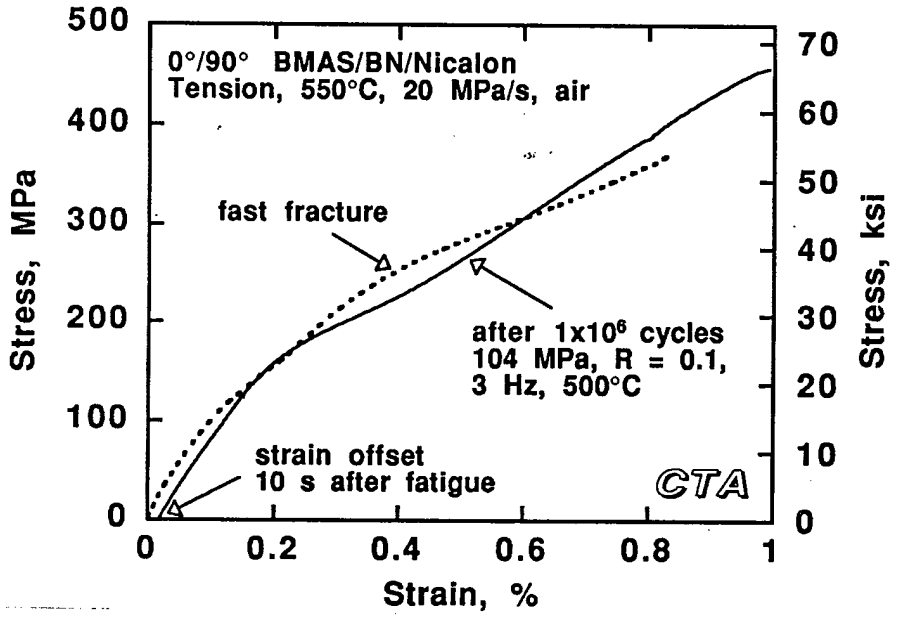

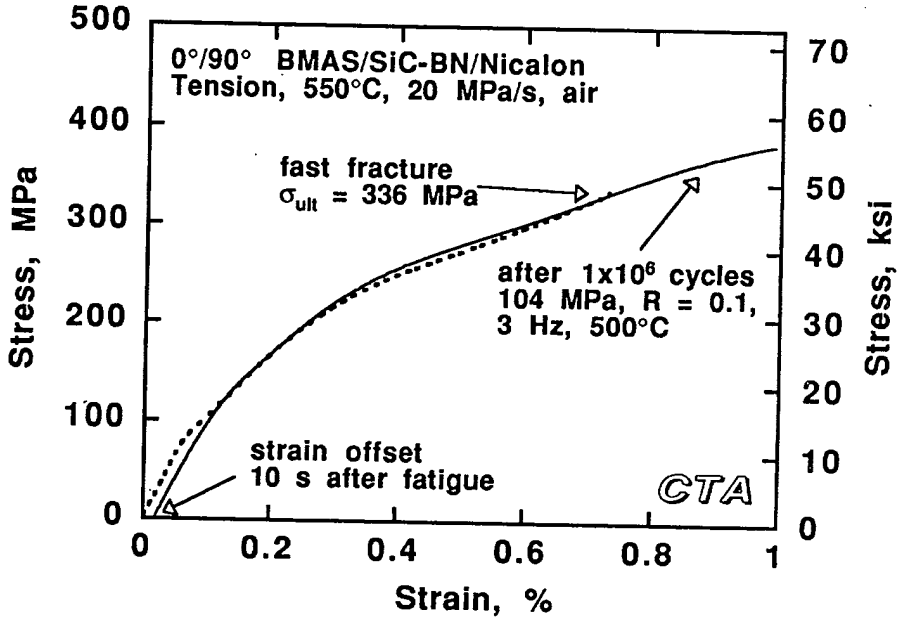

Fig. 7

BMAS Matrix/BN & SiC/BN Coated Nicalon Fiber Composite (0/90°) 1100°C Tensile Results After 1100°C Fatigue

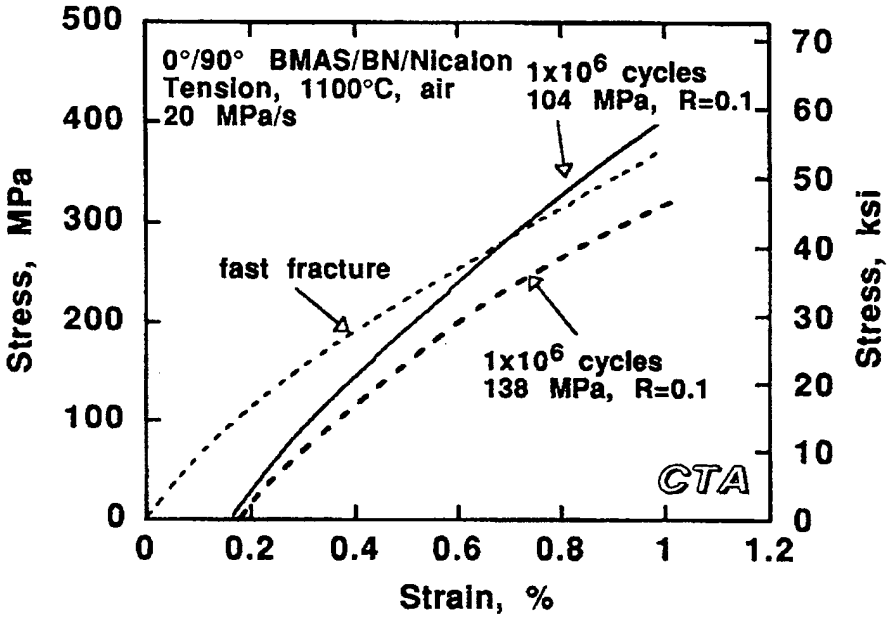

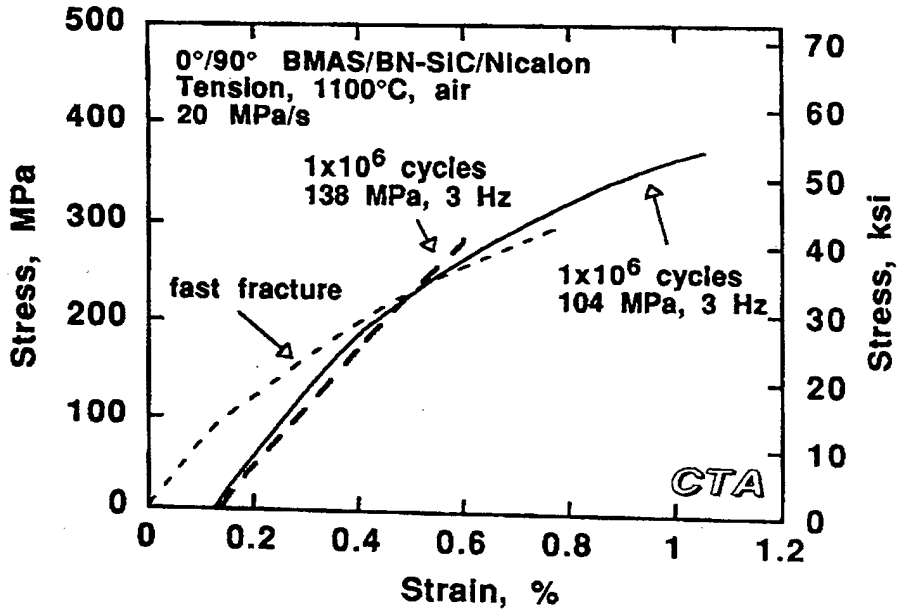

Fig. 8

BMAS Matrix/BN/Nicalon Fiber Composite #29-95-6 (0°/90°)

(500°C, 104 MPa, 10^6 cycle tensile fatigue, residual 500°C UTS = 457 MPa, ε_f =0.99%)

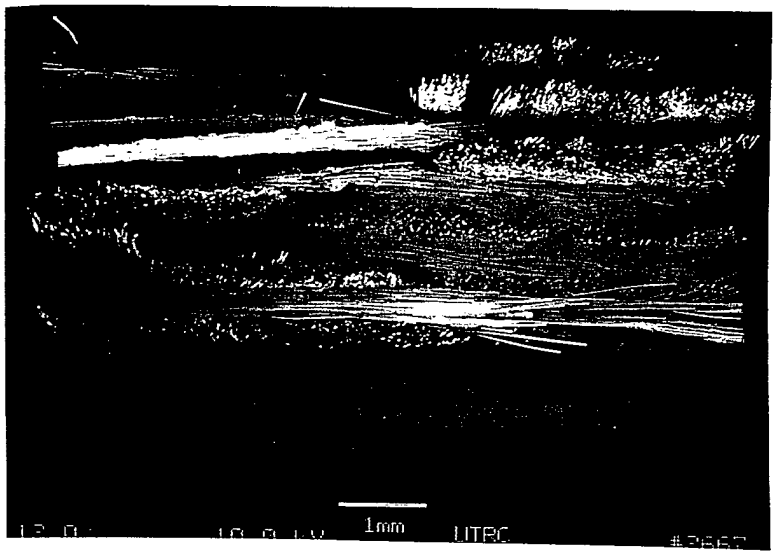

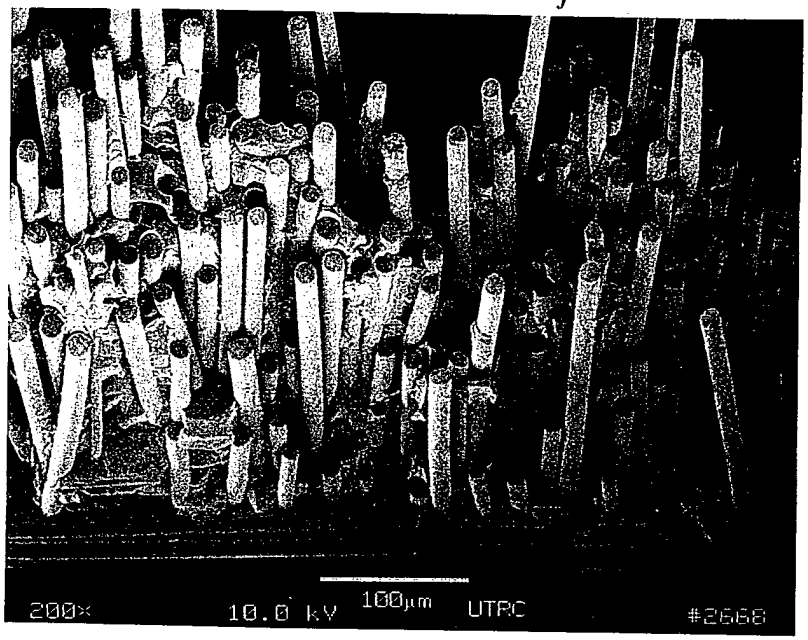

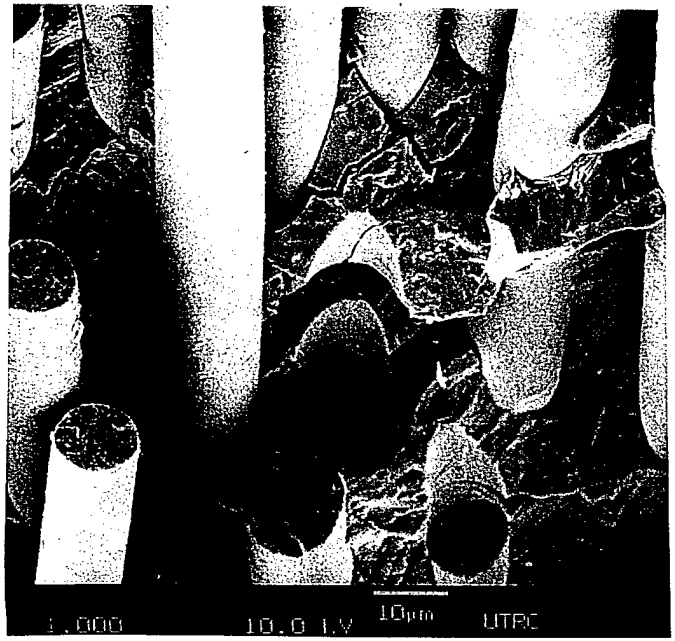

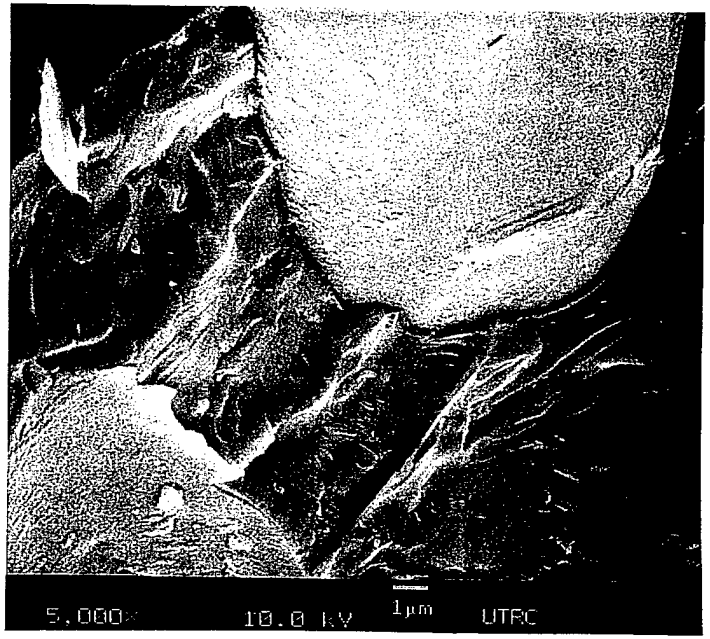

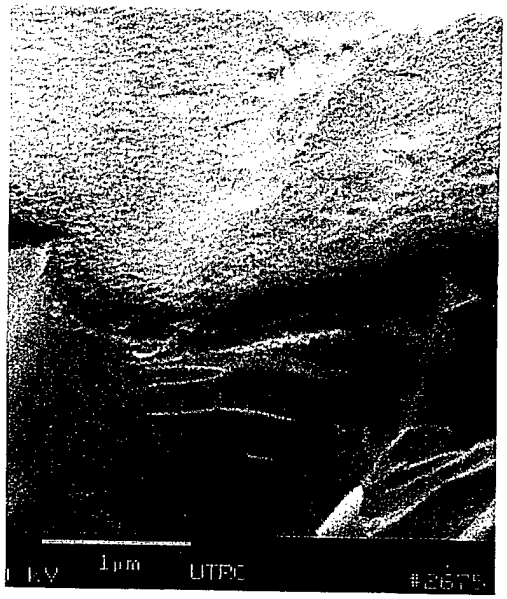

Fig. 9

BMAS Matrix/SiC/BN/Nicalon Fiber Composite #28-95-6 (0°/90°)

(500°C, 104 MPa, 10^6 cycle tensile fatigue, residual 550°C UTS = 384 MPa, ε_f = 0.98%)

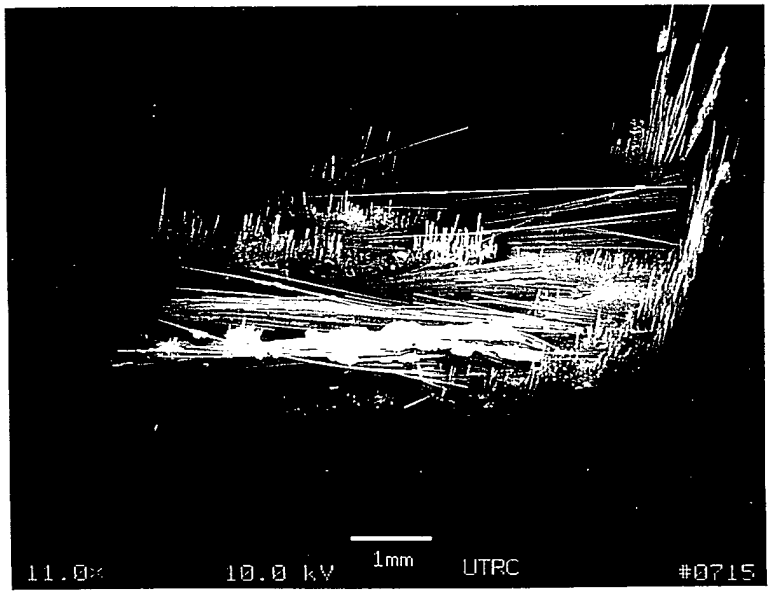

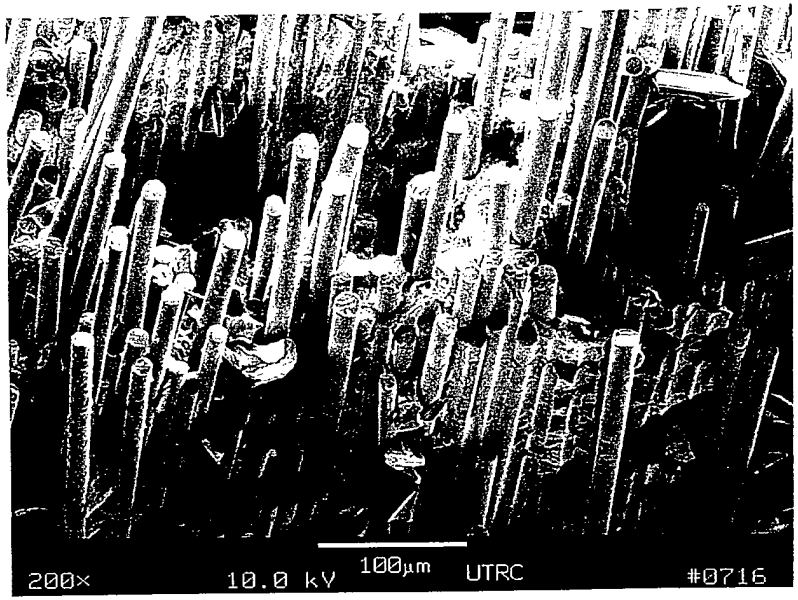

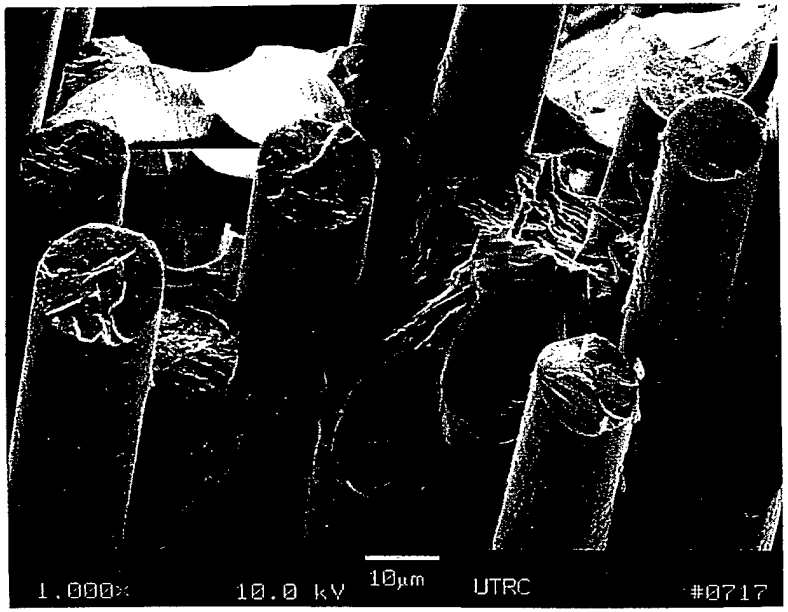

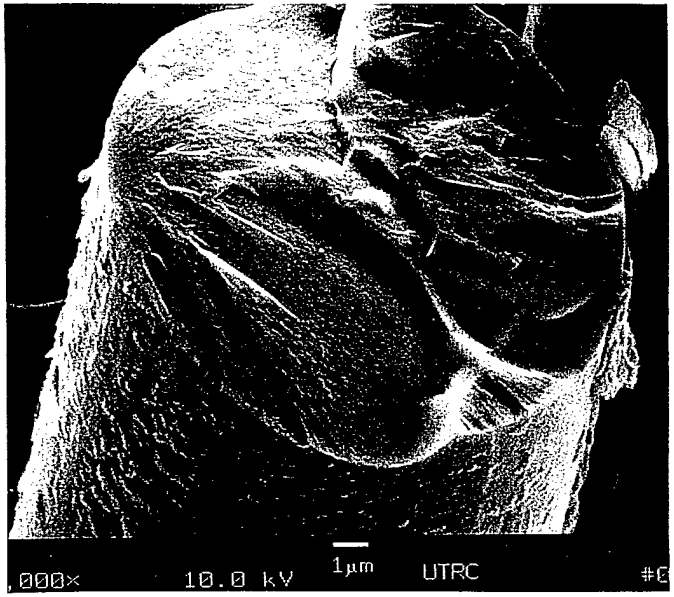

Fig. 10

BMAS Matrix/BN/Nicalon Fiber Composite #29-95-7 (0°/90°)

(1100°C, 104 MPa, 10^6 cycle tensile fatigue, residual 1100°C UTS = 398 MPa, $\varepsilon_f = 0.98\%$)

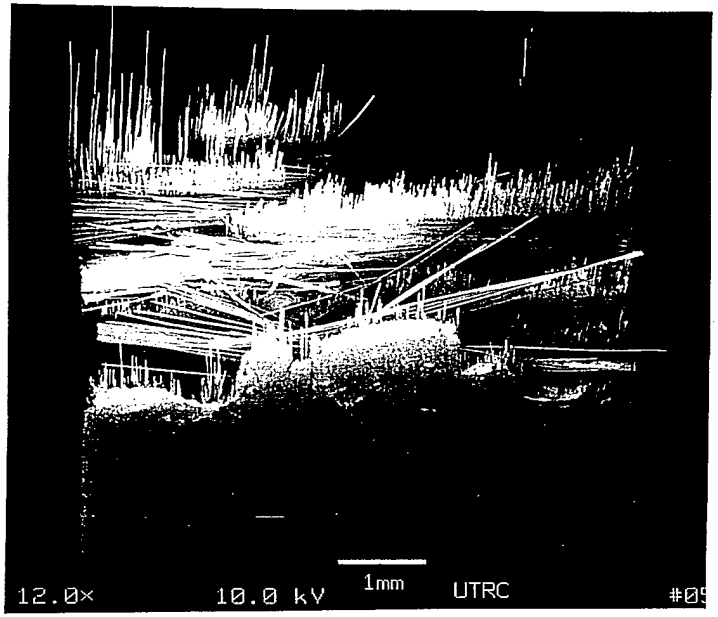

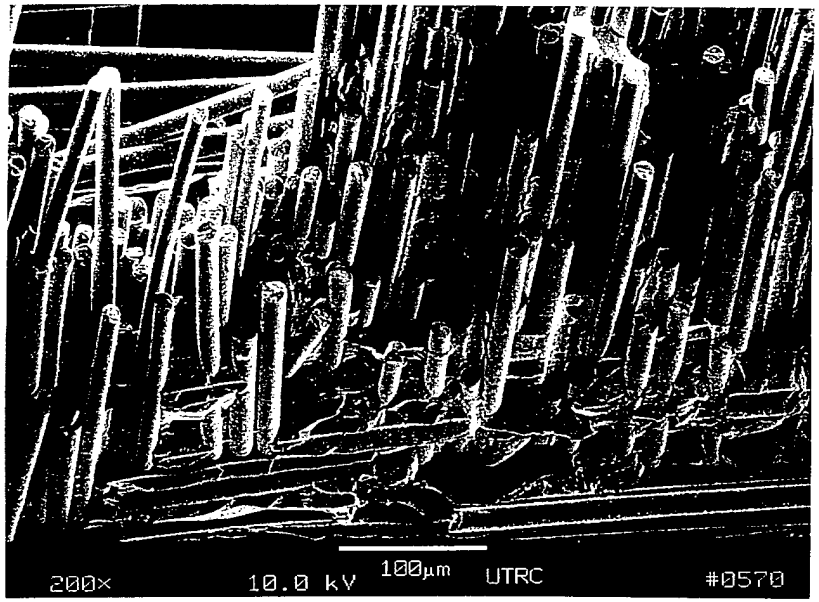

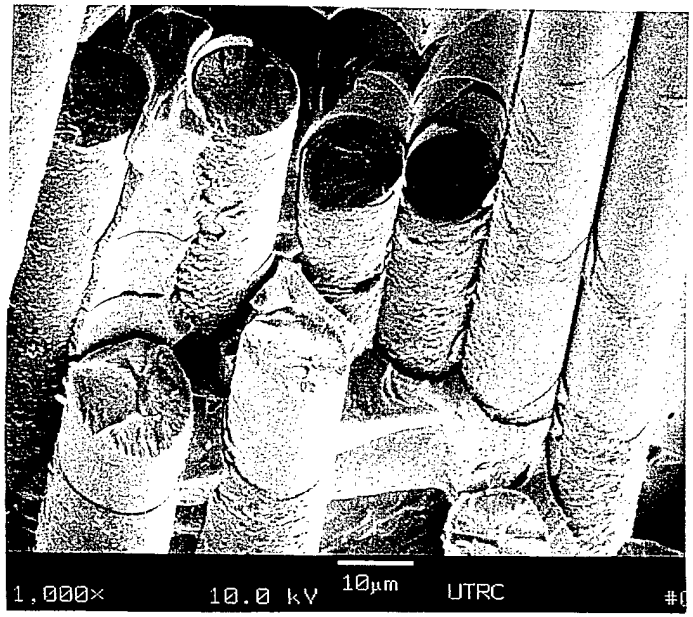

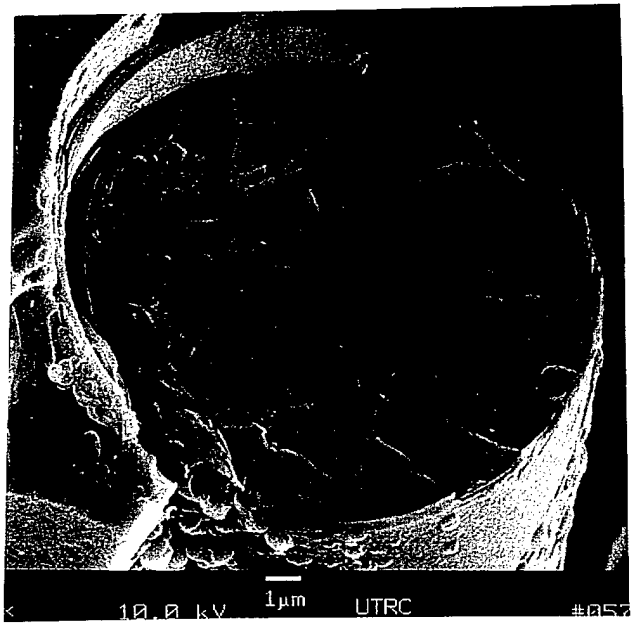

Fig. 11

BMAS Matrix/SiC/BN/Nicalon Fiber Composite #28-95-7 (0°/90°)

(1100°C, 104 MPa, 10^6 cycle tensile fatigue, residual 1100°C UTS = 372 MPa, ε_f = 1.06%)

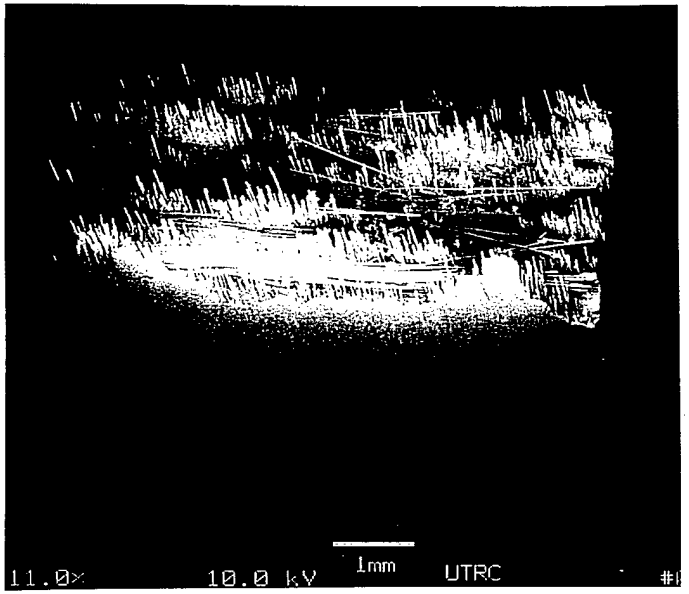

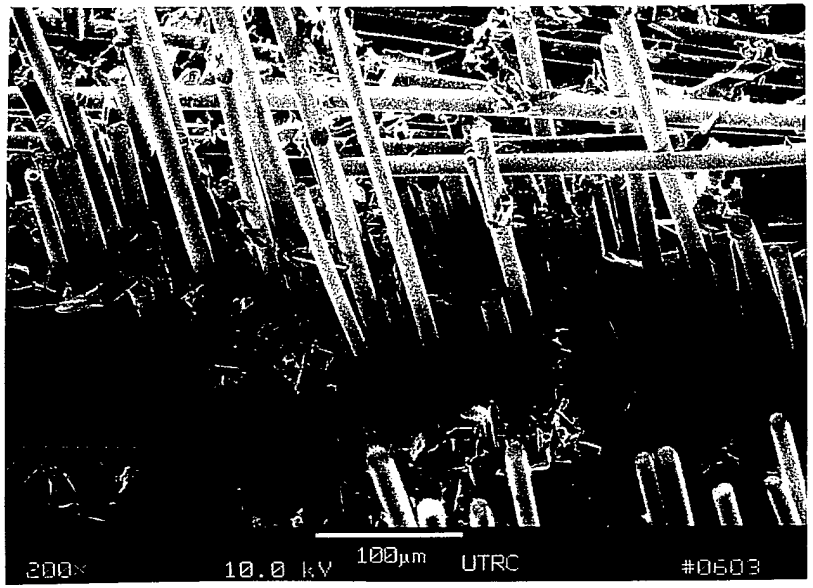

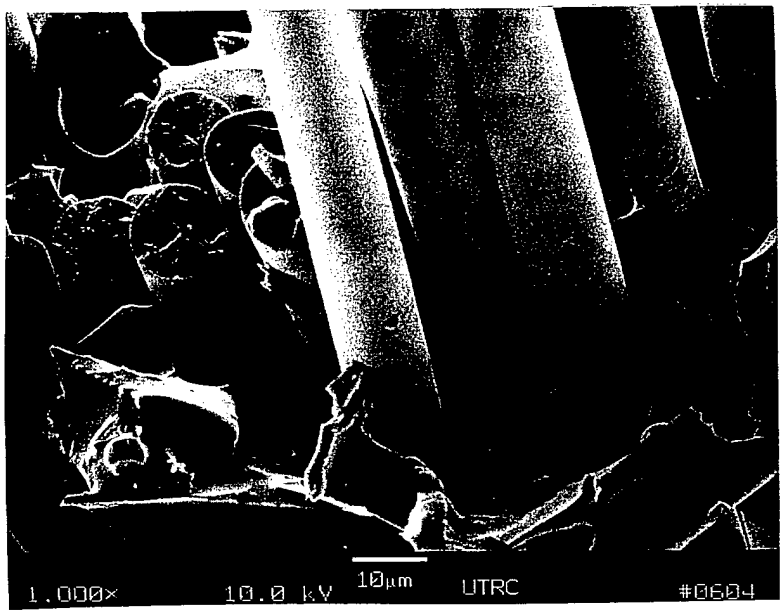

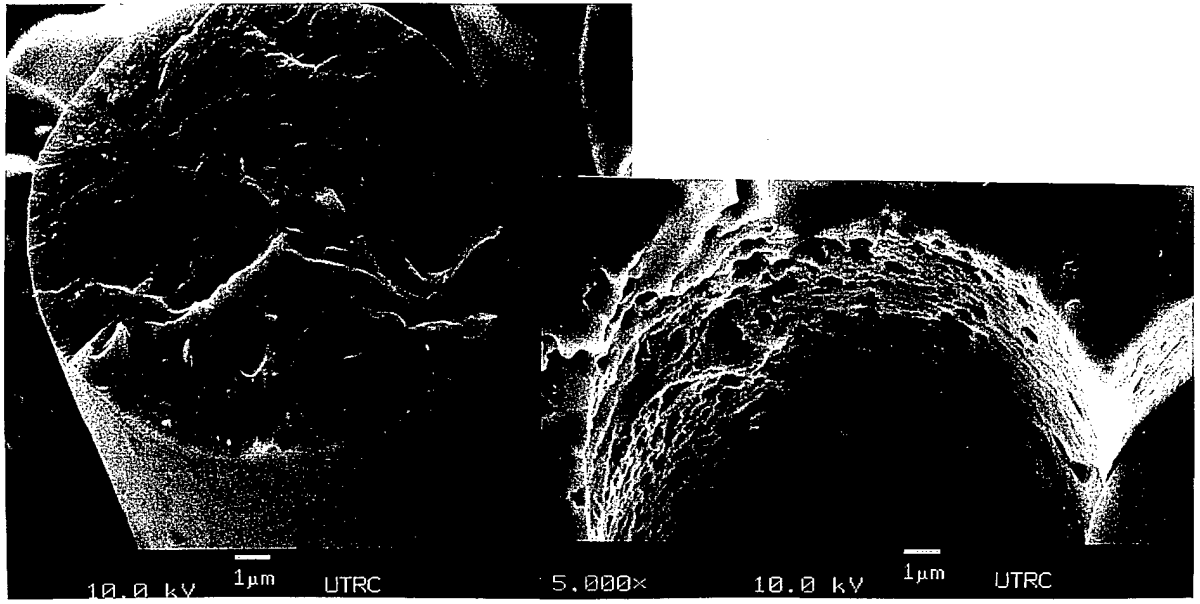

fig. 12

BMAS Matrix/BN/Nicalon Fiber Composite #29-95-8 (0°/90°)

(1100°C, 138 MPa, 10^6 cycle tensile fatigue, residual 1100°C UTS = 323 MPa, ε_f =1.00%)

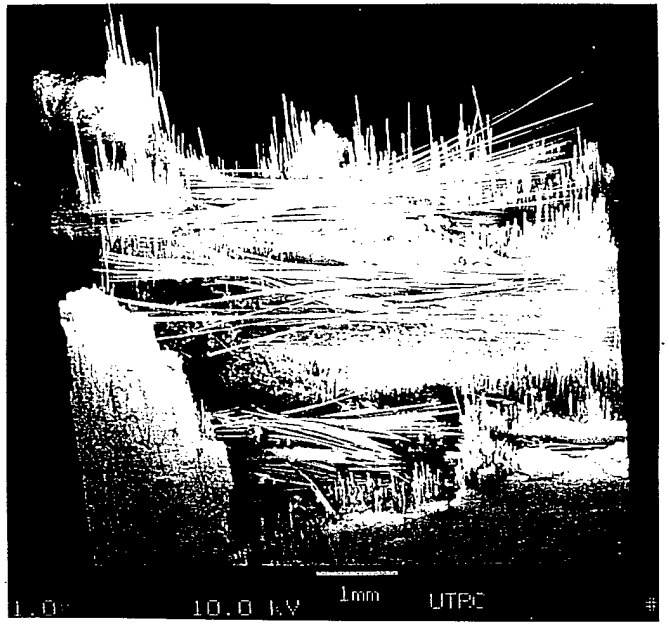

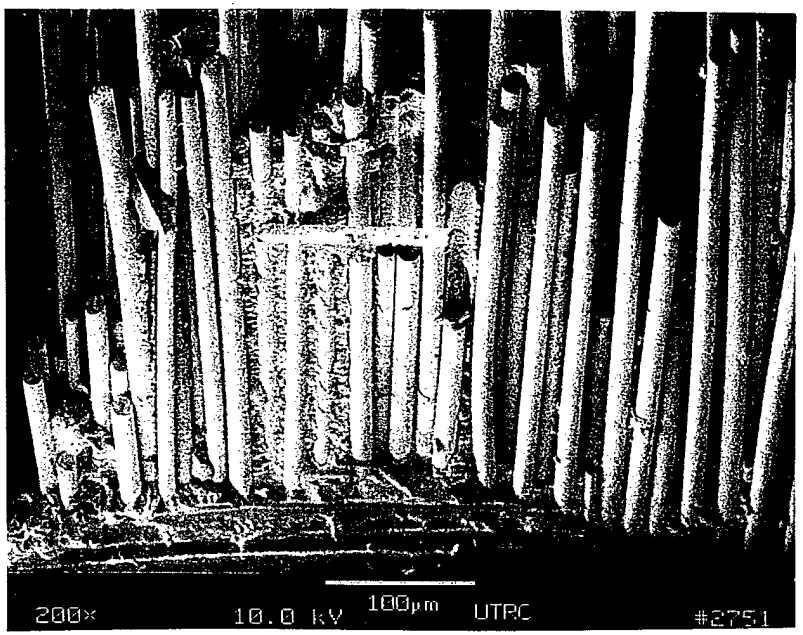

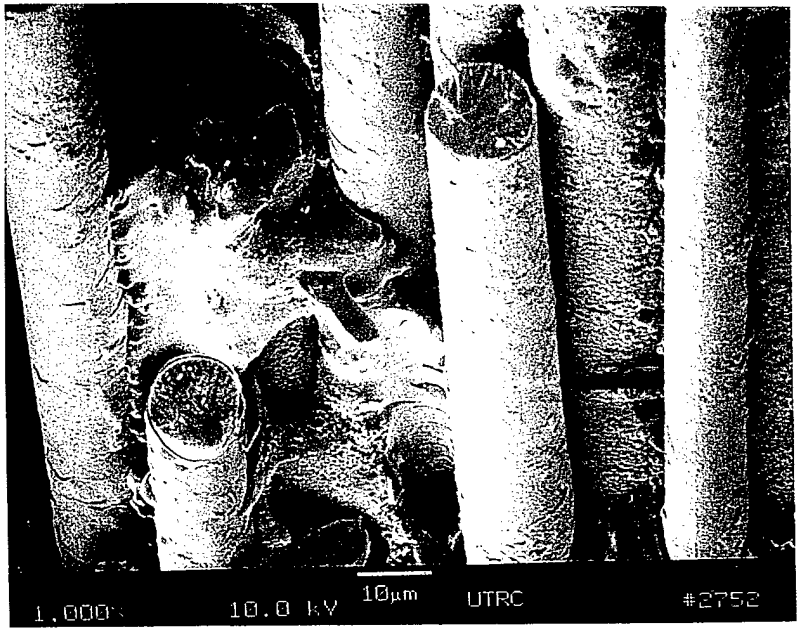

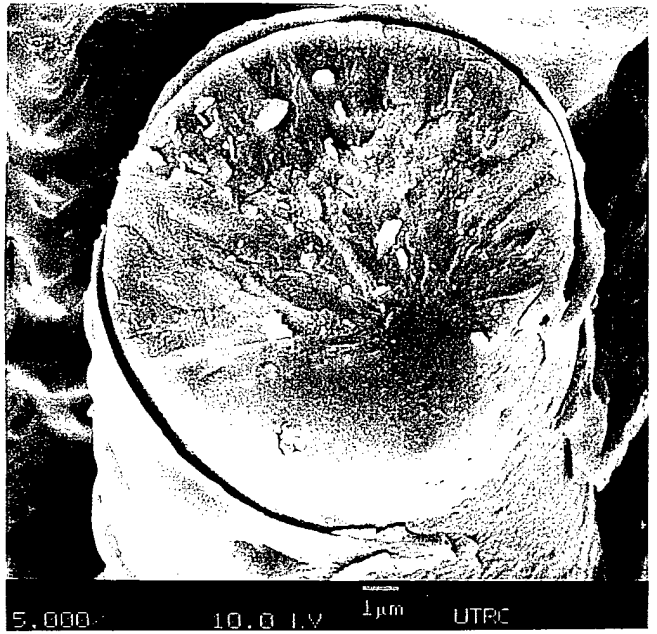

Fig. 13

BMAS Matrix/SiC/BN/Nicalon Fiber Composite #28-95-8 (0°/90°)

(1100°C, 138 MPa, 10^6 cycle tensile fatigue, residual 1100°C UTS = 284 MPa, ε_f = 0.56%)

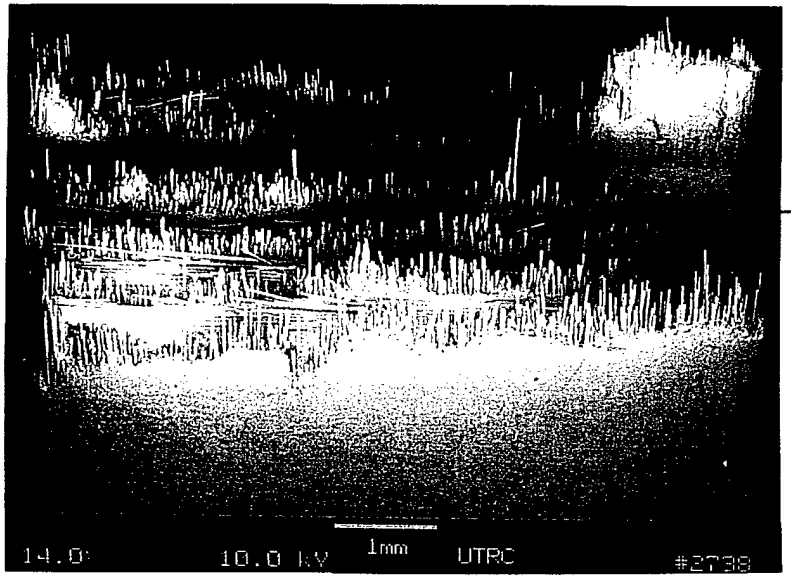

Brittle Region

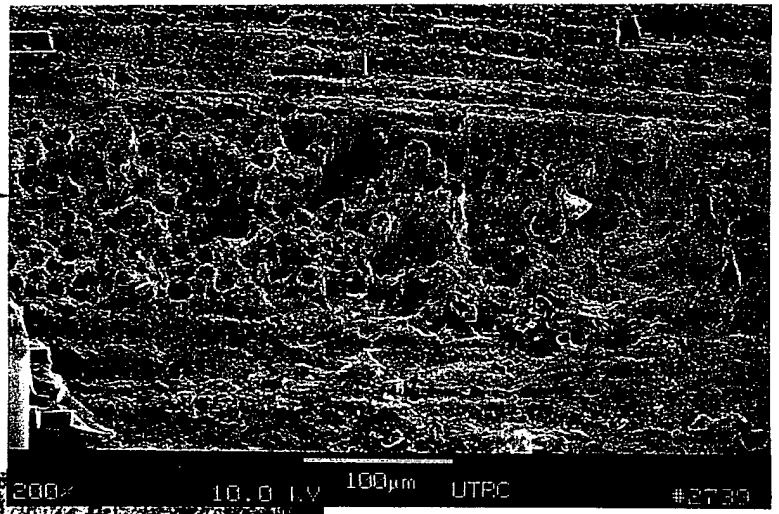

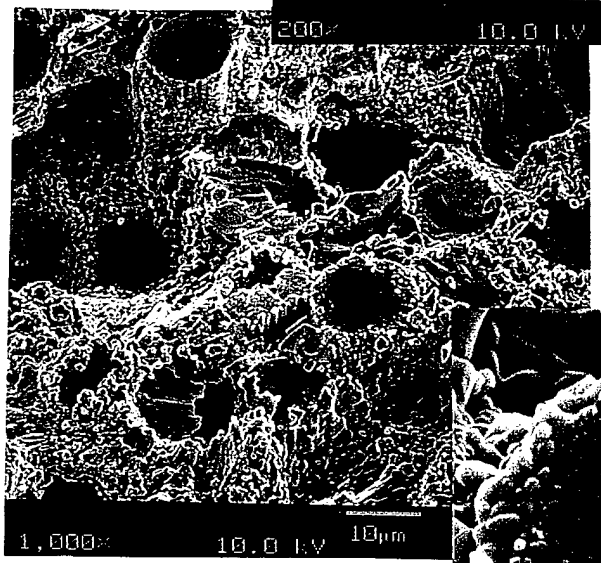

Tough Region

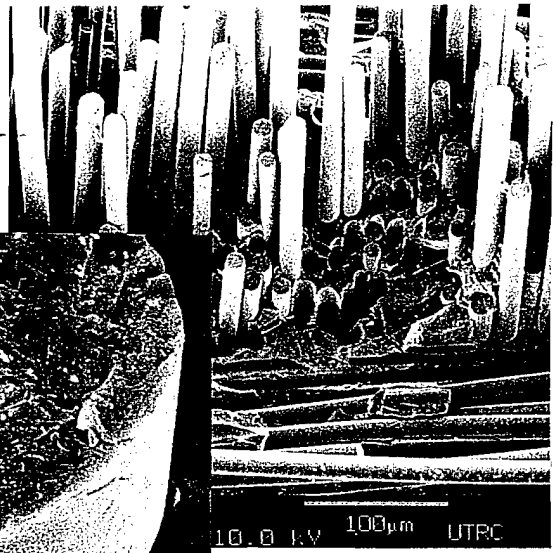

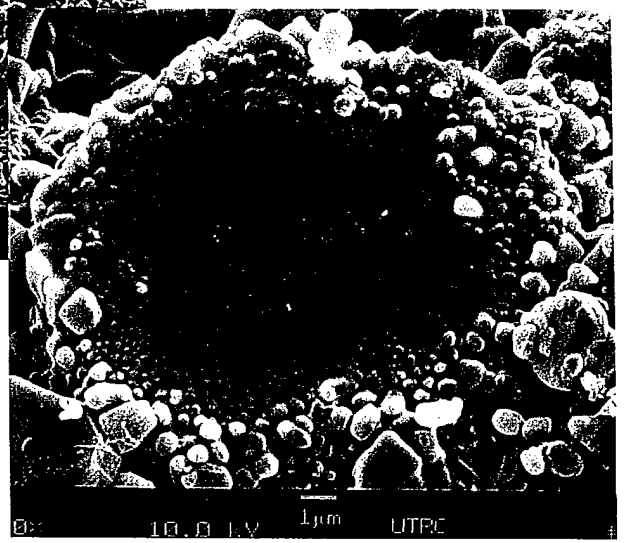

Fig. 14

BMAS Matrix/BN/Nicalon Fiber Composite #29-95-8 (0°/90°)

(1100°C, 138 MPa, 10^6 cycle tensile fatigue, residual 1100°Ç UTS = 323 MPa, εf = 1.00%)

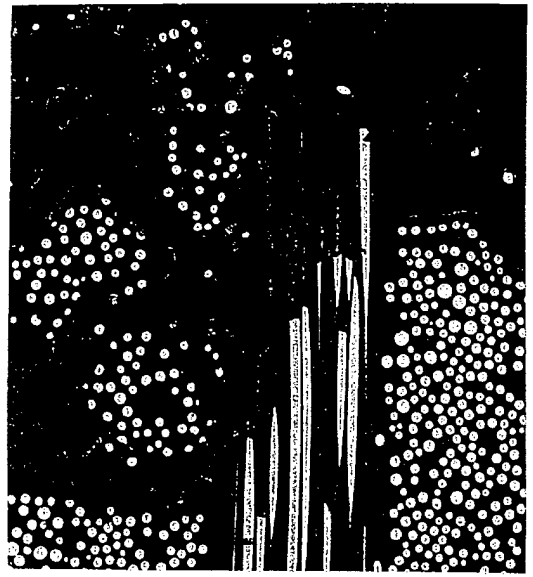

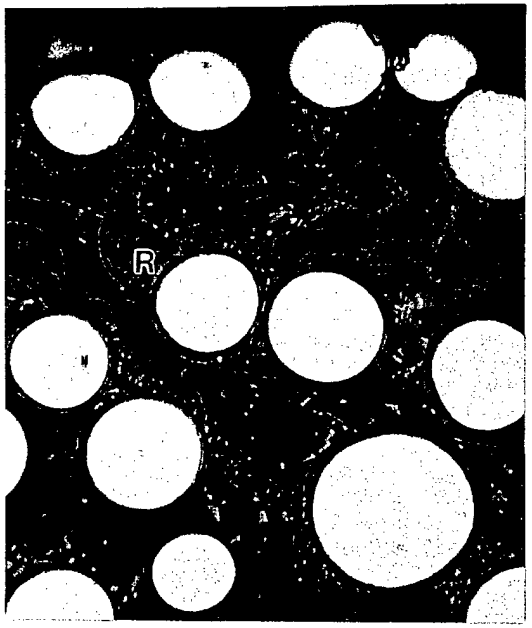

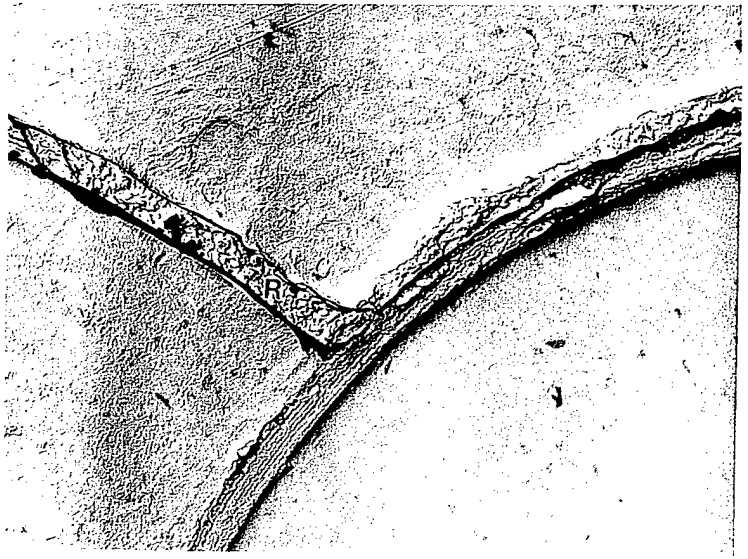

Fig. 15

BMAS Matrix/SiC/BN Coated Nicalon Fiber Composite #56-95-1

[700° UTS = 275 MPa (40 ksi), εf = 0.89%]

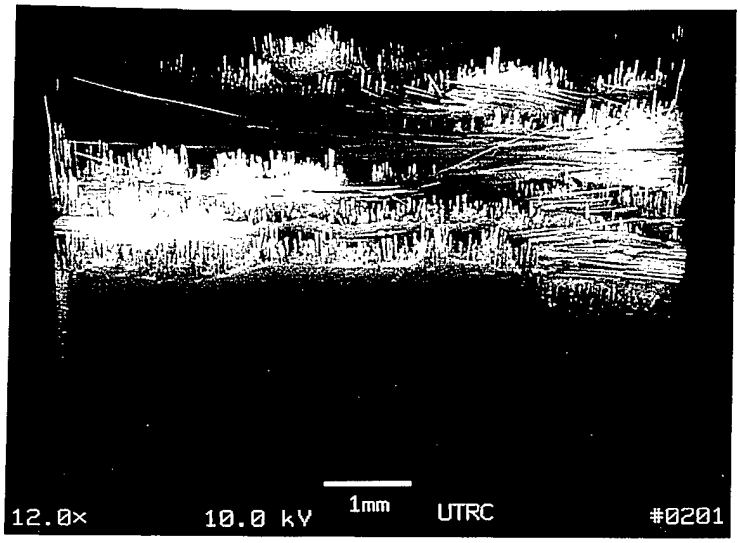

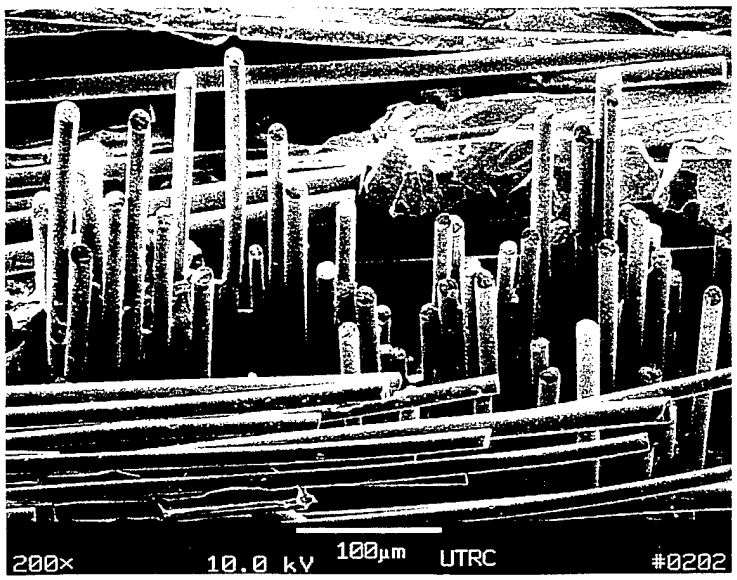

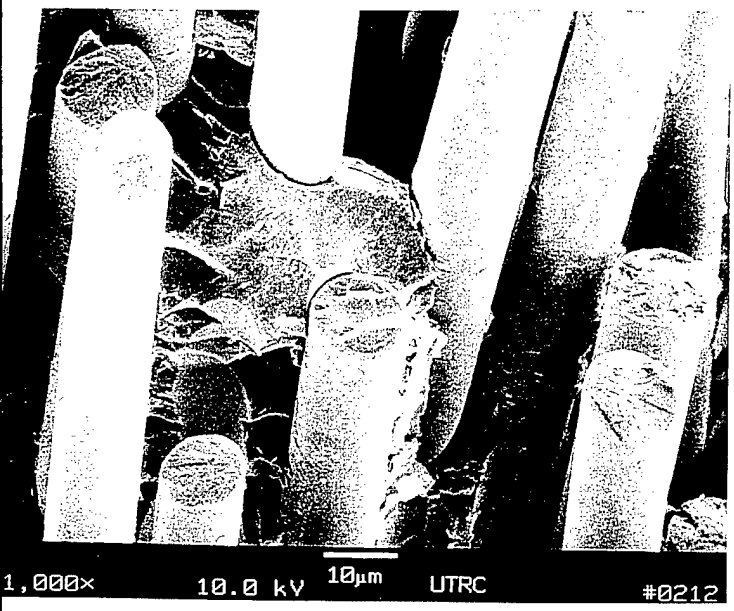

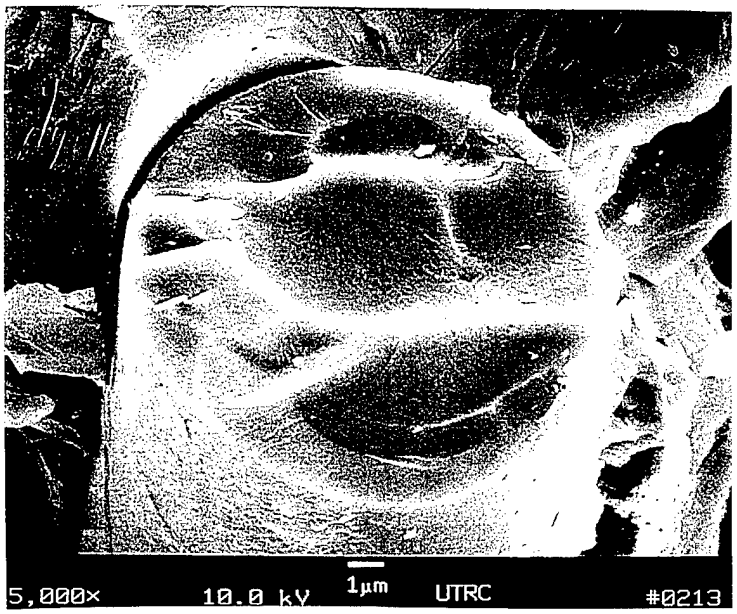

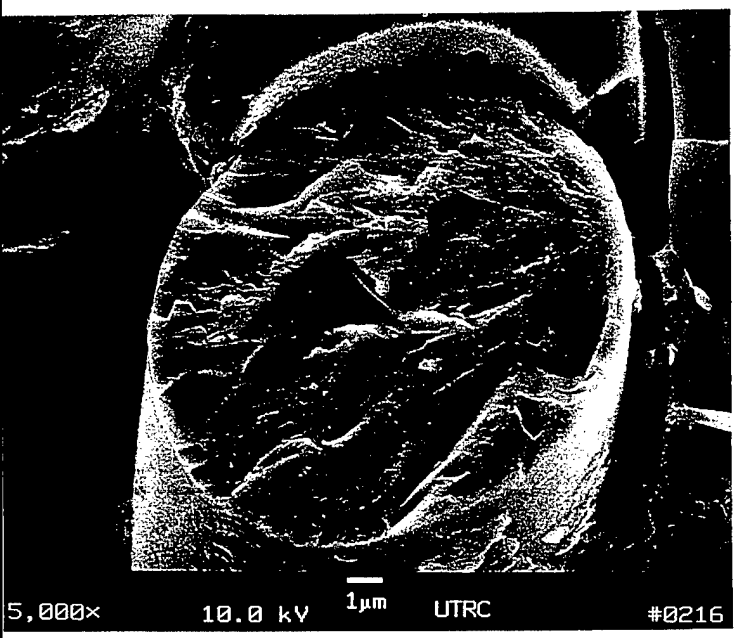

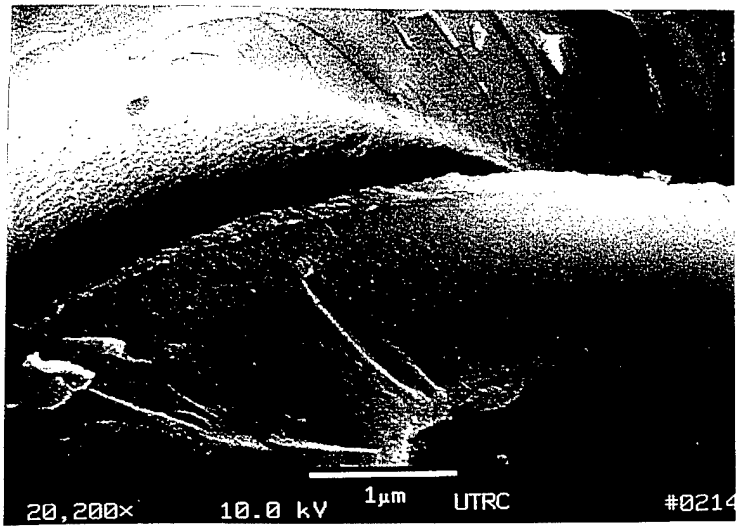

BMAS Matrix/SiC/BN Nicalon Fiber Composite #56-95-4

[900°C UTS = 260 MPa (38 ksi), ε_f = 0.81%]

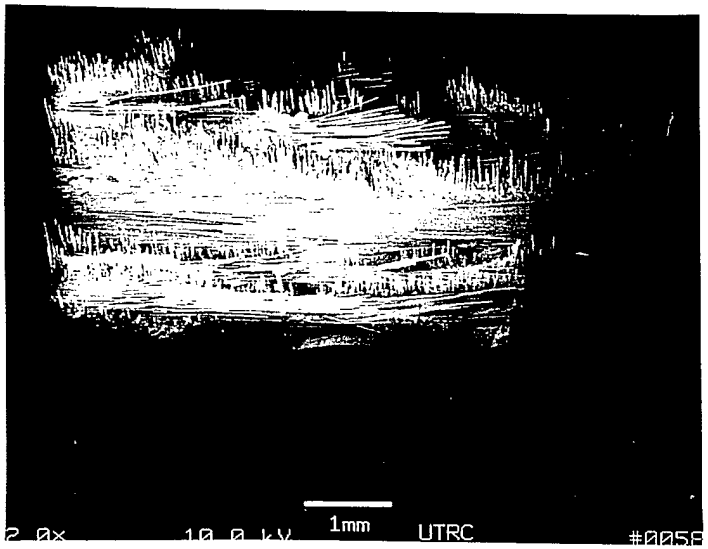

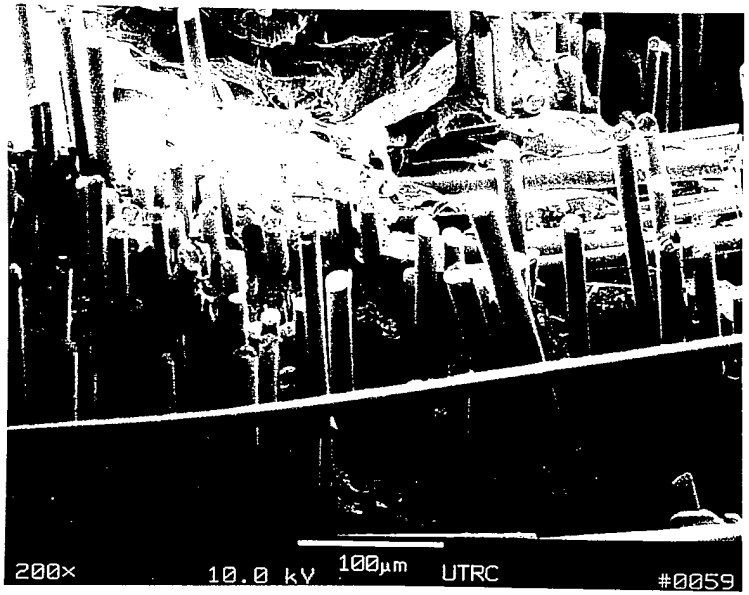

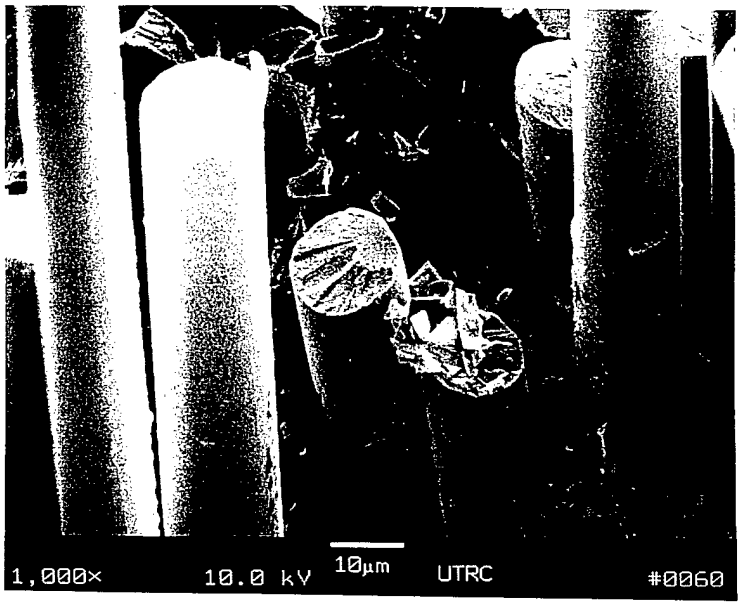

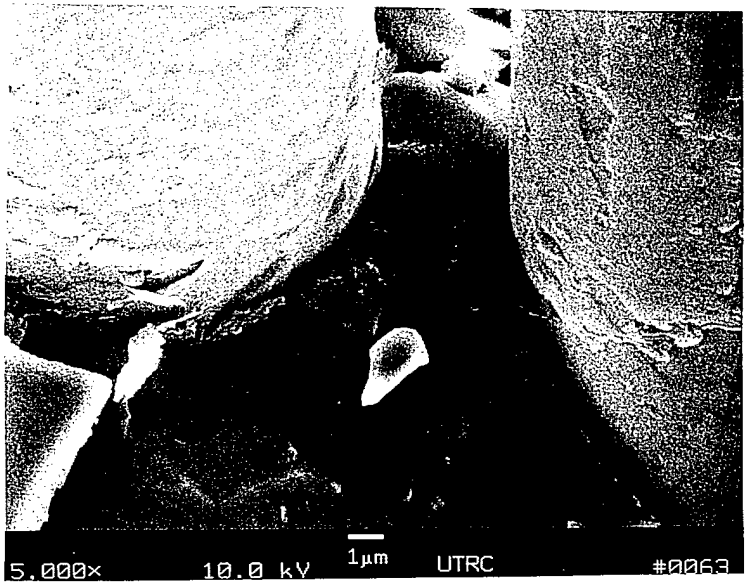

Fig. 17

BMAS Matrix/SiC/BN Nicalon Fiber Composite #56-95-2

[700°C tensile fatigue, 104 MPa (15 ksi), 10^6 cycle runout]

[residual UTS = 269 MPa (39 ksi), ε_f = 0.73%]

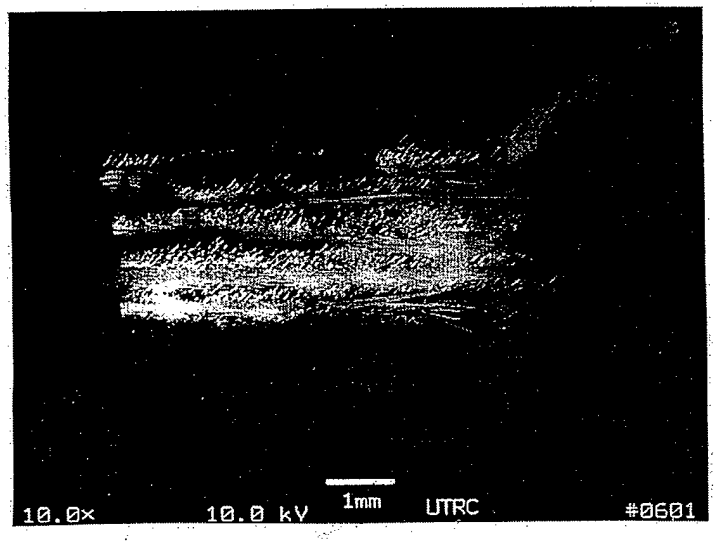

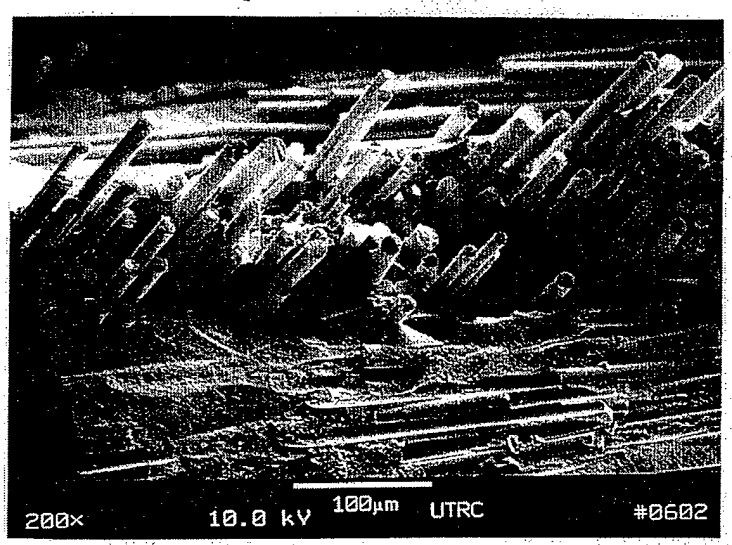

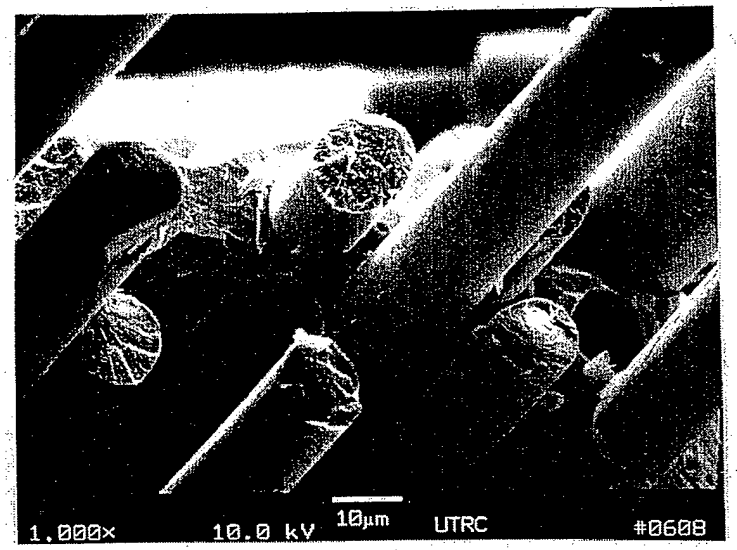

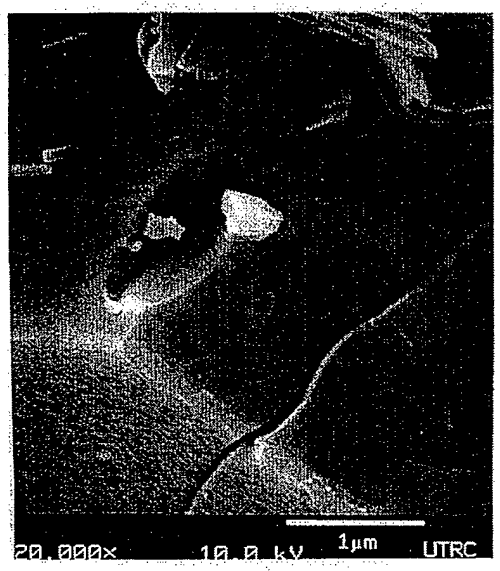

Fig. 18

BMAS Matrix/SiC/BN Nicalon Fiber Composite #56-95-5

[900°C tensile fatigue, 104 MPa (15 ksi), 10^6 cycles to runout]
(Residual 900°C UTS = 285 MPa (41 ksi), ε_f = 0.99%)

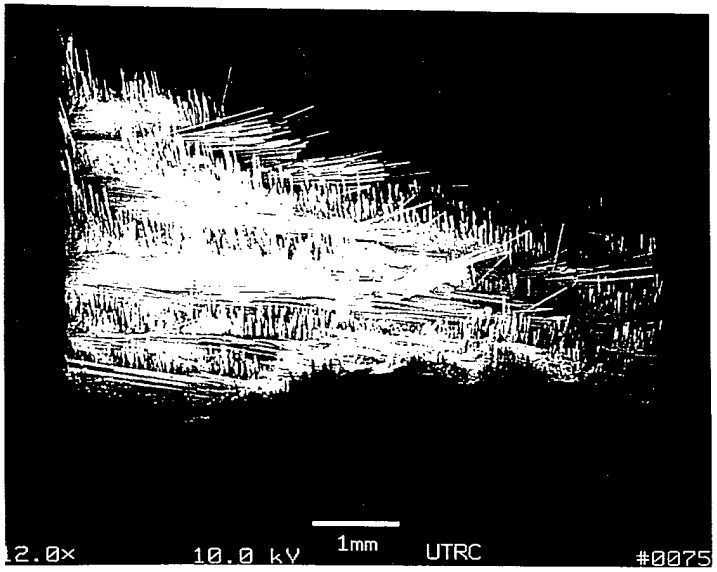

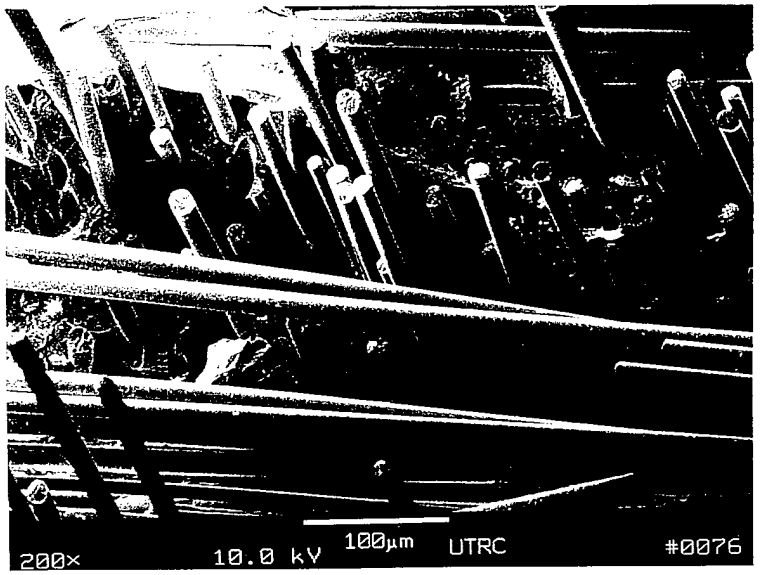

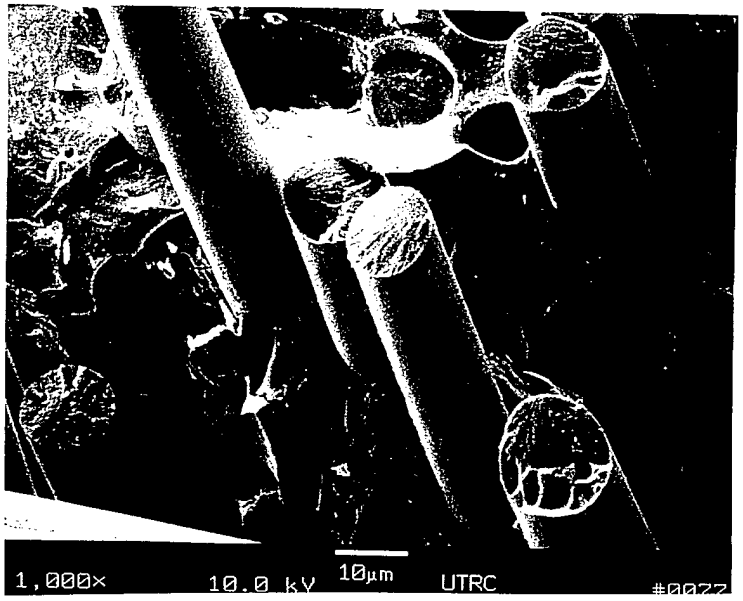

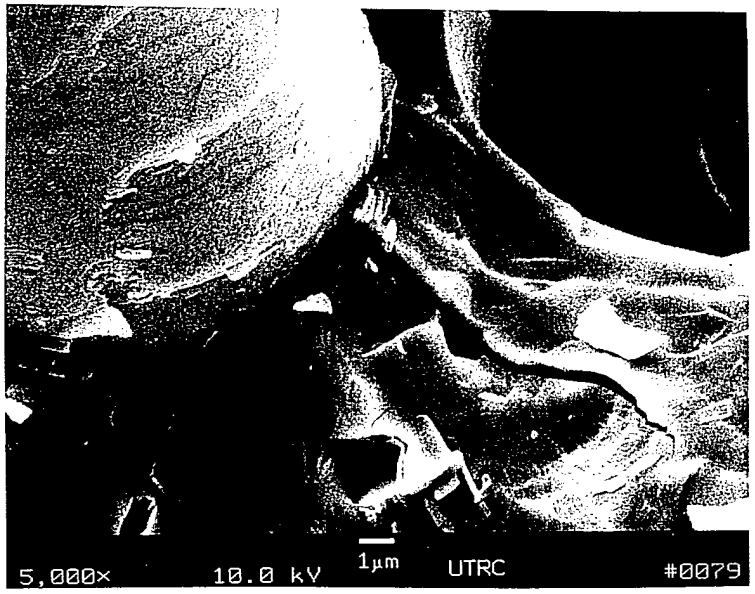

Fig. 19

BMAS Matrix/SiC/BN Nicalon Fiber Composite #56-95-3

[700°C tensile fatigue, 138 MPa (20 ksi), 349,216 cycles to failure]

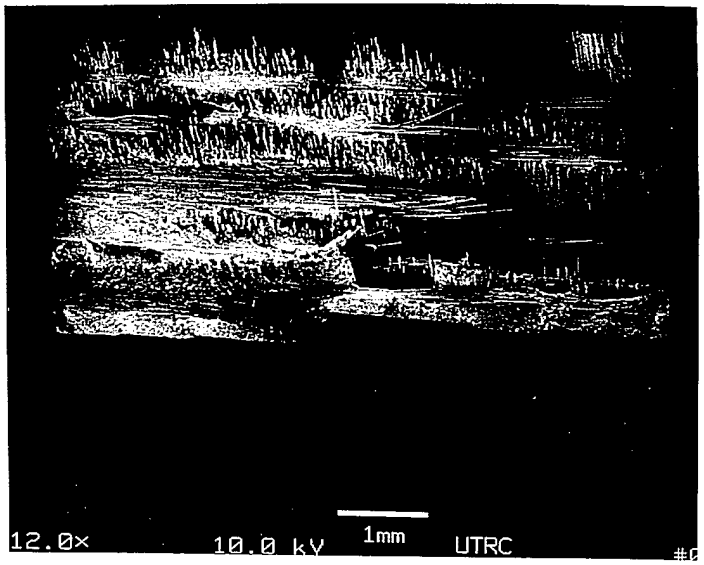

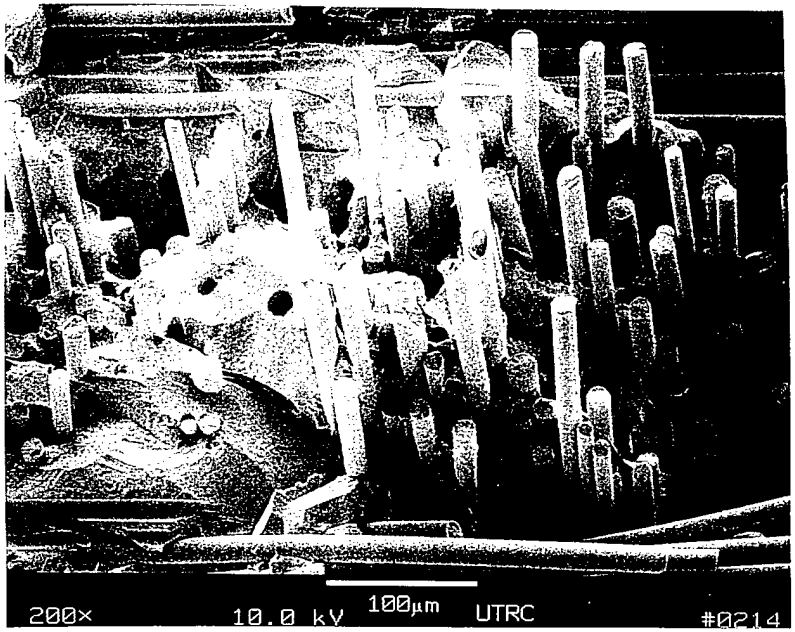

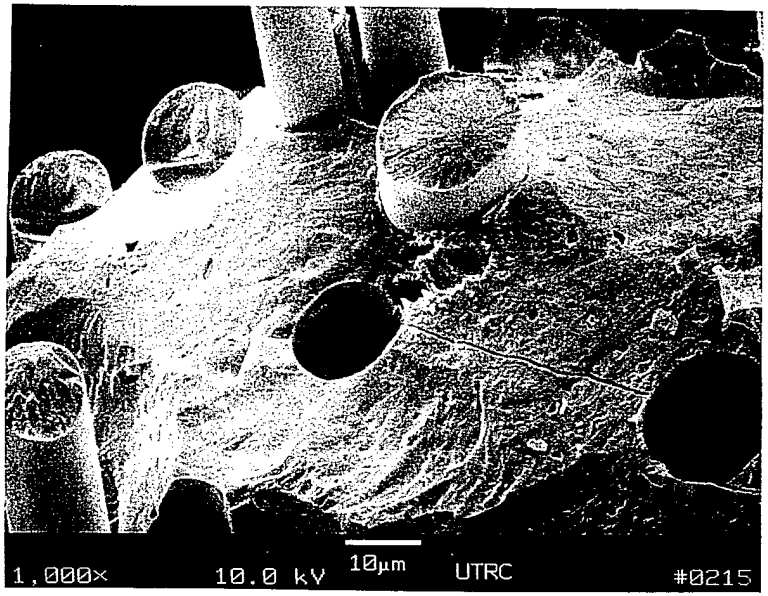

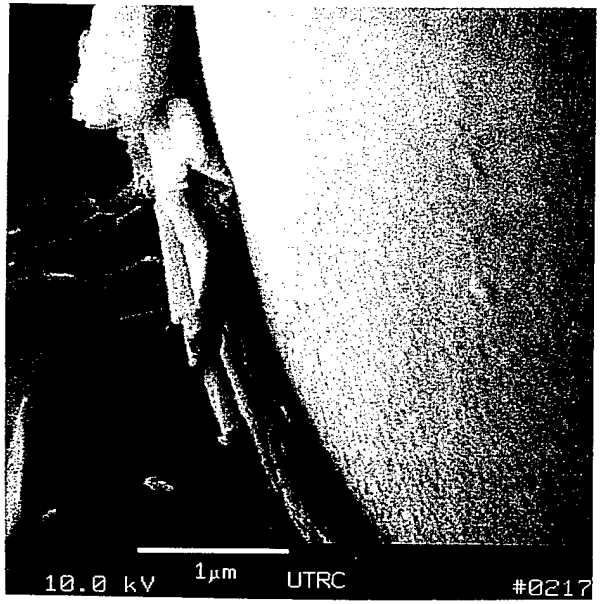

Fig. 20

BMAS Matrix/SiC/BN Nicalon Fiber Composite #56-95-3

[700°C tensile fatigue, 138 MPa (20 ksi), 349,216 cycles to failure]

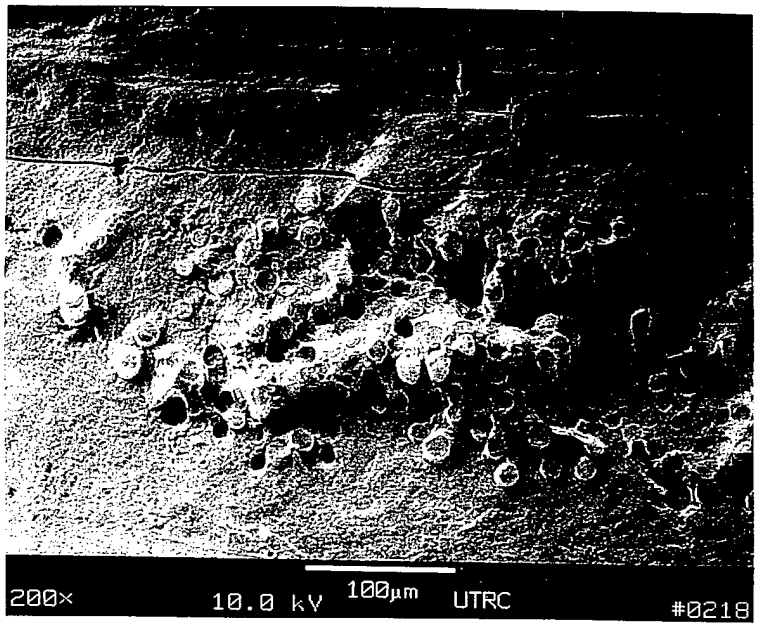

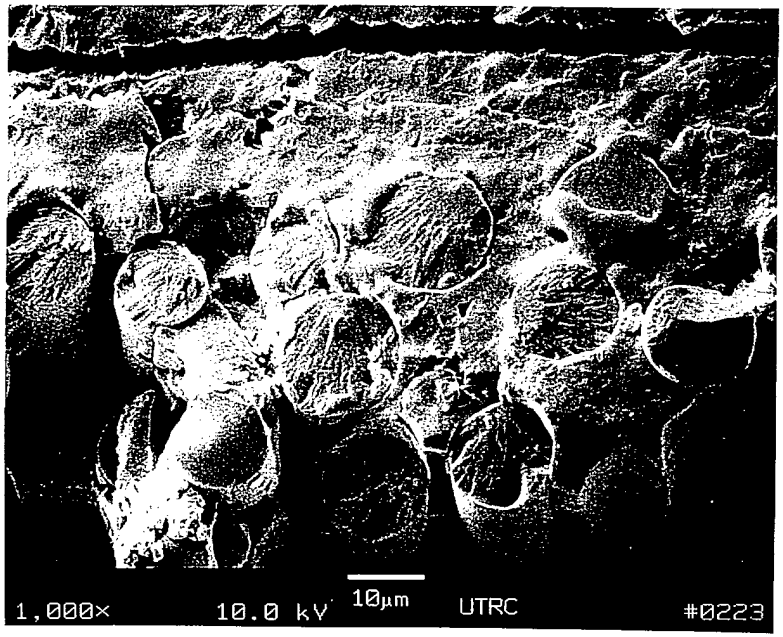

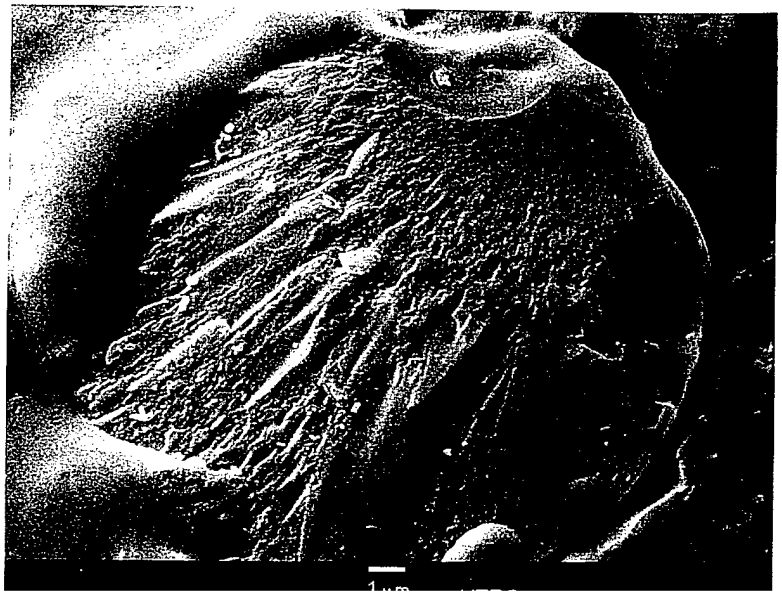

Fig. 21

BMAS Matrix/SiC/BN Nicalon Fiber Composite #56-95-6

[900°C tensile fatigue, 138 MPa (20 ksi), 719,710 cycles to failure]

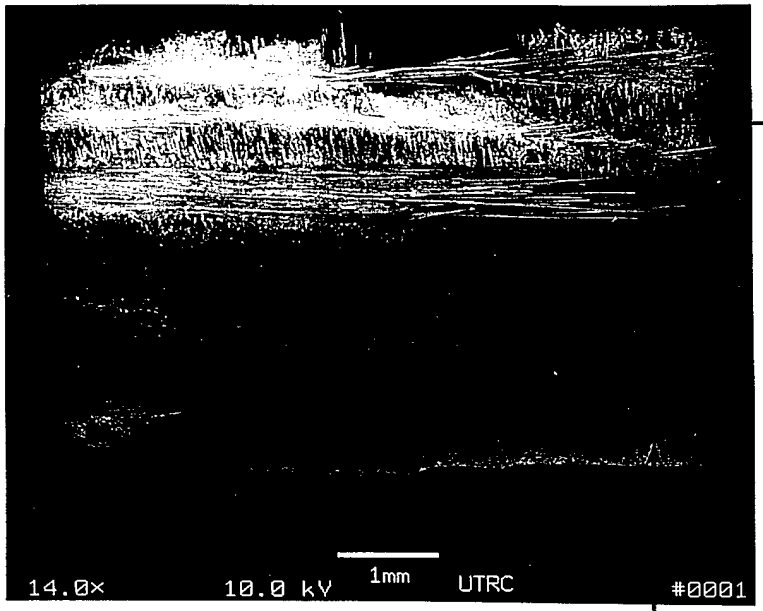

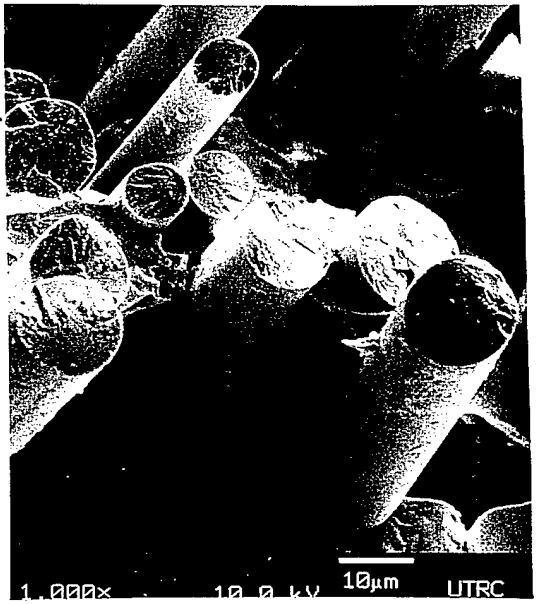

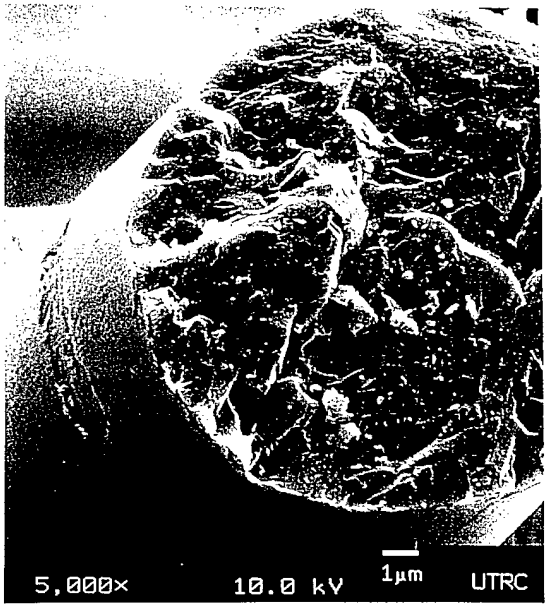

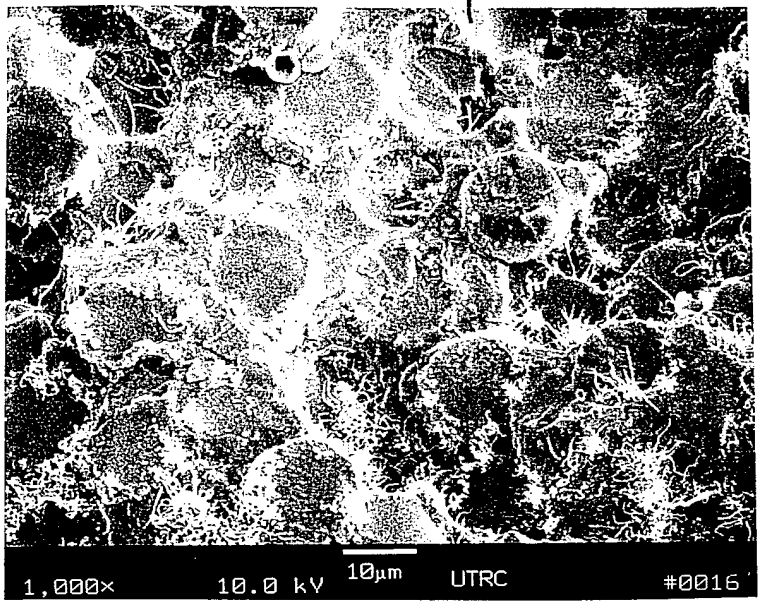

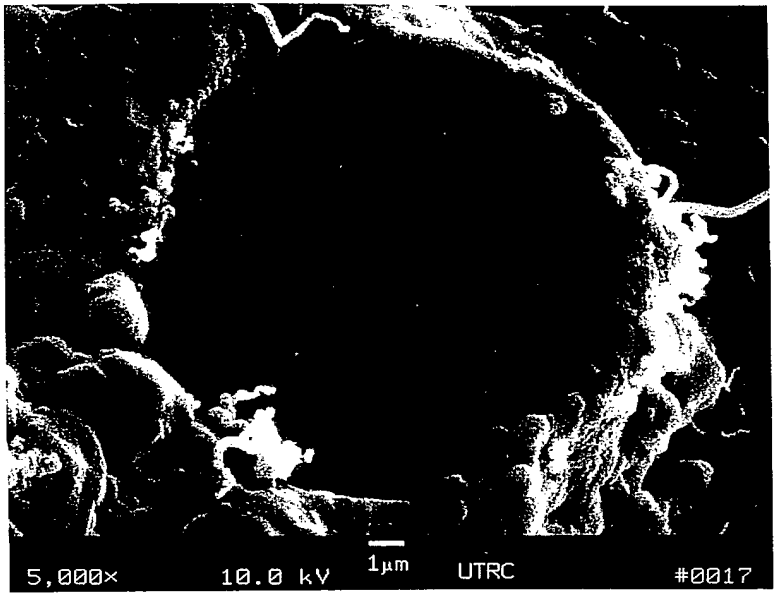

Fig. 22

BMAS Matrix/BN/Nicalon Fiber Composite #7-95-3 (0°/90°)

(550°C Tensile Stepped Stress-Rupture, 69-234 MPa, 678 hrs)

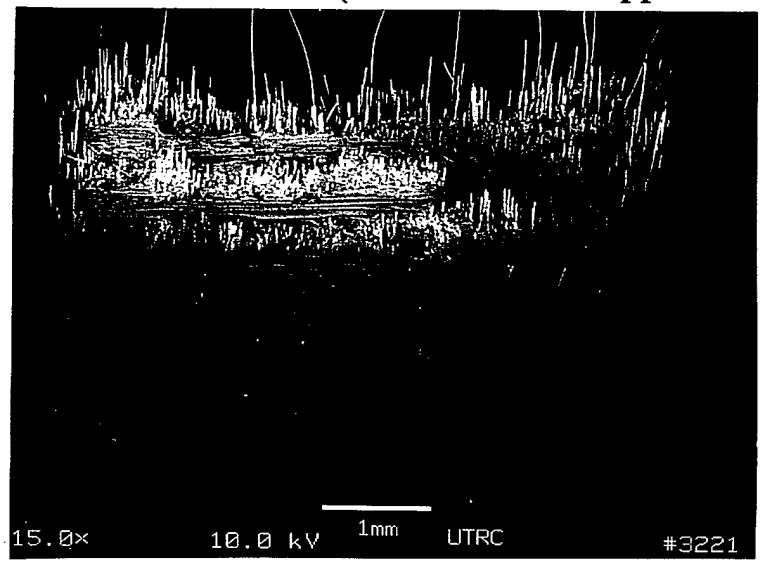

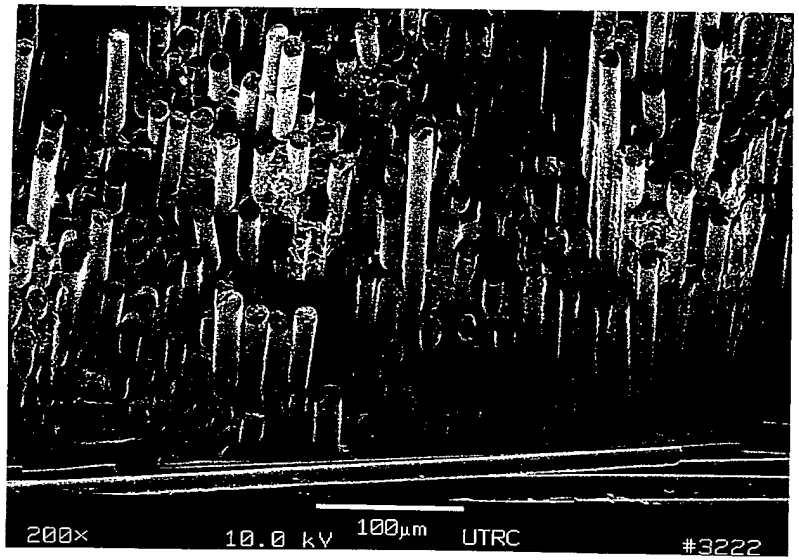

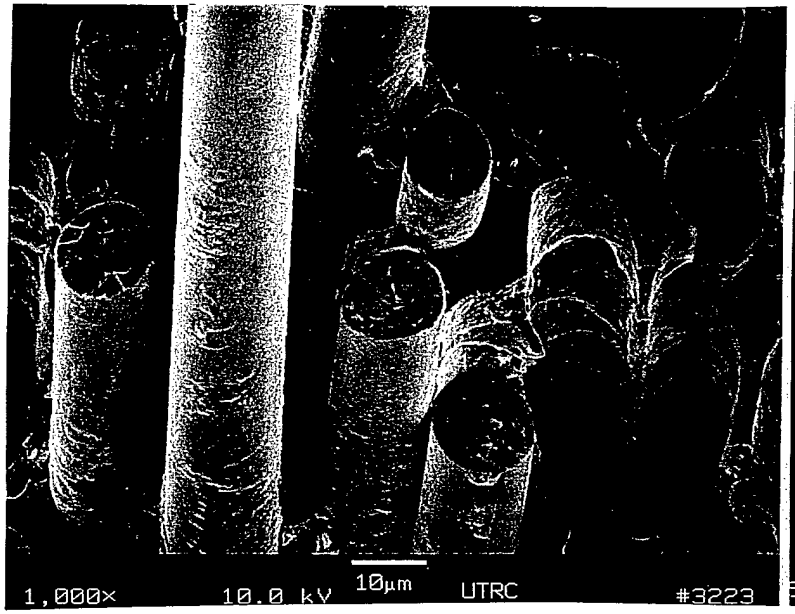

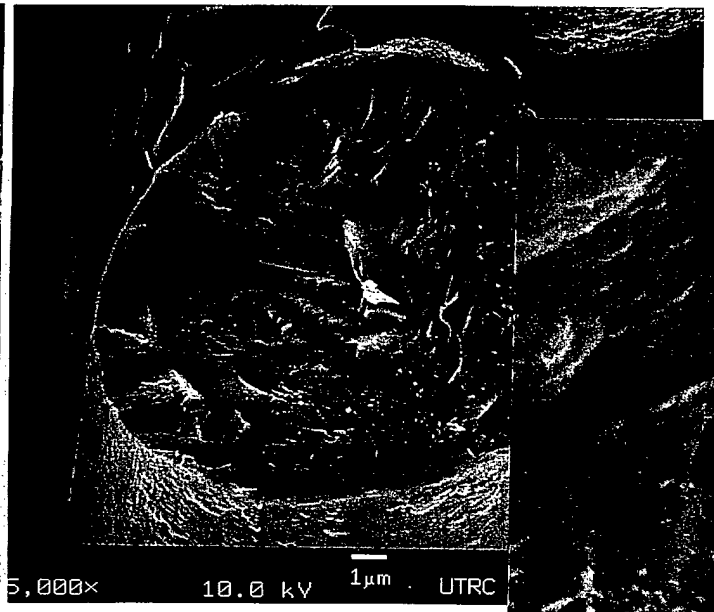

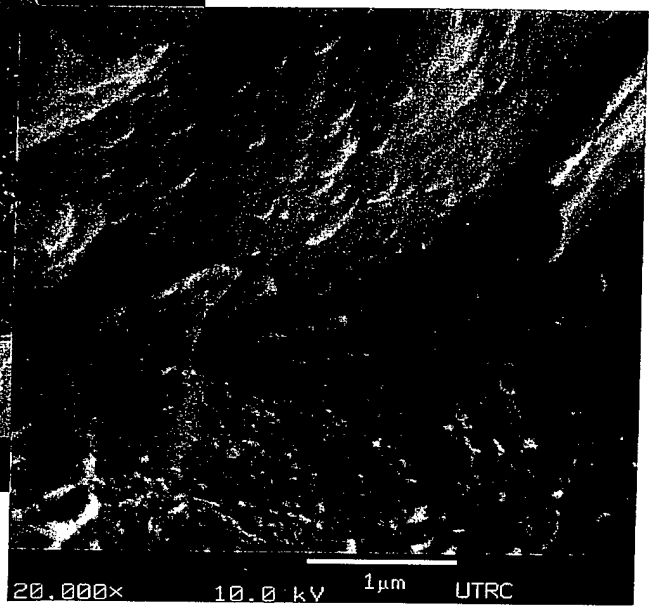

Fig. 23

BMAS Matrix/SiC/BN/Nicalon Fiber Composite #3-95-3 (0°/90°)

(550°C Tensile Stepped Stress-Rupture, 69-220 MPa, 632 hrs)

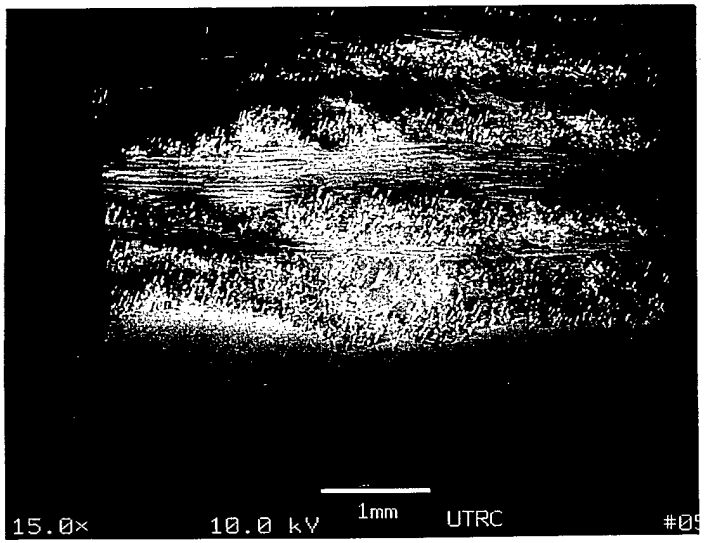

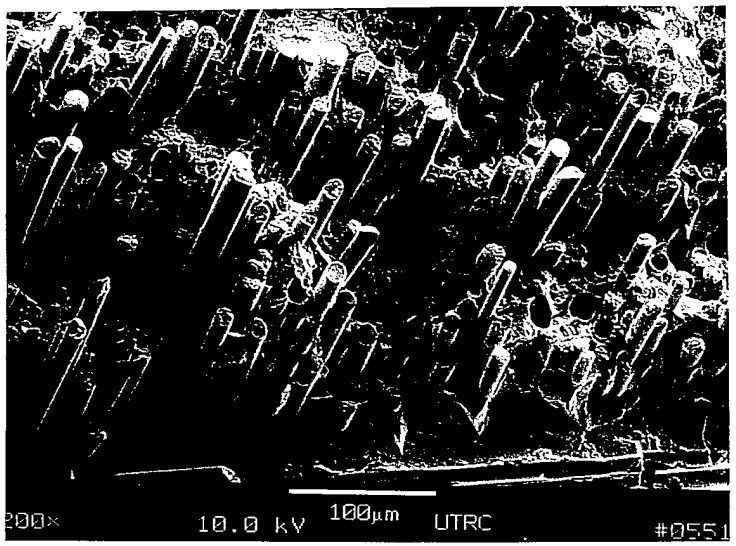

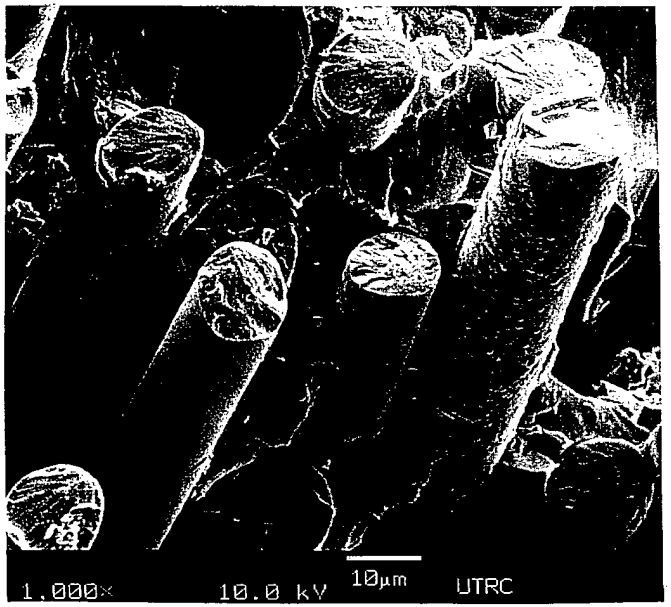

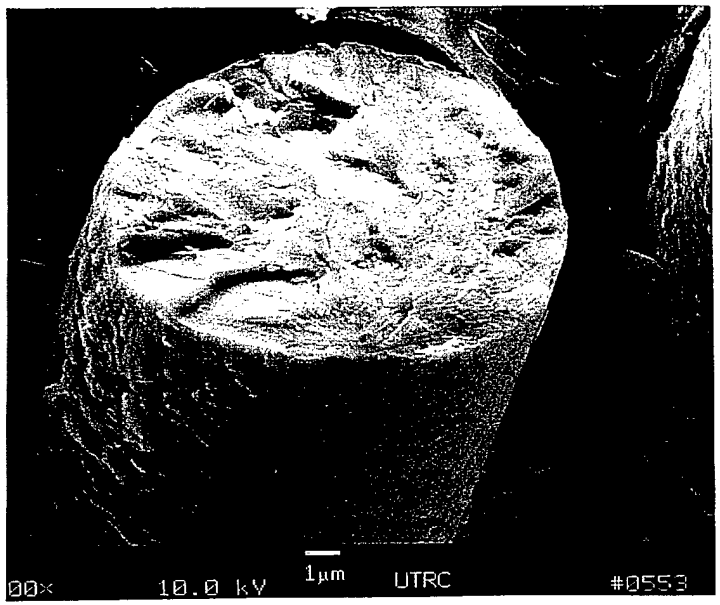

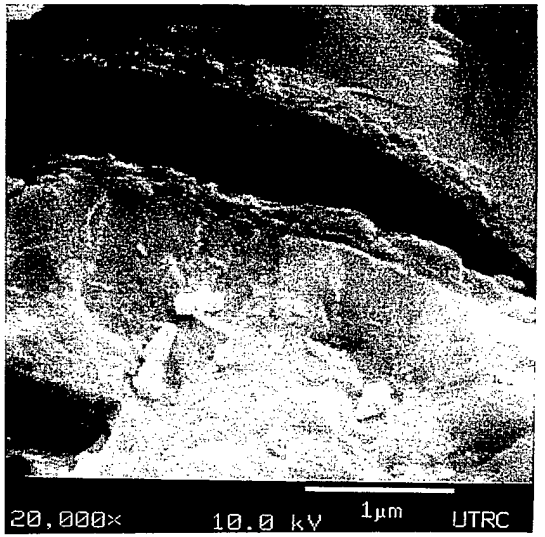

Fig. 24

BMAS Matrix/BN/Nicalon Fiber Composite #7-95-3 (0°/90°)

(550°C Tensile Stepped Stress-Rupture, 69-234 MPa, 678 hrs)

Note crack path consistently between matrix and BN-coating

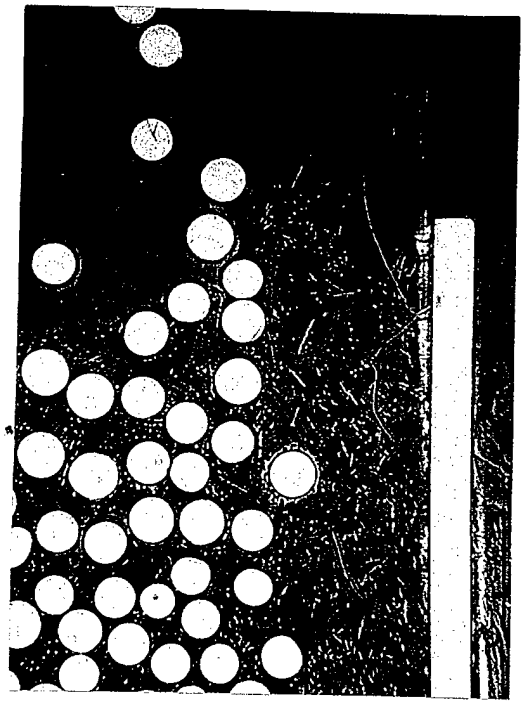

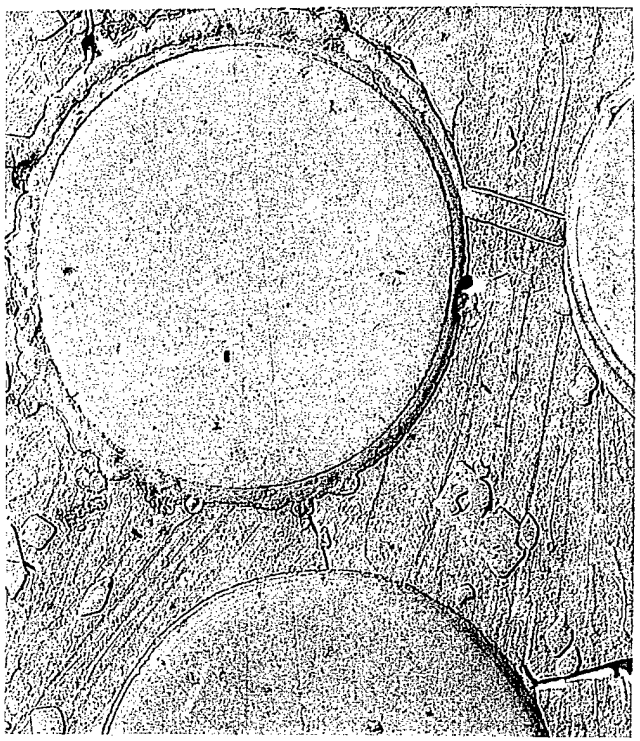

Fig. 25

BMAS Matrix/BN/Nicalon Fiber Composite #7-95-2 (0°/90°)

(1100°C Tensile Stepped Stress-Rupture, 69-207 MPa, 598 hrs)

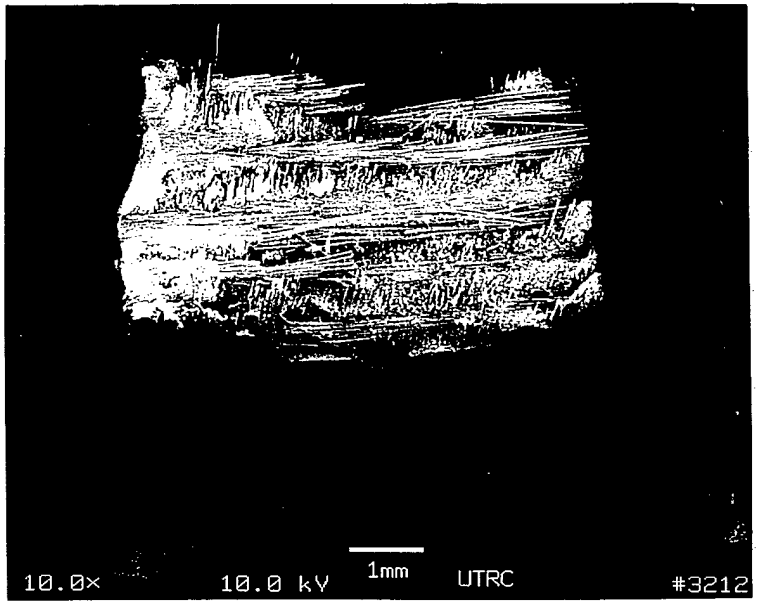

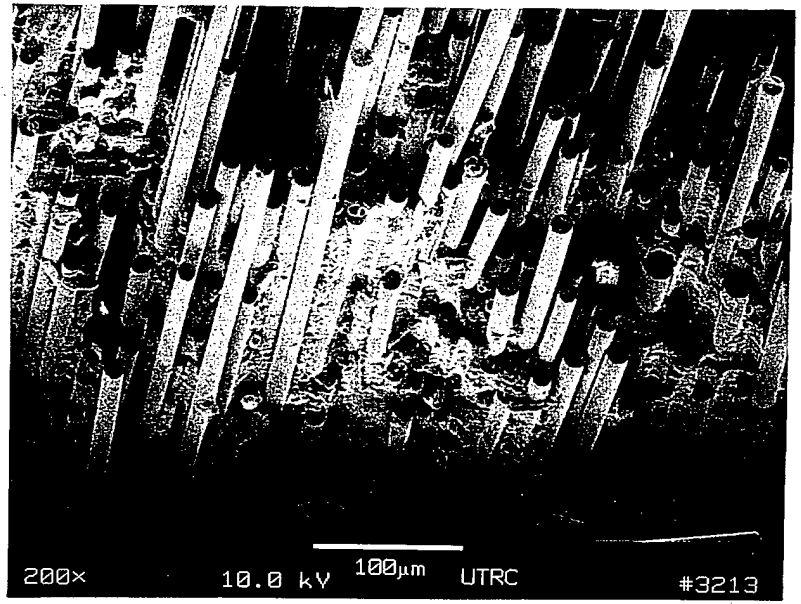

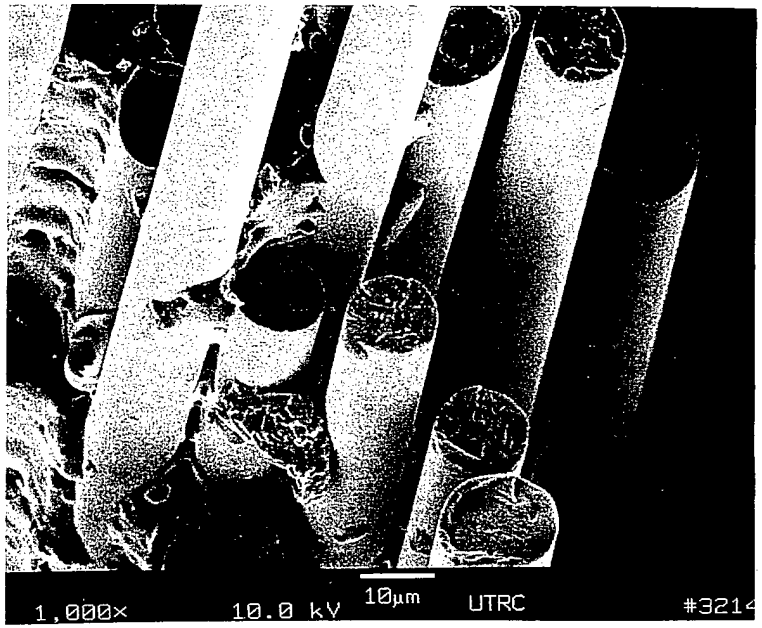

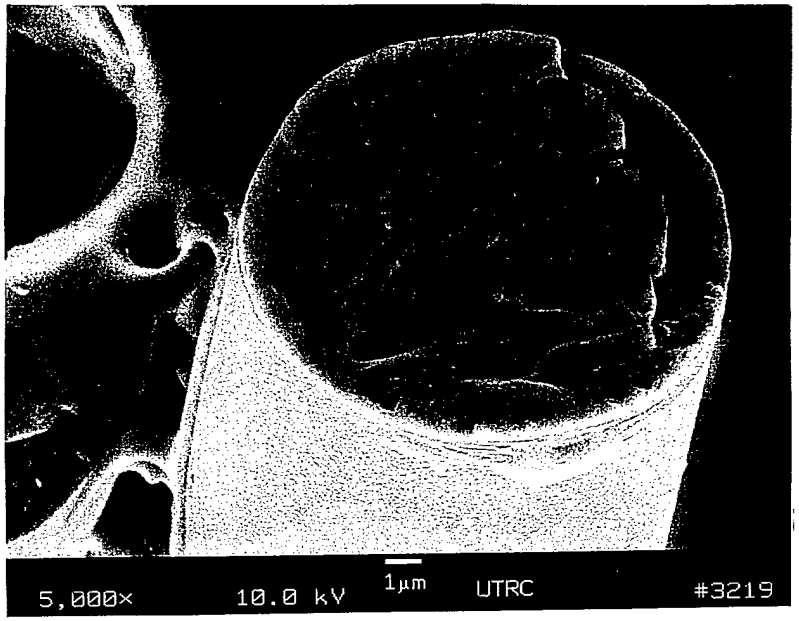

Fig. 26

BMAS Matrix/SiC/BN/Nicalon Fiber Composite #3-95-2 (0°/90°)

(1100°C Tensile Stepped Stress-Rupture, 69-180 MPa, 436 hrs)

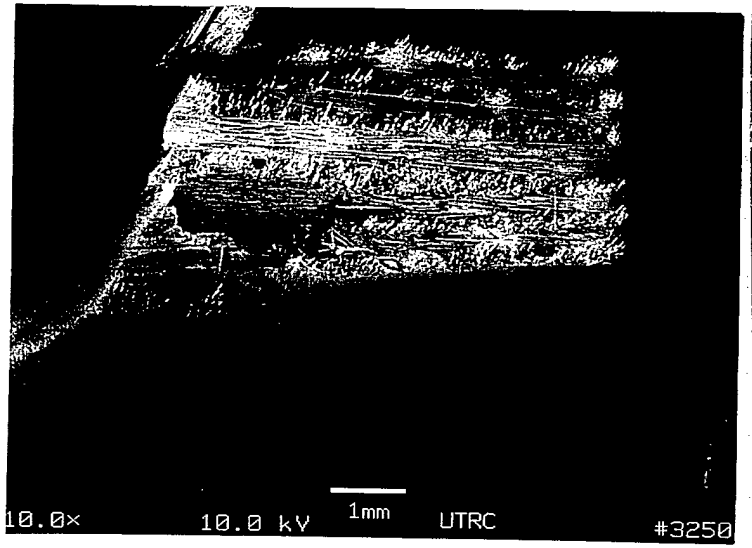

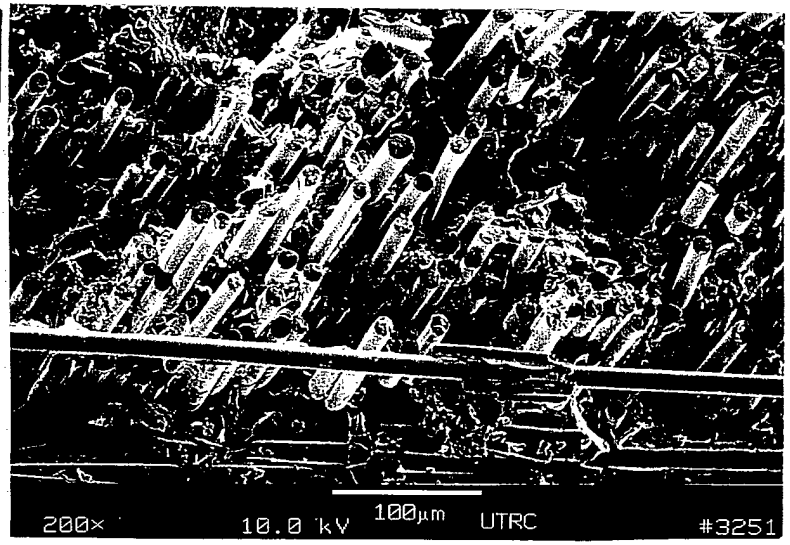

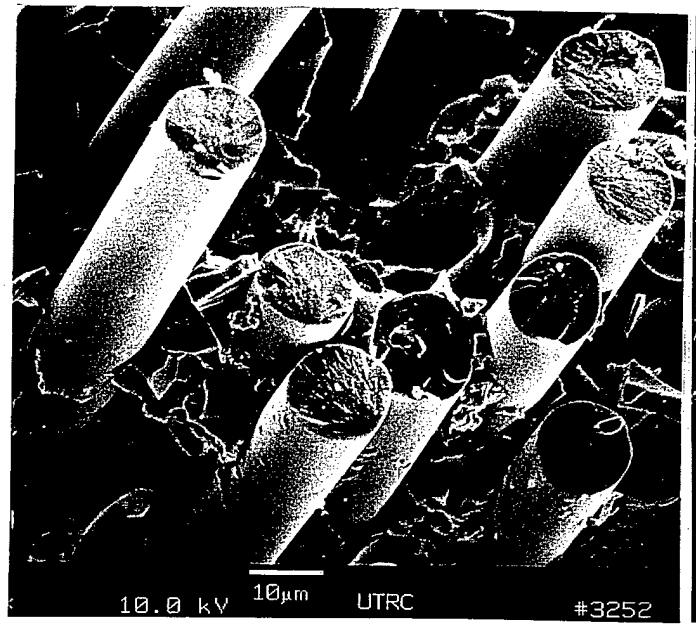

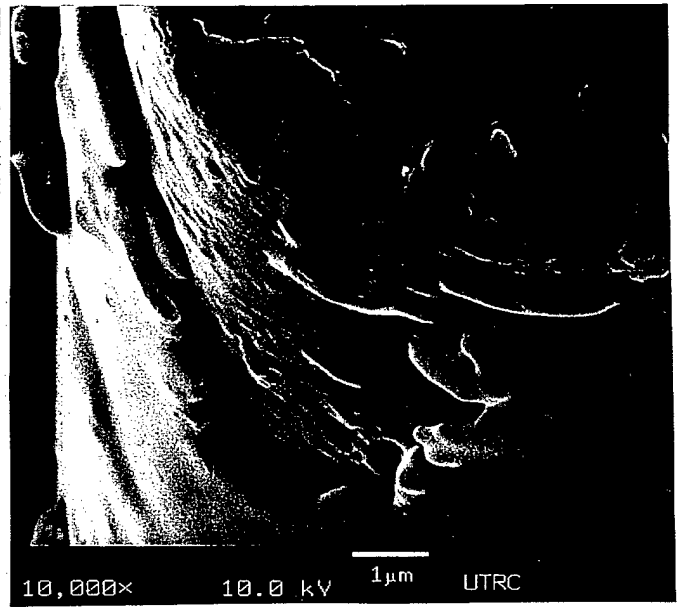

Fig. 27

BMAS Matrix/BN/Nicalon Fiber Composite #7-95-2 (0°/90°)

(1100°C Tensile Stepped Stress-Rupture, 69-207 MPa, 598 hrs)

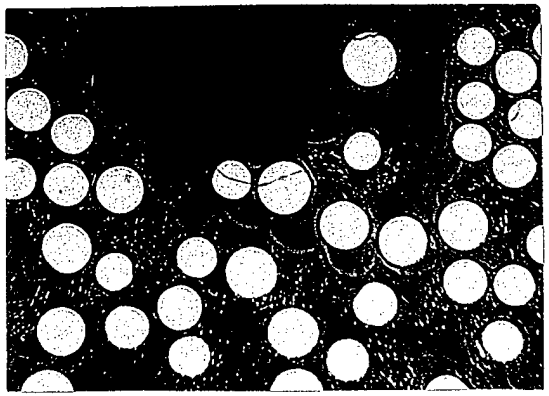

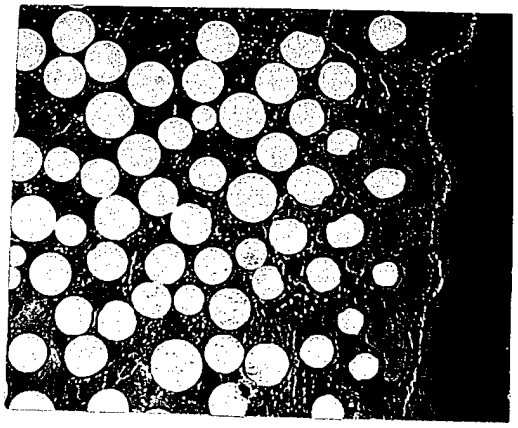

Note crack path consistently between matrix and BN-coating

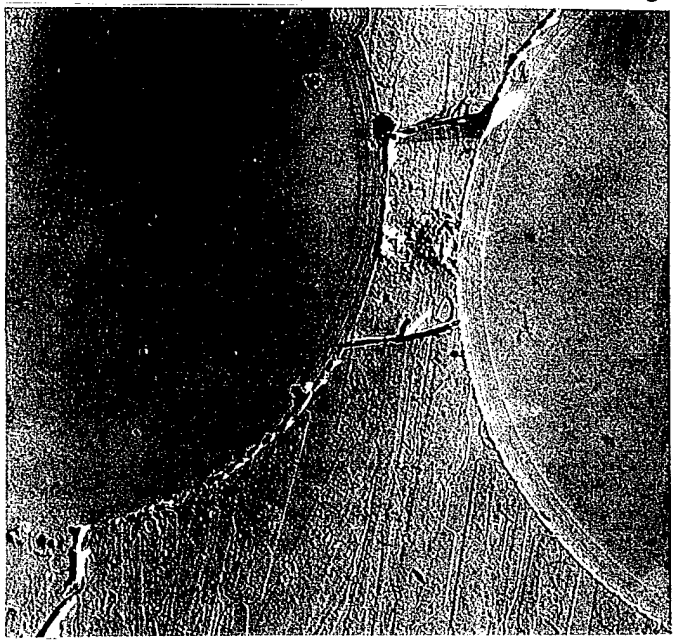

Note surface oxidation of fibers and interface

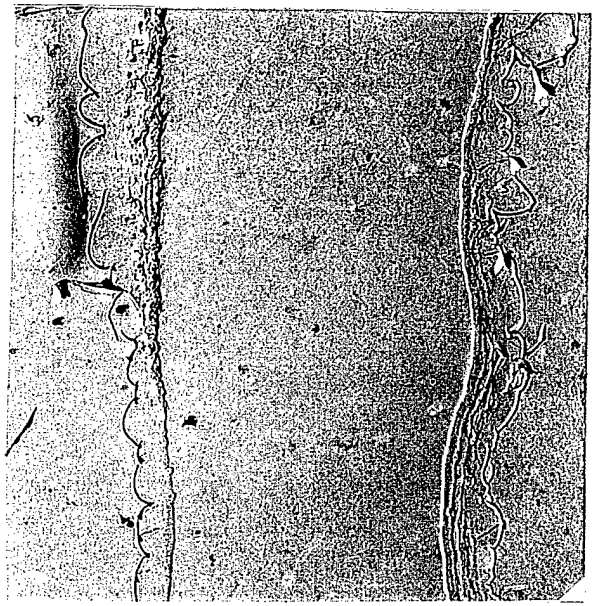

Fig. 28

BMAS Matrix/BN Coated Nicalon Fiber Composite #15-95-5 (0°/90°)

(650°C, 138 MPa (20 ksi) TSR, 6269 hrs to failure)

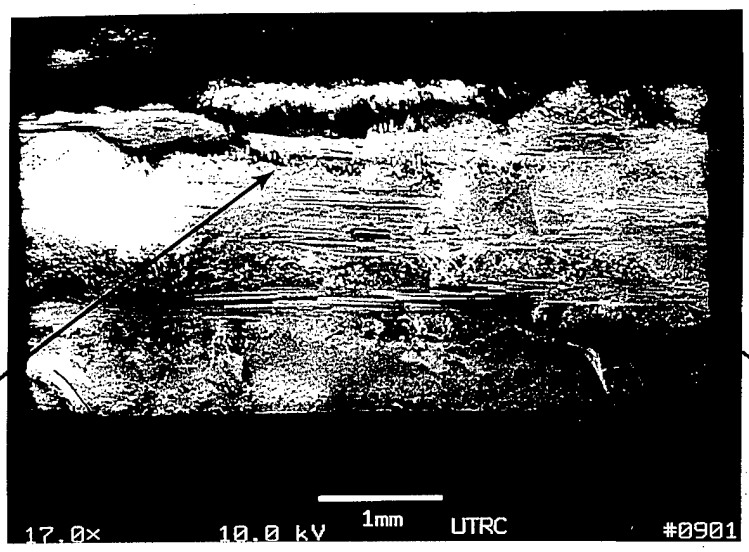

"Tough" Region

"Brittle" Region

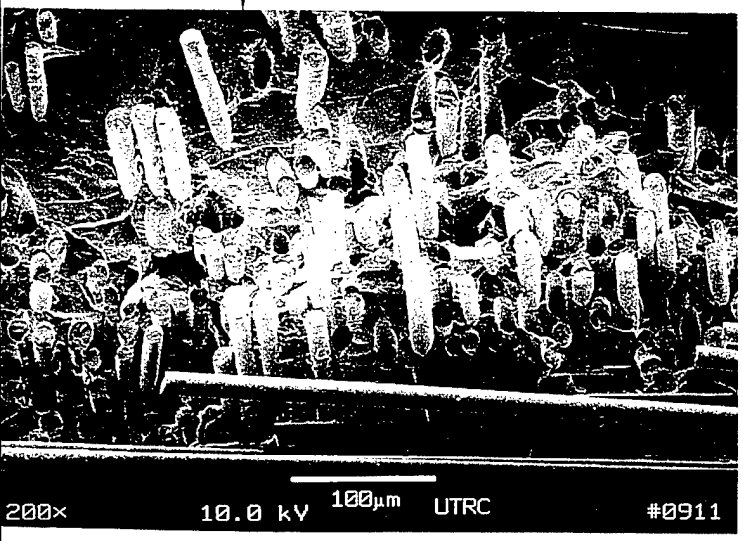

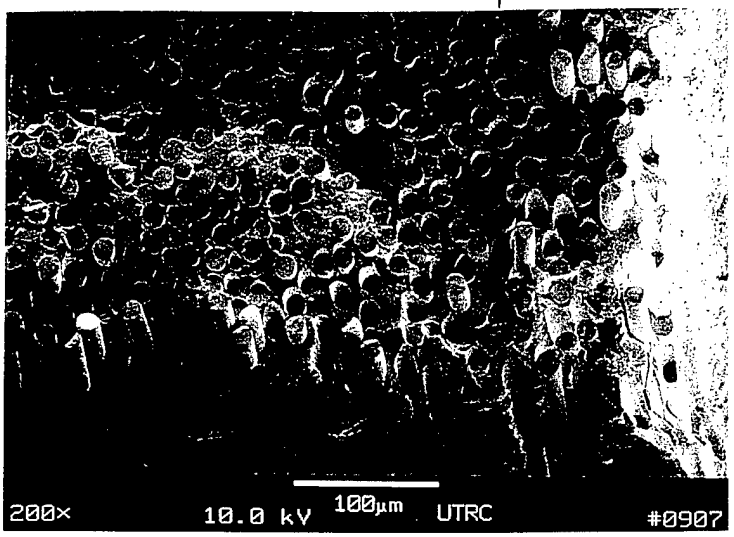

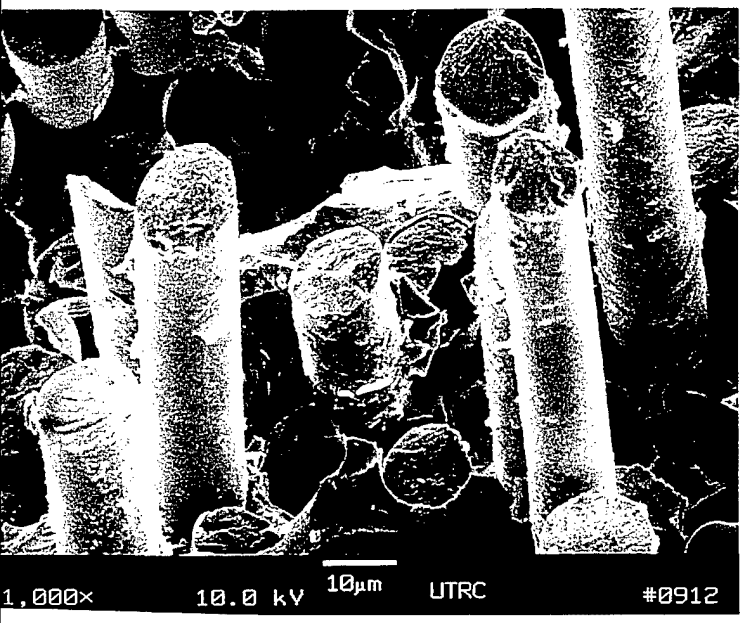

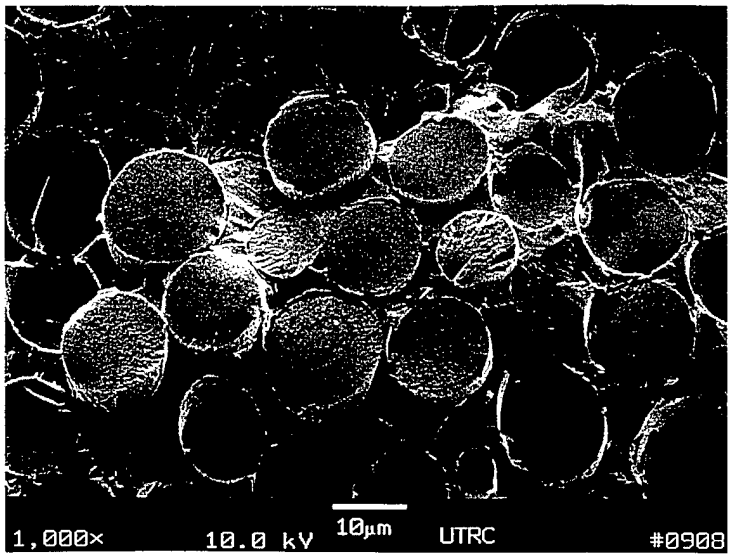

BMAS Matrix/BN Coated Nicalon Fiber Composite #15-95-5 (0°/90°)

(650°C, 138 MPa (20 ksi) TSR, 6269 hrs to failure)

[Longitudinal section, near edge]

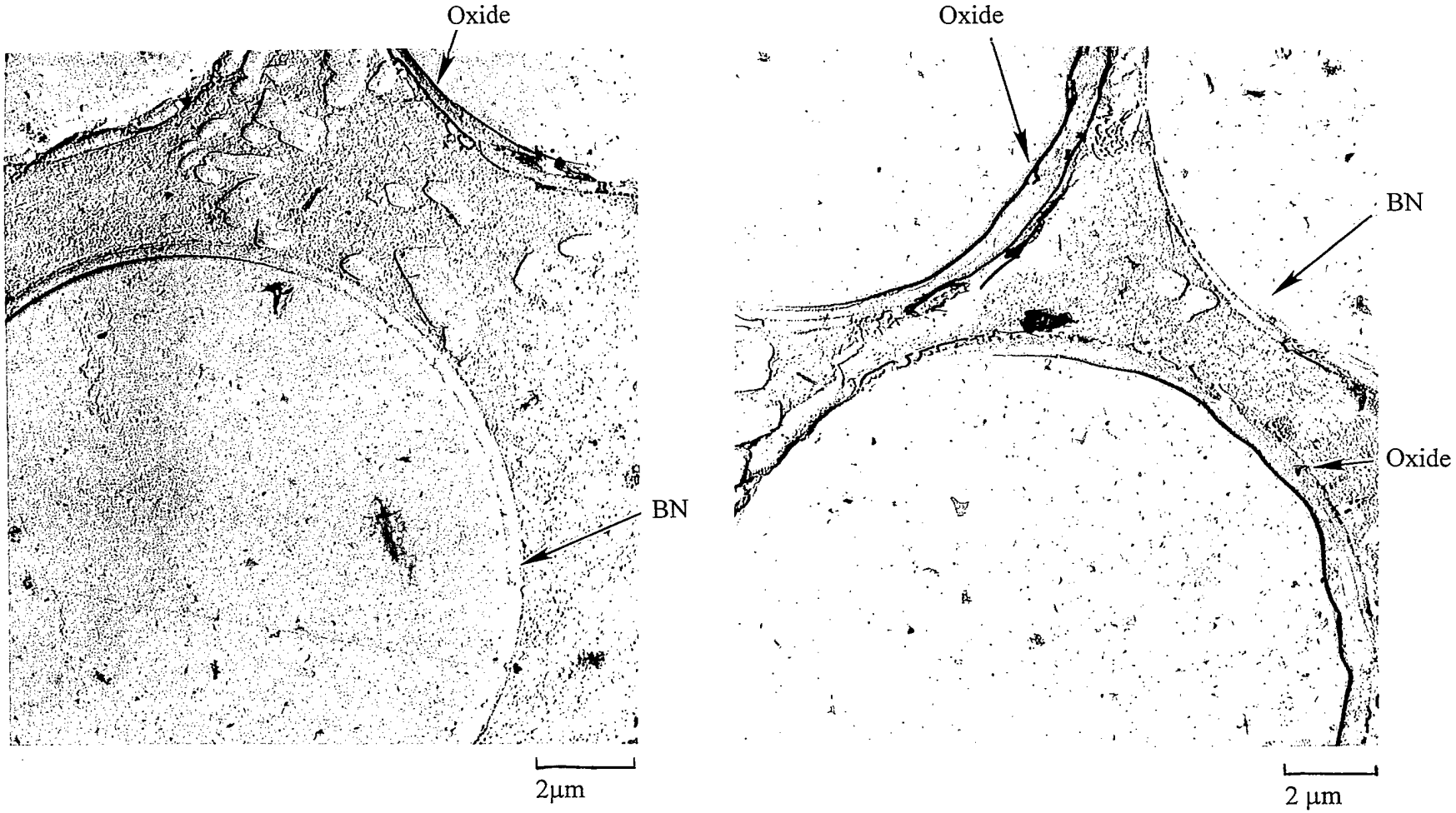

Fig. 30

BMAS Matrix/SiC/BN Coated Nicalon Fiber Composite (0/90°) 1100°C Tensile Results After 1100°C Fatigue and Creep

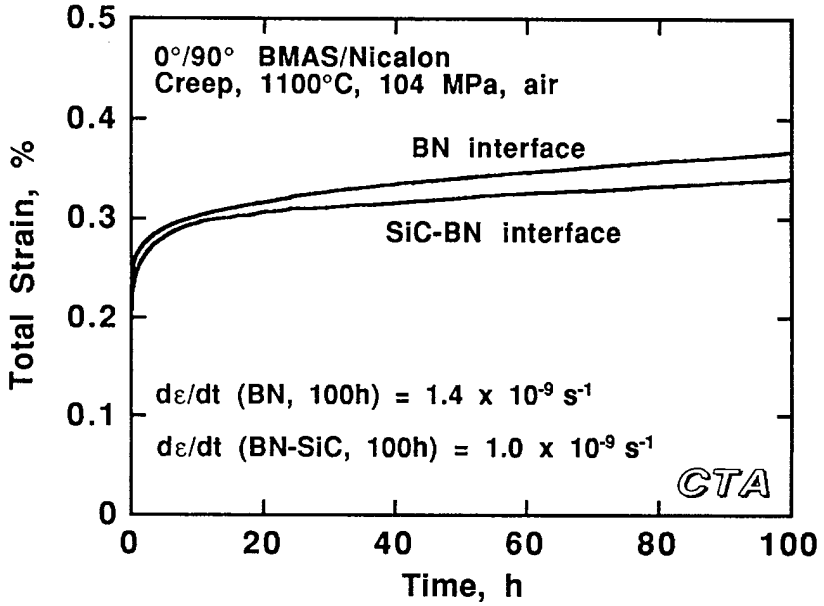

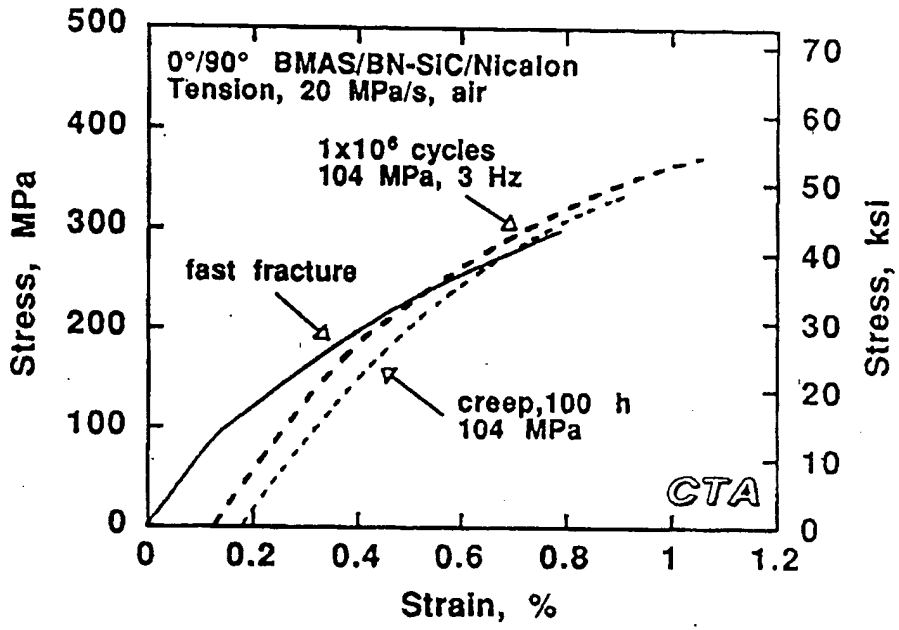

Fig. 31

BMAS Matrix/SiC/BN/Nicalon Fiber Composite #28-95-9 (0°/90°)

(1100°C, 104 MPa, 100 hr tensile creep, 1100°C UTS = 333 MPa, $\varepsilon_f = 0.91\%$)

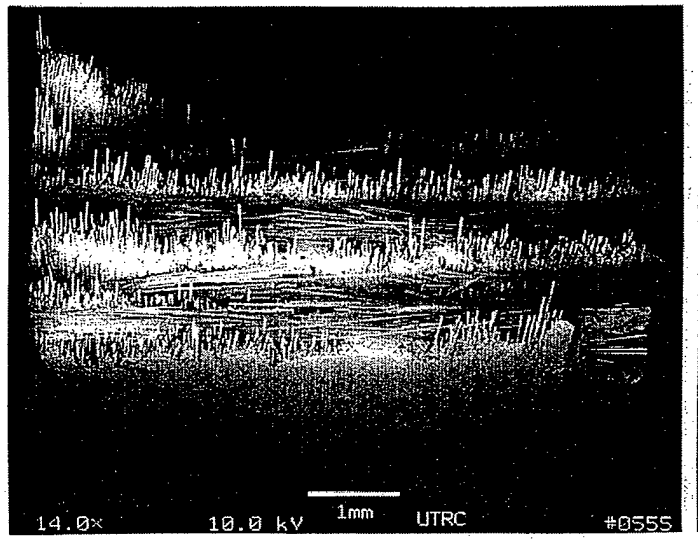

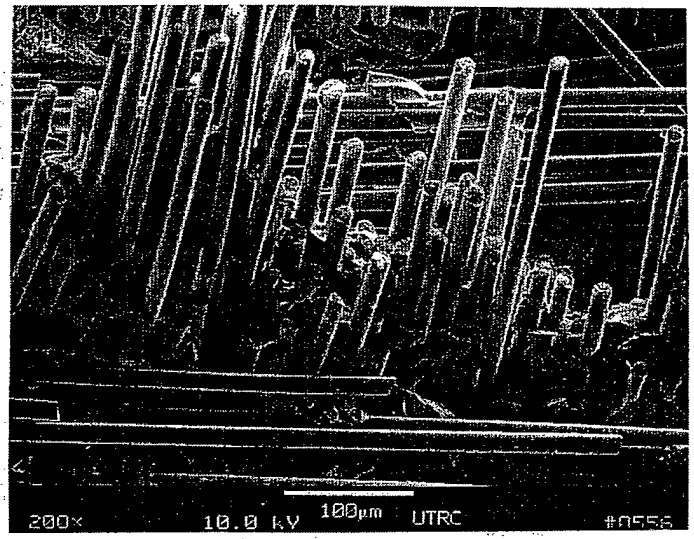

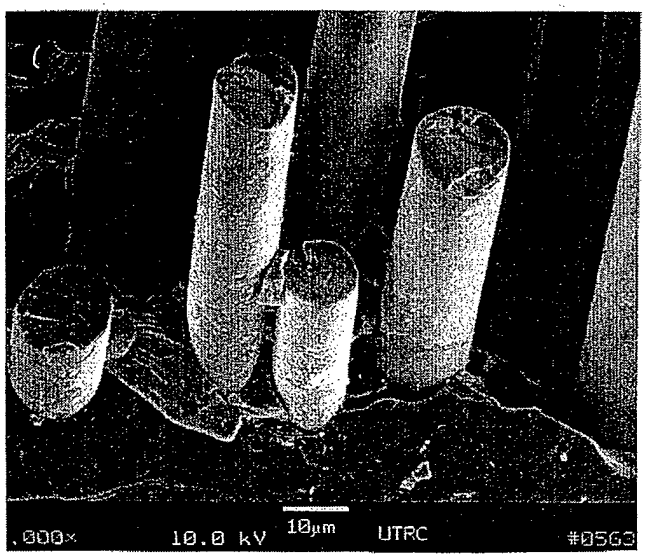

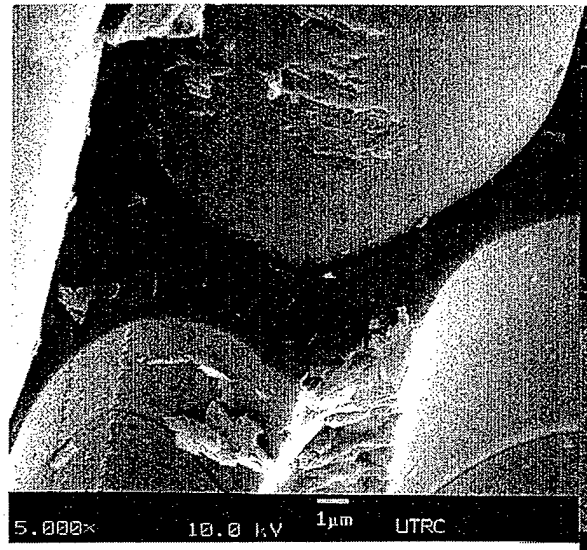

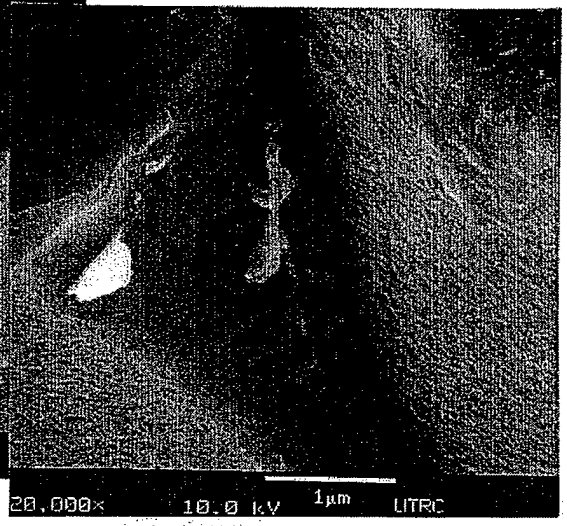

Fig. 32

Stepped Temperature Tensile Creep of BMAS Matrix Composites (0°/90°)

(Applied Stress = 138 MPa)

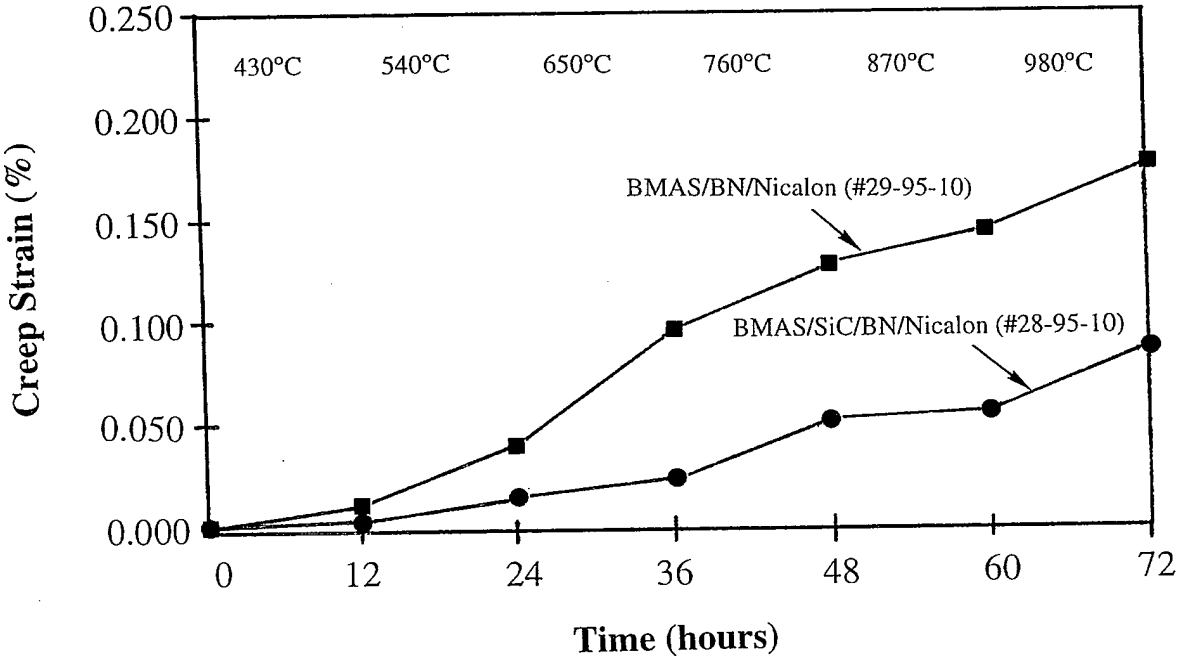

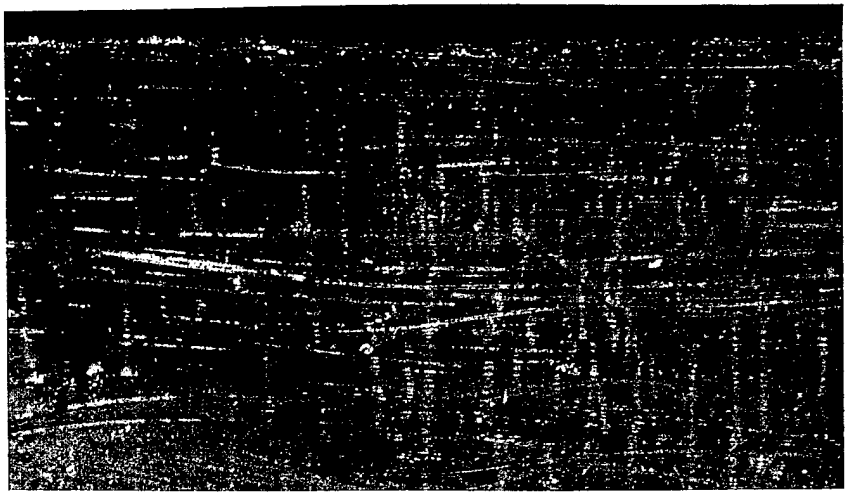

#28 -95-10 (Unsaturated, discontinuous cracks) 400 μm

#29-95-10 (Saturated crack spacing = 232 μm) 400 μm

Fig. 33

BMAS/NICALON COMPOSITE STEPPED TEMPERATURE TENSILE CREEP

(430 - 980°C, 72hrs./138Mpa)

9000X

A. #28-95 (SiC/BN Interface)

B. #29-95 (BN Interface)

2.0μ

MML 34524

United Technologies

Research Center Transmission Electron Microscope Laboratory

Fig. 34

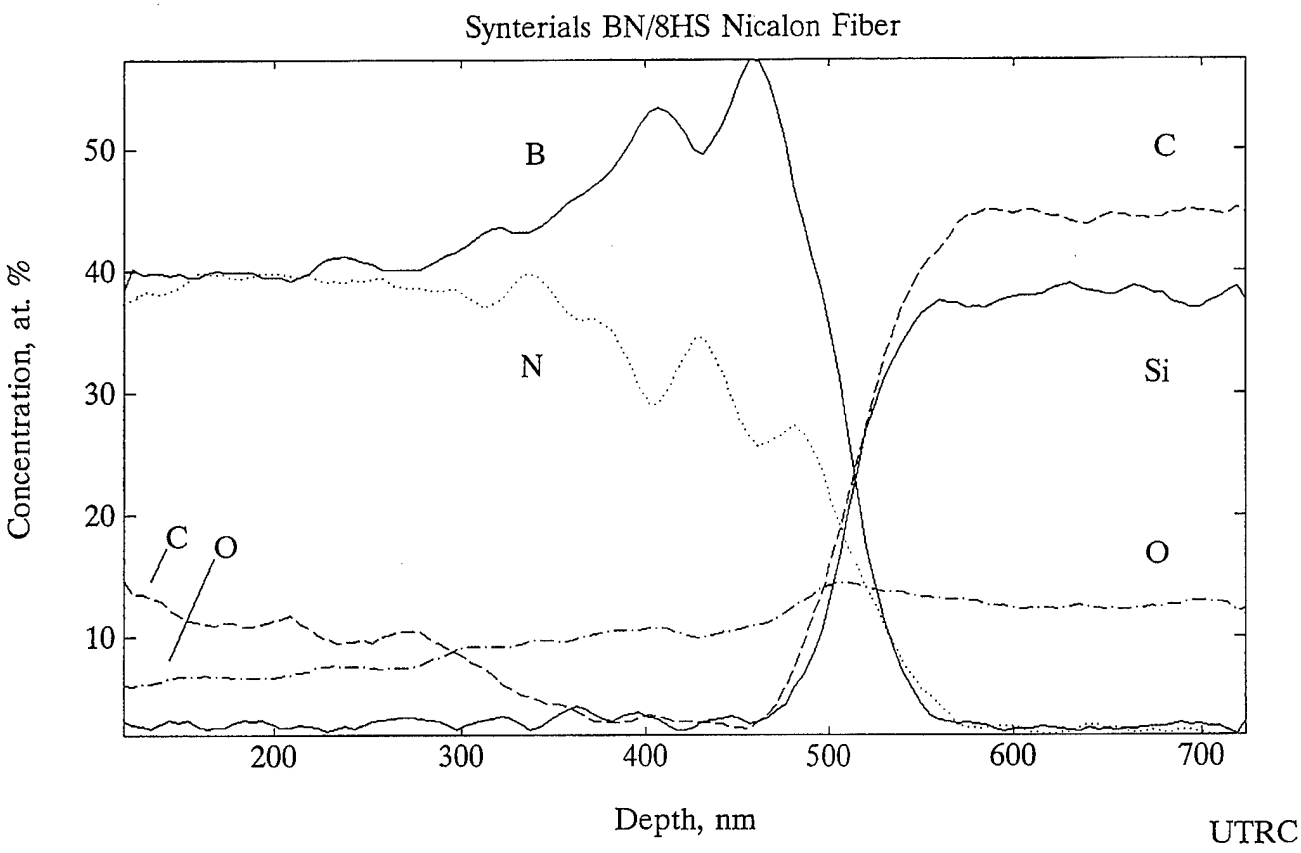

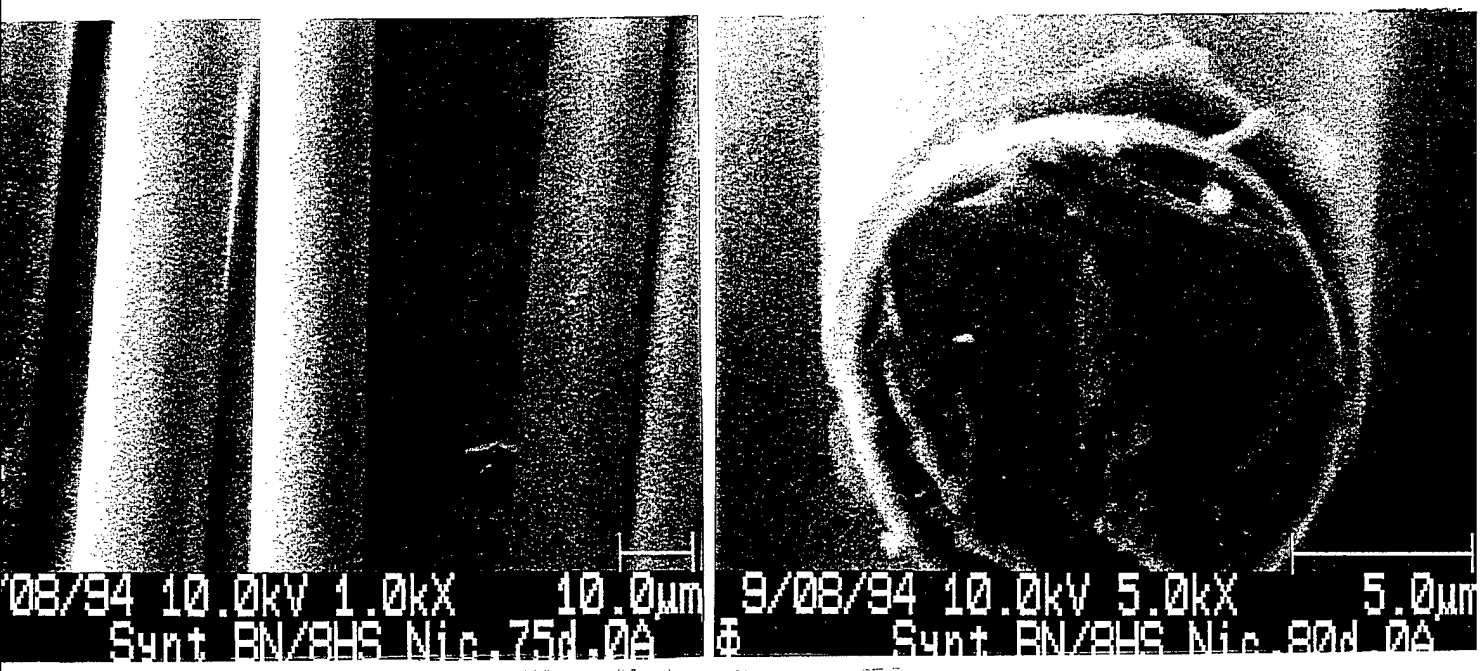

Difference in BN Layer Crystallization During Composite Fabrication Between 3M Carbon Containing BN and Synterials BN

#7-95 BMAS/3M BN/Nicalon (RTσ = 640 MPa)

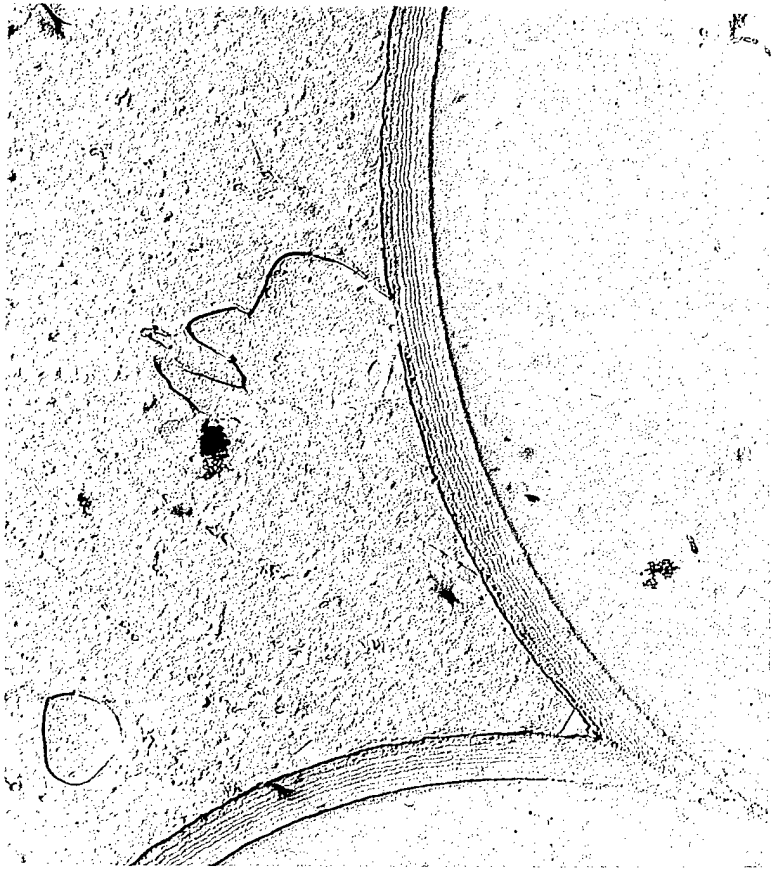

#131-94 BMAS/Synterials BN/Nicalon (RTσ = 340 MPa)

Fig. 36

BMAS MATRIX/ADVANCED CERAMICS BN COATED/CARBON COATED 8HS NICALON FIBERS (0°/90°), CERAMED - COMPOSITE #41-96-2A

(RT 4ptσ = 72 ksi (495Mpa), Ef = 0.65%)

Middle of composite, edge of tow

Middle of composite, middle of tow **15000X**

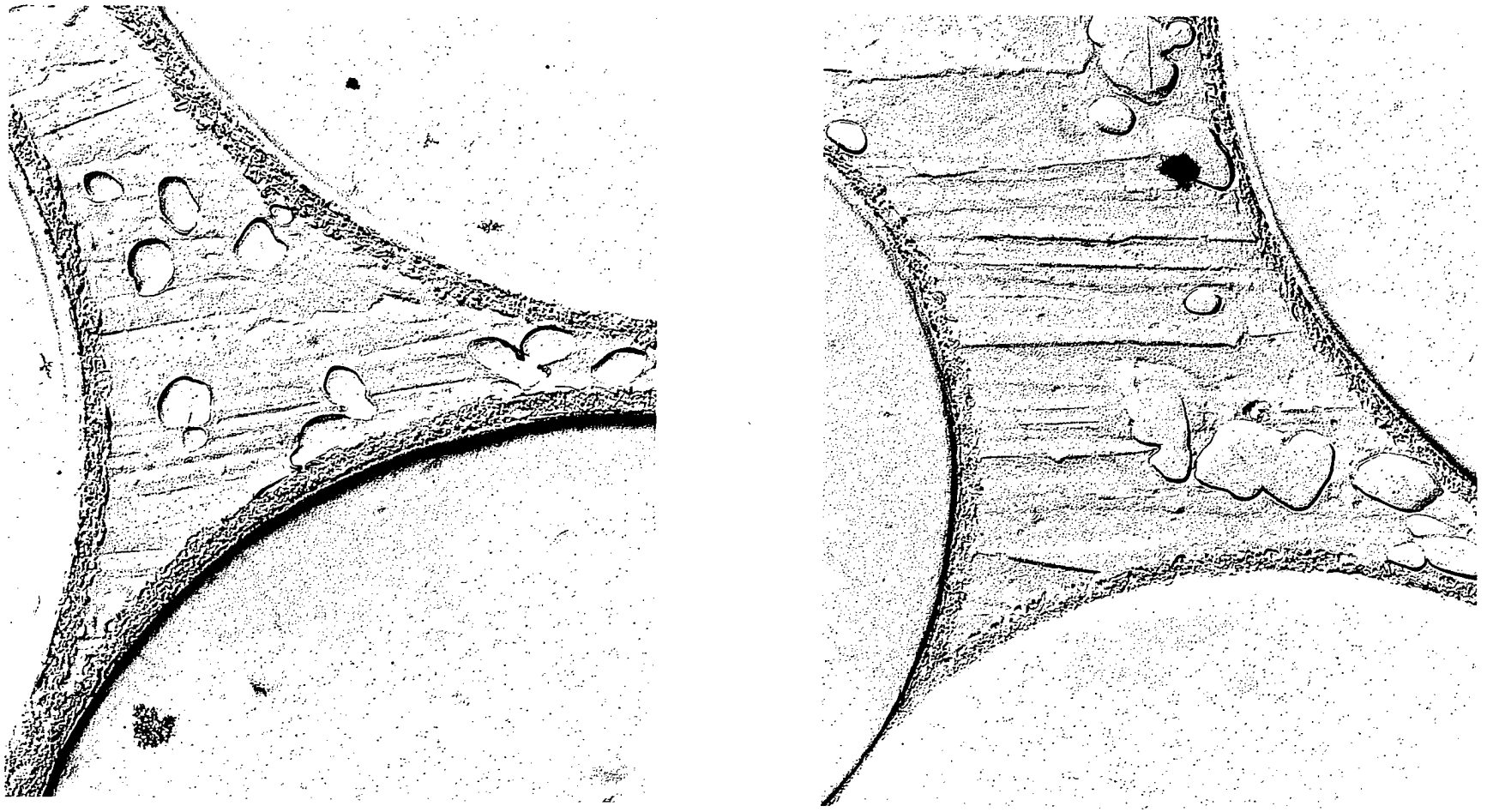

BN Thickness = 200 -330nm

1.0μ

Fig. 37

United Technologies

BMAS MATRIX/BF GOODRICH BN COATED 5HS Hi-NICALON FIBERS (0°/90°), CERAMED - COMPOSITE #30-96-3

(RT 3ptσ = 73 ksi (505Mpa), Ef = 0.50%)

Middle of composite, edge of tow

Middle of composite, middle of tow **15000X**

BN Thickness = 400 - 930nm

1.0μ

MML 34570

United Technologies

Research Center Transmission Electron Microscope Labor

Fig. 38

BMAS/SiC/BN/NICALON COMPOSITE (800°C, 90%H2O, 88Hrs.)
Composite #29-95

500X

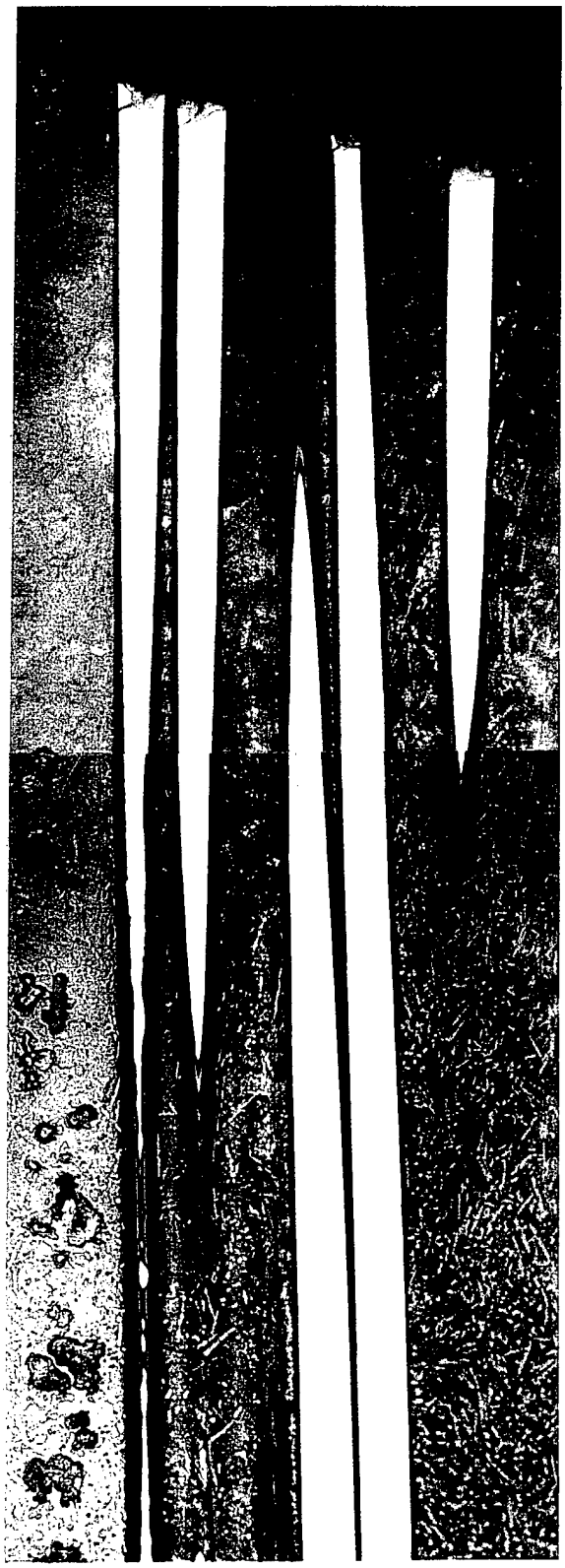

1000X

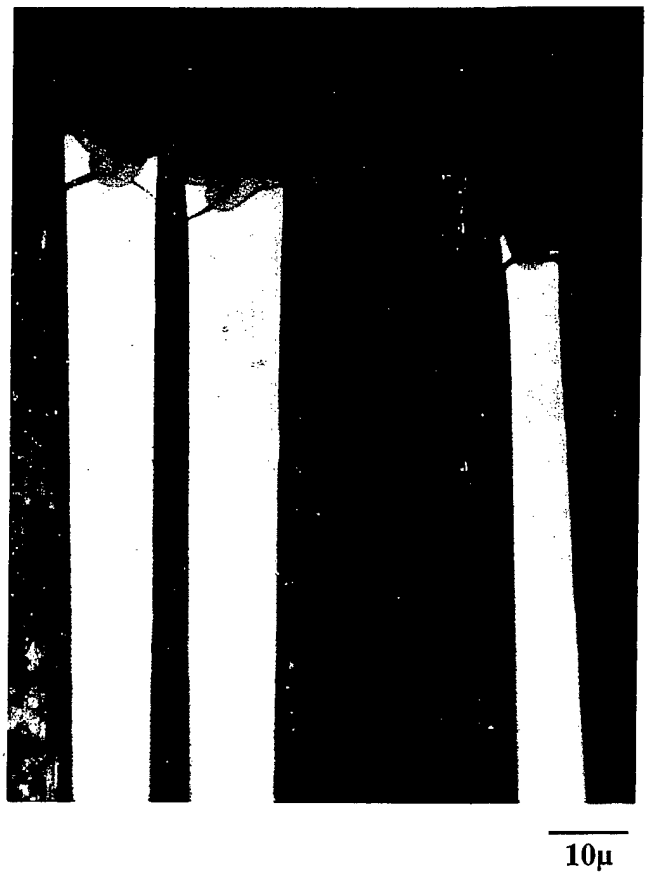

BMAS/SiC/BN/NICALON COMPOSITE (800°C, 90%H2O, 88Hrs.)
Composite #29-95

2000X

3.0μ

4200X

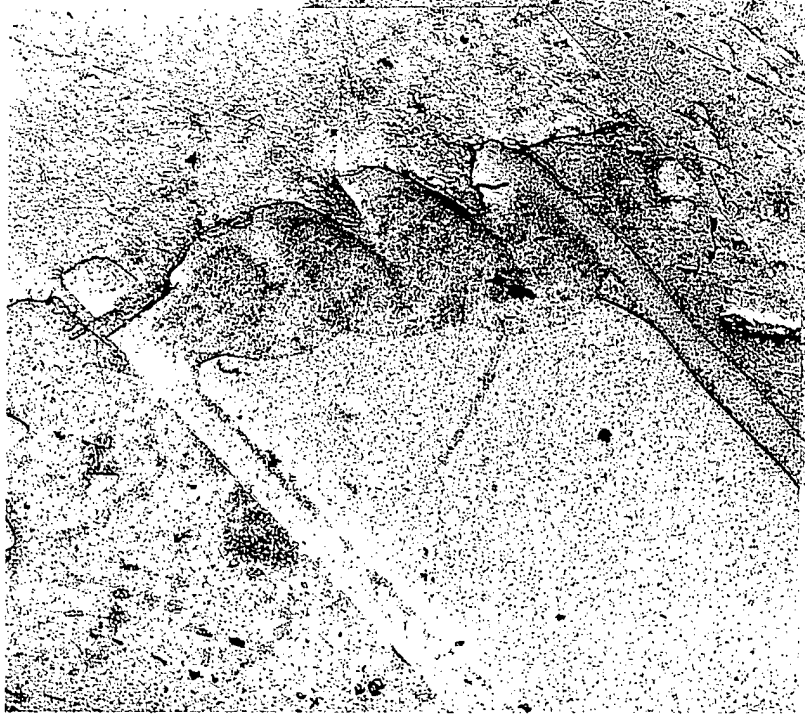

3.0μ

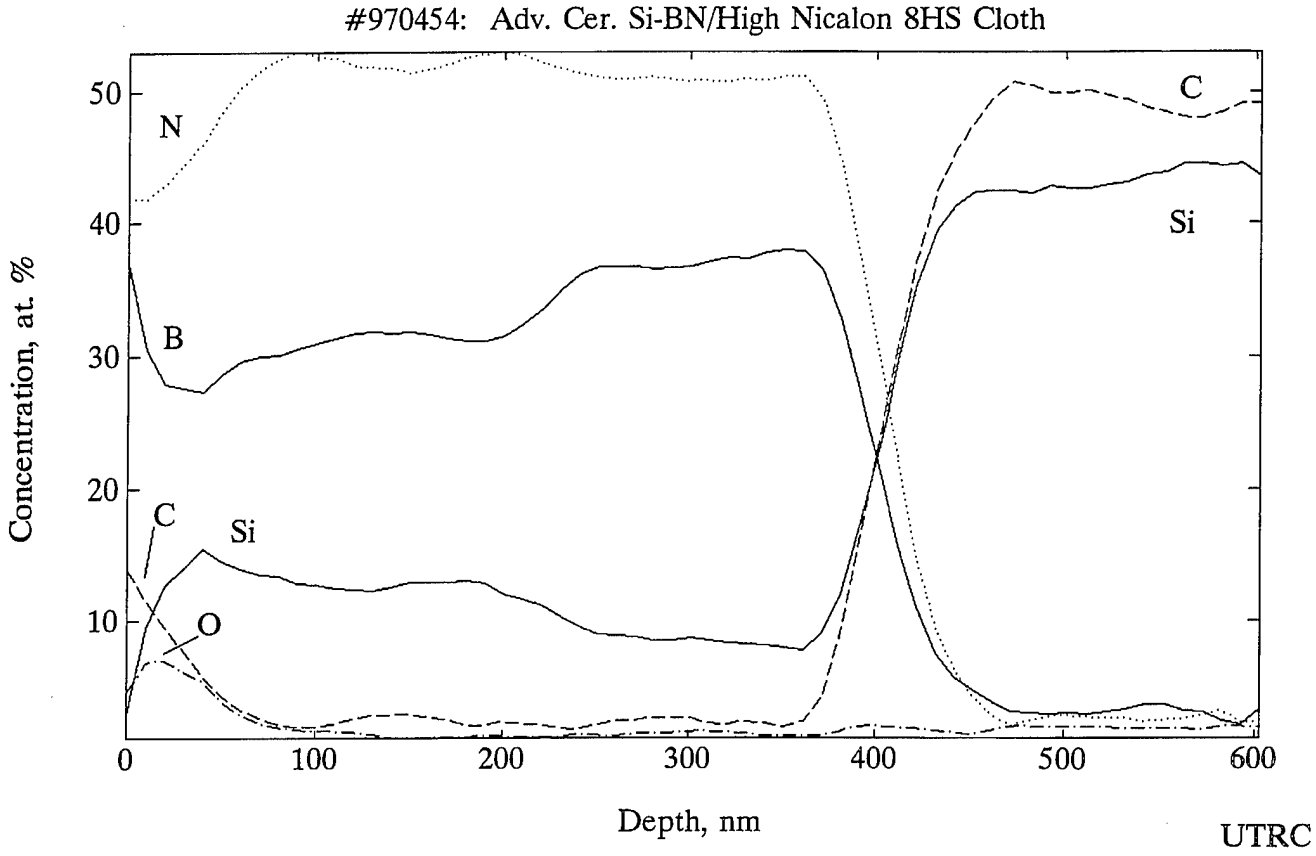
#970454: Adv. Cer. Si-BN/High Nicalon 8HS Cloth
Concentration, at. %
Depth, nm
N
B
C
Si
O
C
Si
50
40
30
20
10
0
100
200
300
400
500
600
UTRC

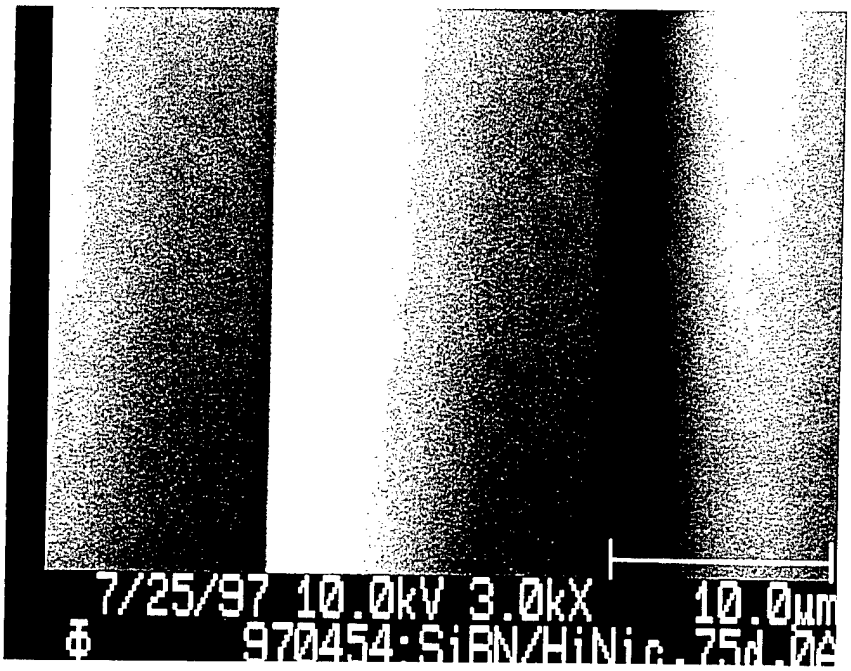
7/25/97 10.0kV 3.0kX 10.0µm
970454:SiBN/HiNic.75d.0

ADVANCED CERAMICS Si-DOPED BN COATED 8HS HI-NICALON
(Lot 970454C - End Section)

5400X

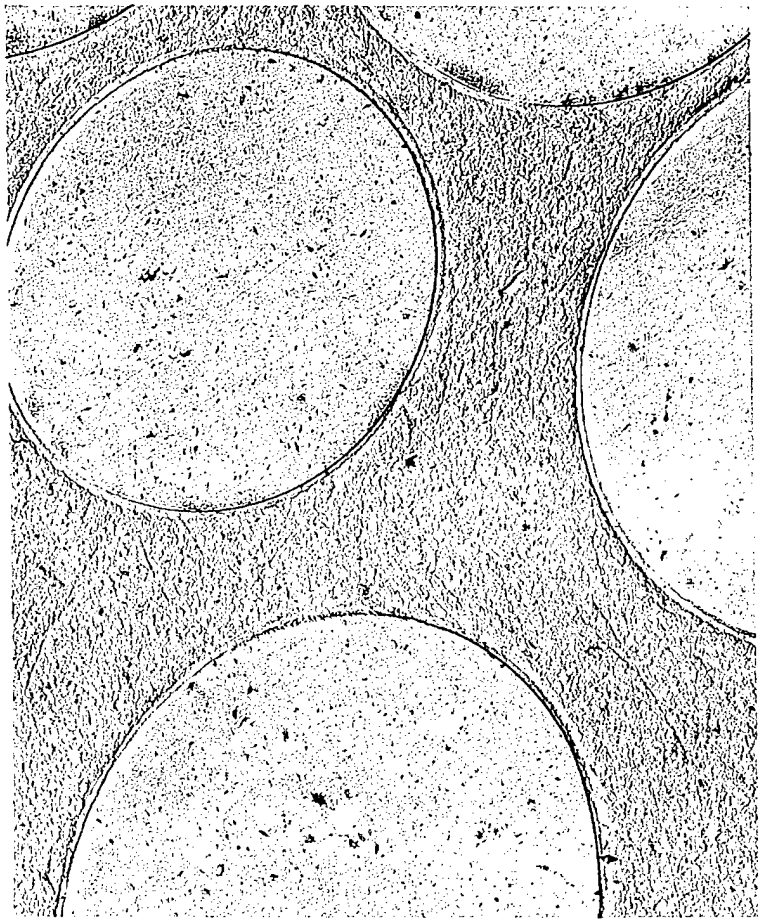

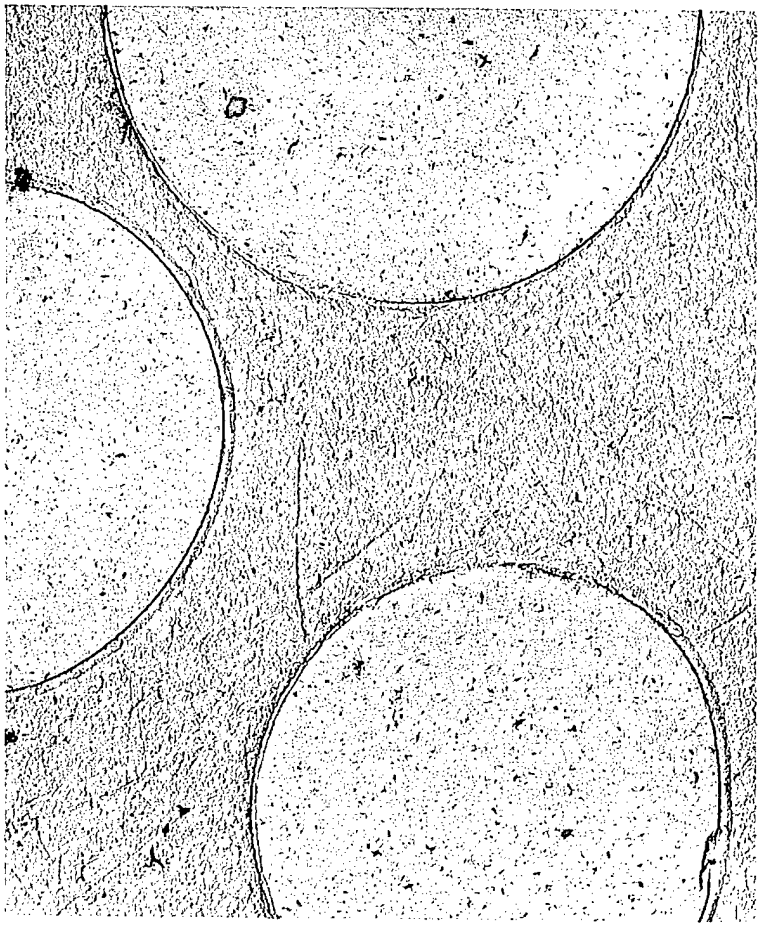

3.0μ

Fig. 42

MML 34547

United Technologies

Research Center Transmission Electron Microscope Laboratory

ADVANCED CERAMICS Si-DOPED BN COATED 8HS HI-NICALON (Lot 970454C - End Section)

Fig. 43

437,000X

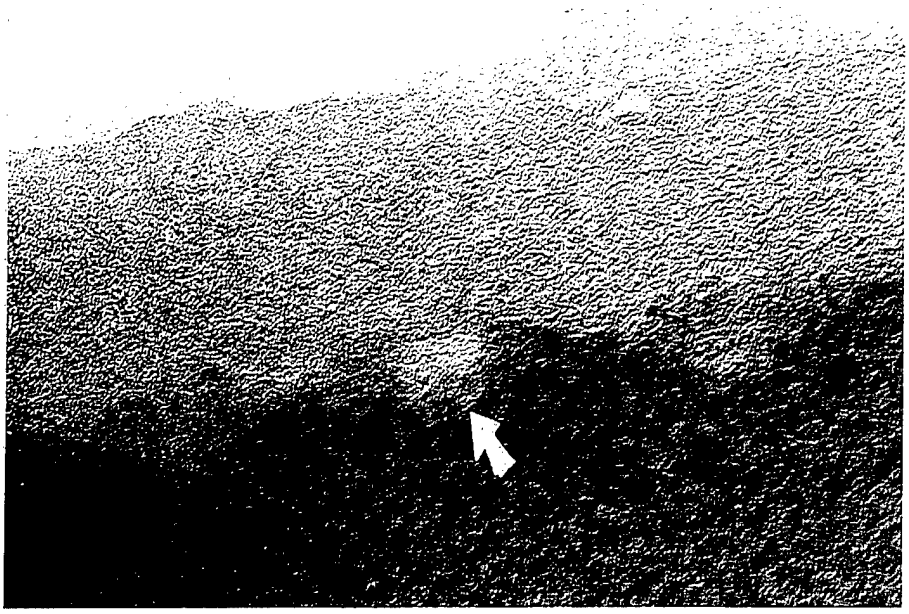

0.05μ

182,000X

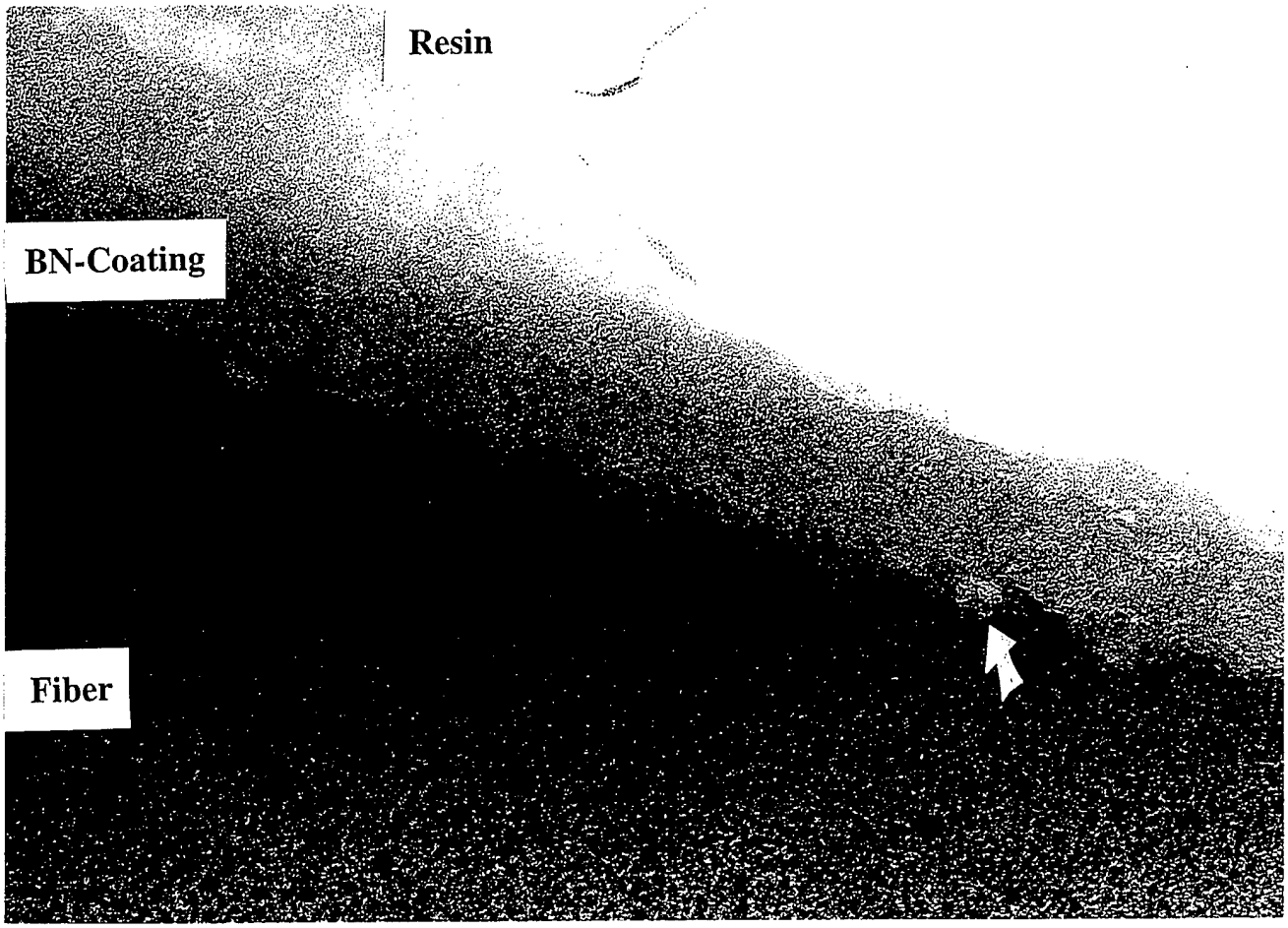

0.1μ

ML 34647 UNITED TECHNOLOGIES RESEARCH CENTER TRANSMISSION ELECTRON MICROSCOPE LABORATORY

ADVANCED CERAMICS Si-DOPED BN COATED 8HS HI-NICALON
(Lot 970454C - End Section)

Fig. 44

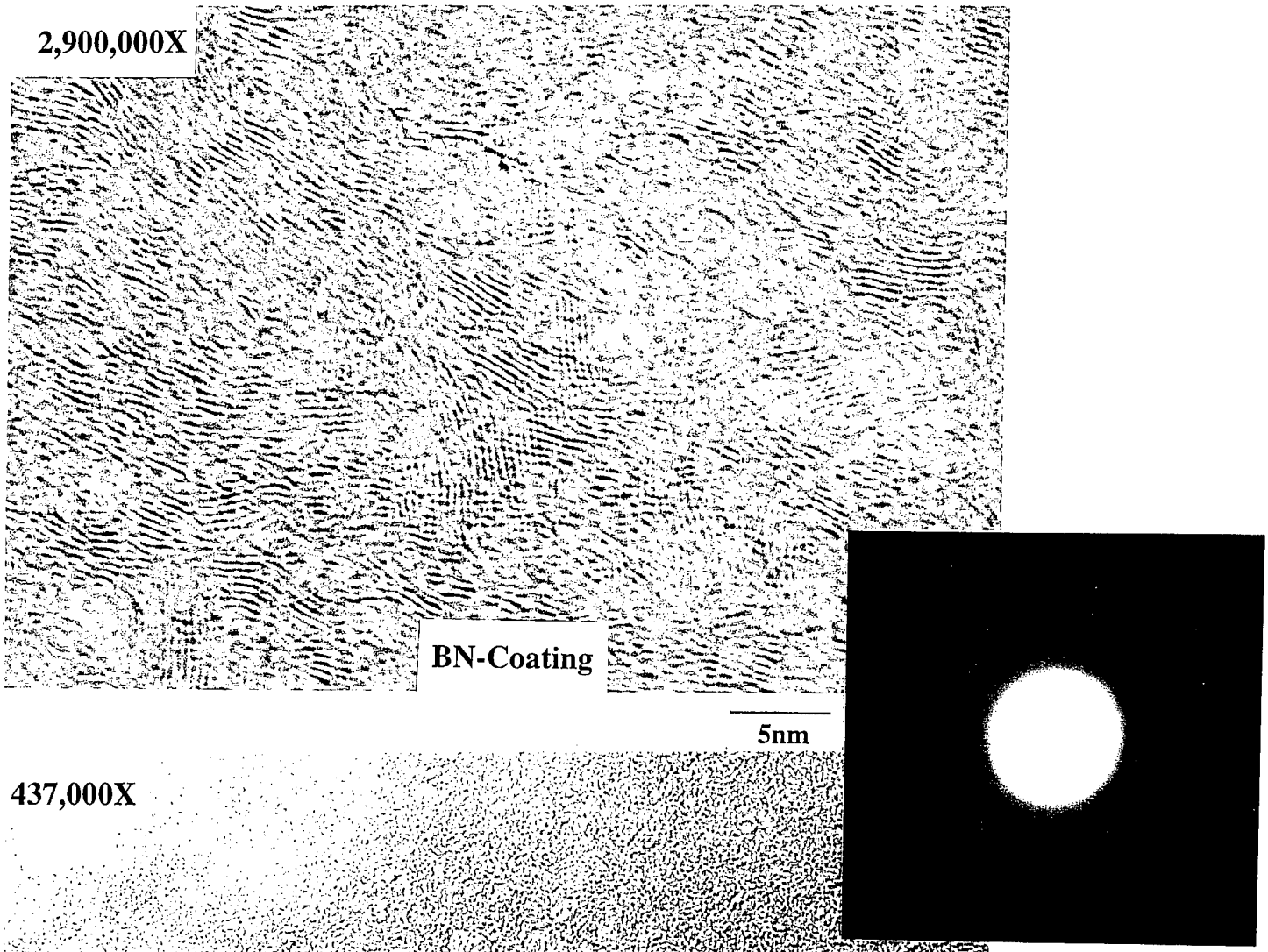

IML 34647 UNITED TECHNOLOGIES RESEARCH CENTER TRANSMISSION ELECTRON MICROSCOPE LABORATORY

Fracture Surface of BMAS Matrix/Advanced Ceramics Si-Doped BN/High Nicalon 8HS Composite #24-97-1

RTσ = 21.5 ksi (170 Mpa)

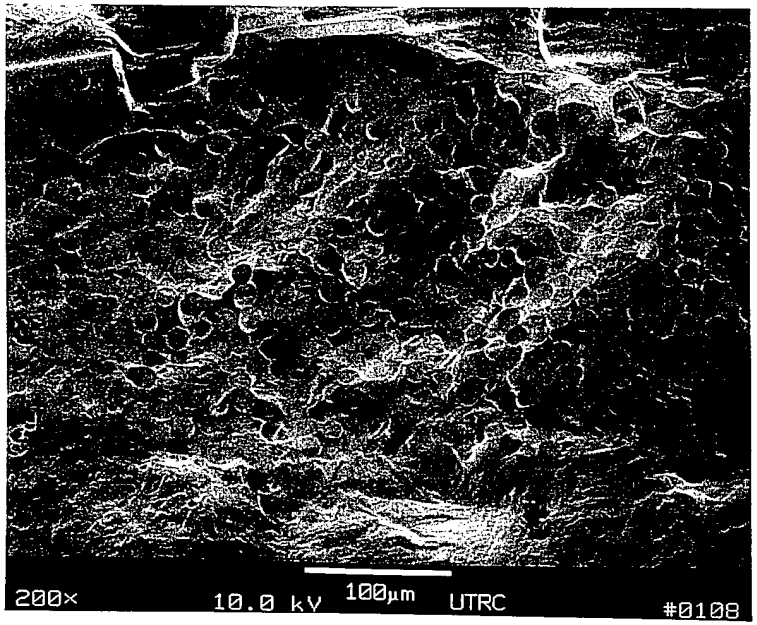

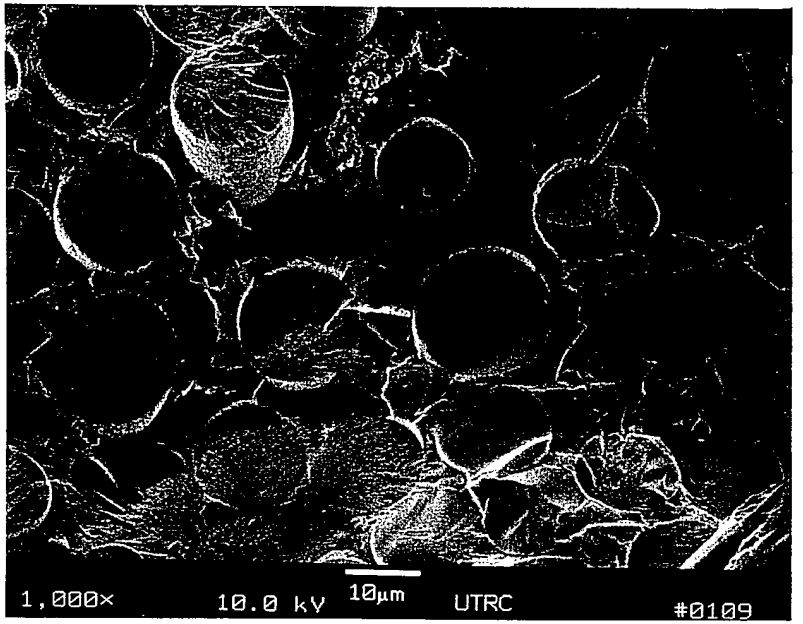

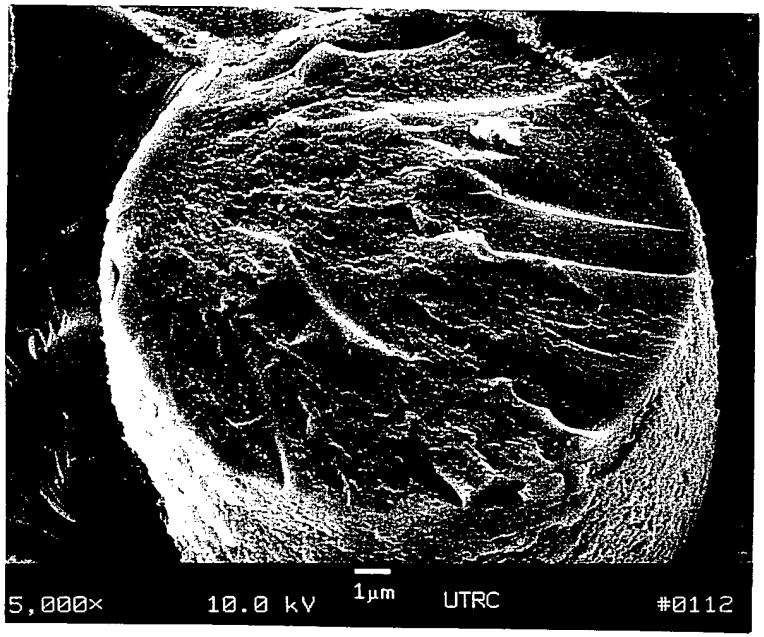

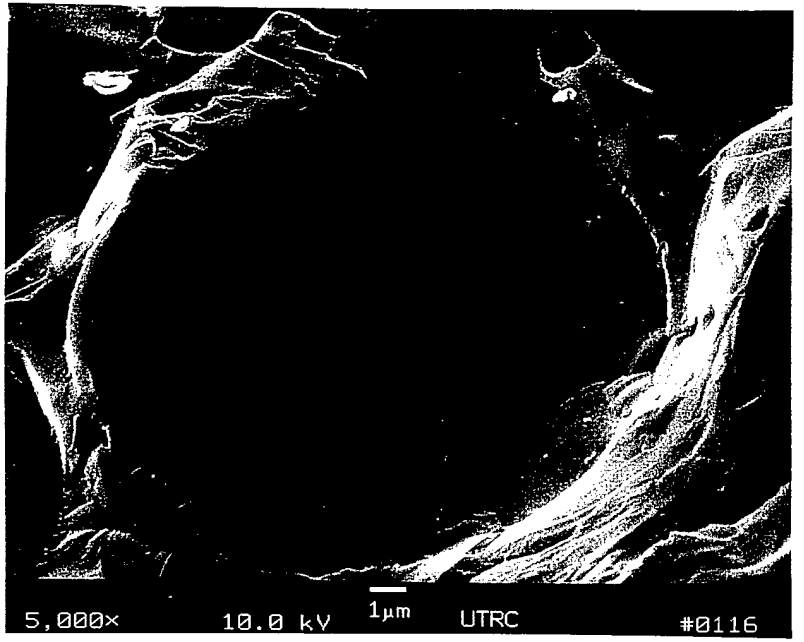

Fig. 45

BMAS MATRIX/ADVANCED CERAMICS Si-DOPED BN/8HS HIGH NICALON (RT Flex = 21.5 ksi) - COMPOSITE #24-97-1

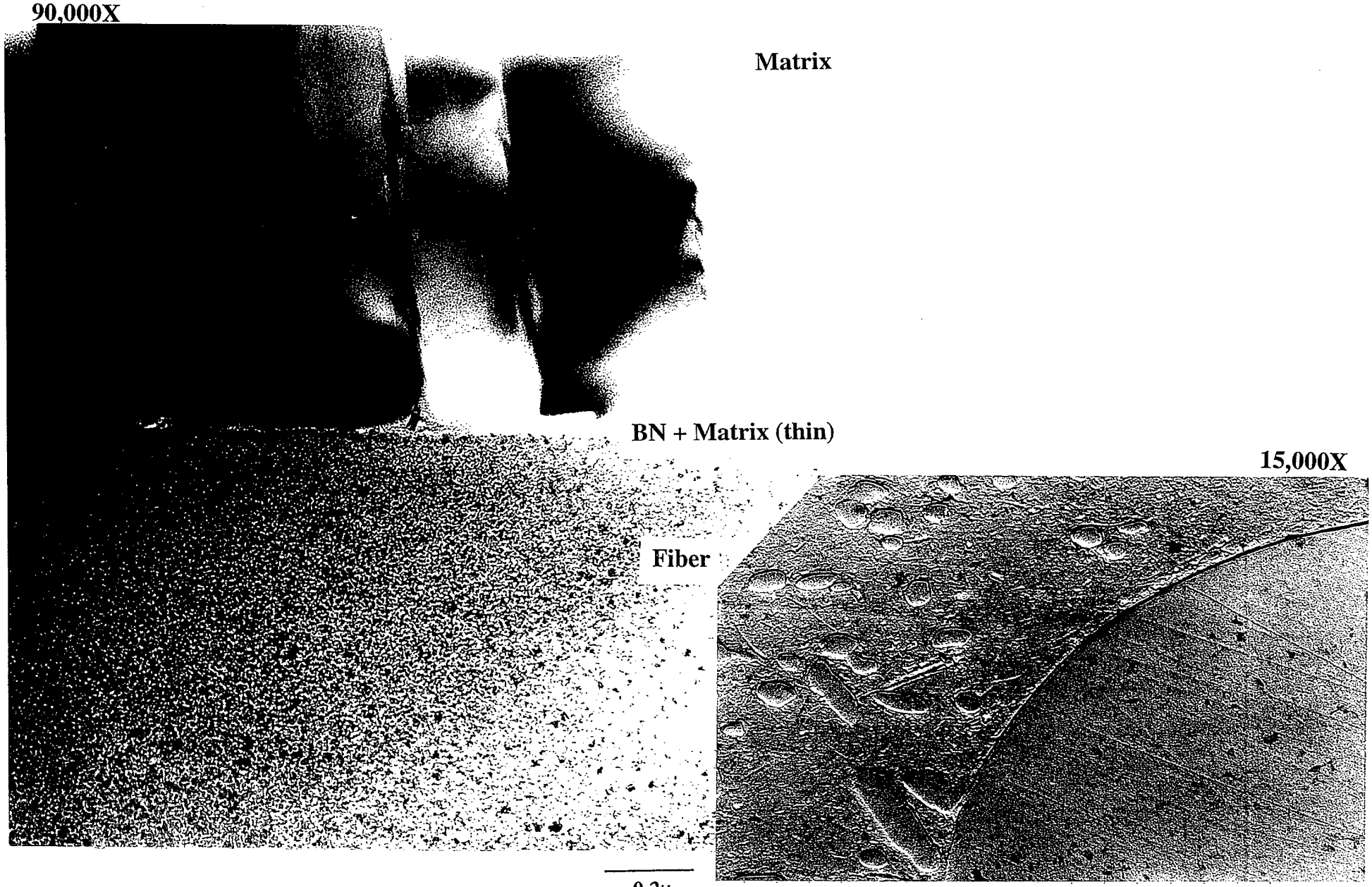

United Technologies Research Center Transmission Electron Microscope Laboratory

MML 24654

Fig. 46

BMAS MATRIX/ADVANCED CERAMICS Si-DOPED BN/8HS HIGH NICALON (RT Flex = 21.5 ksi) - COMPOSITE #24-97-1

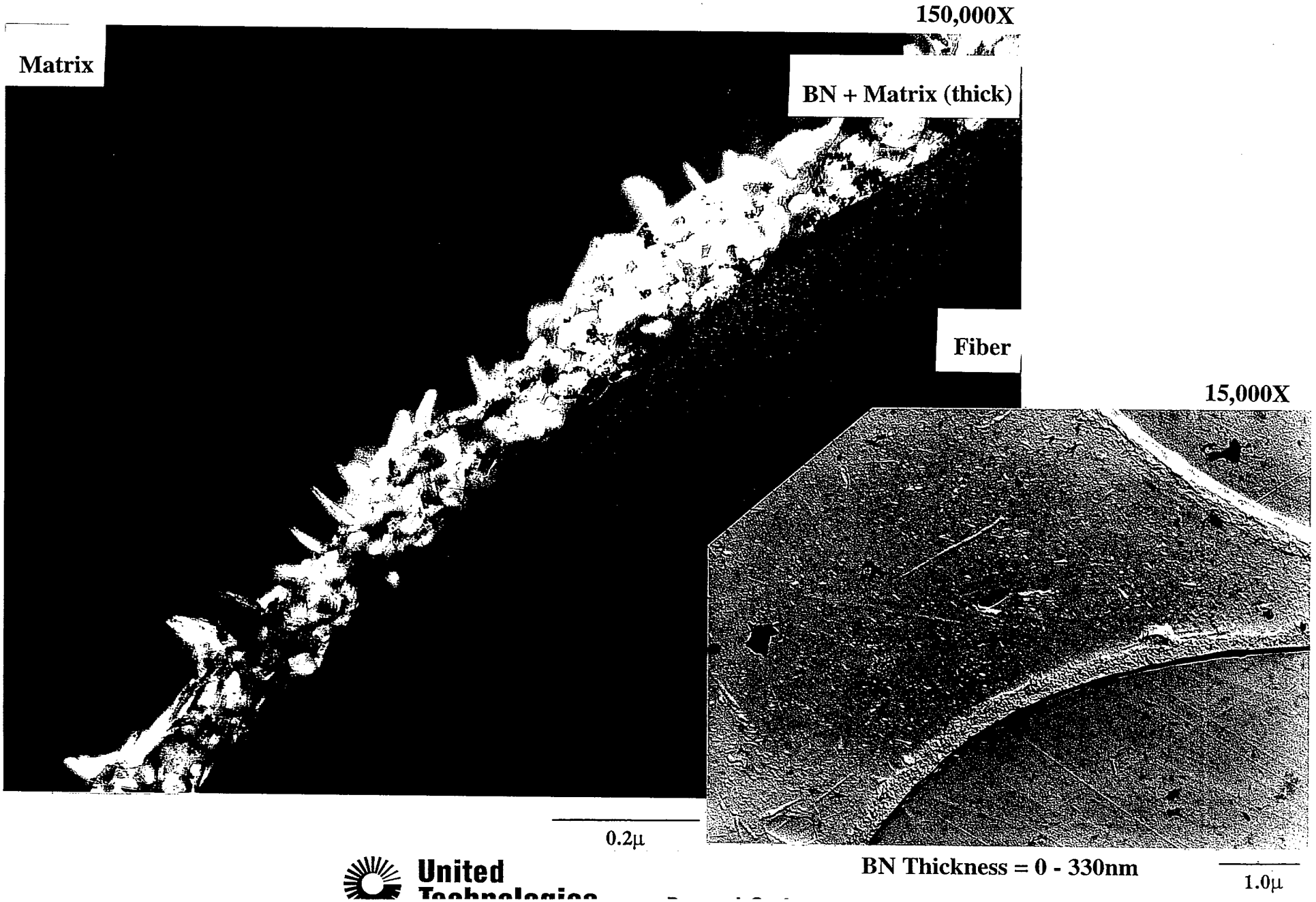

United Technologies

Fig. 47

BMAS MATRIX/ADVANCED CERAMICS Si-DOPED BN/8HS HIGH NICALON (RT Flex = 21.5 ksi) - COMPOSITE #24-97-1

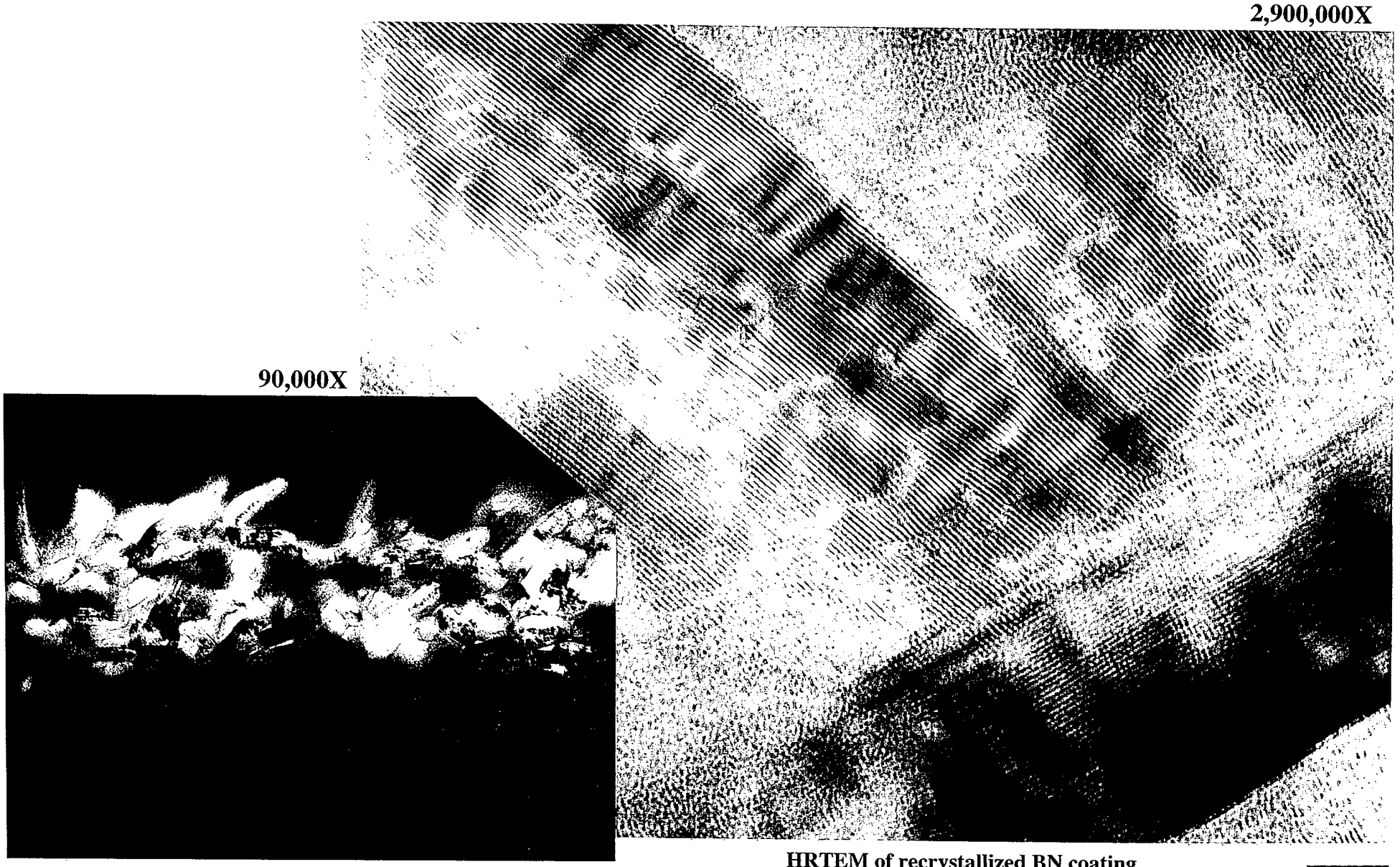

HRTEM of recrystallized BN coating

United Technologies

Fig. 48

Scanning Auger Interfacial Chemistry of BMAS Matrix/Advanced Ceramics Si-Doped BN/High Nicalon 8HS Composite #24-97-1

RTσ = 21.5 ksi (170 Mpa)

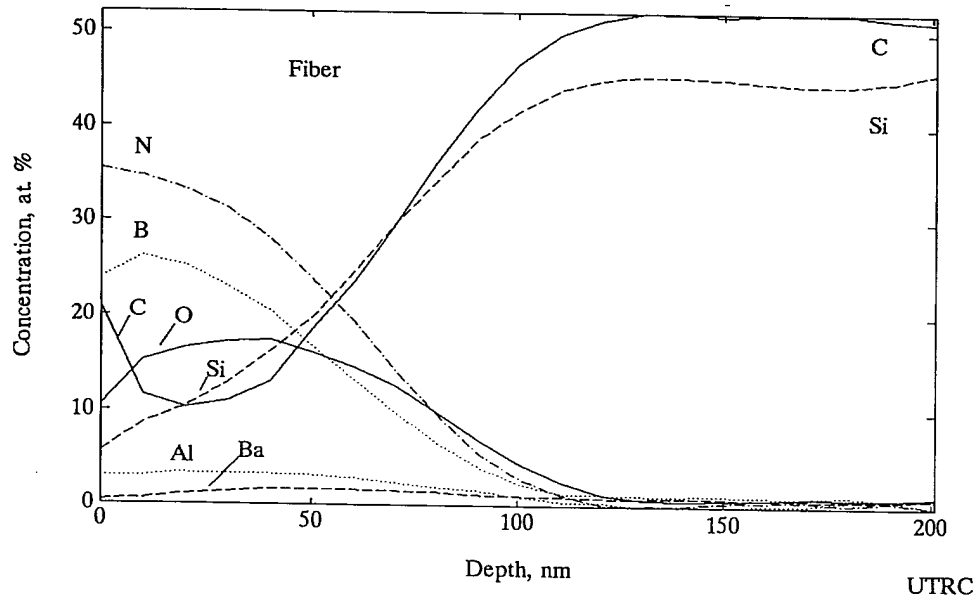

UTRC

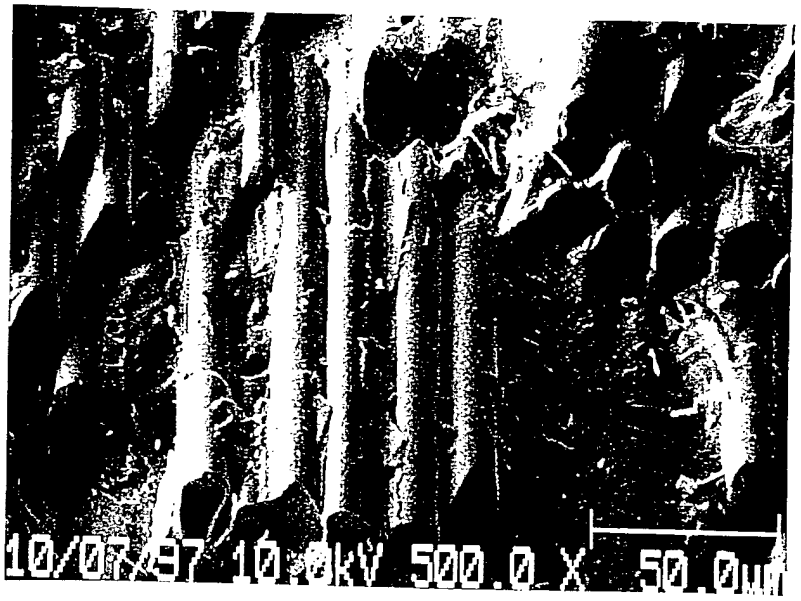

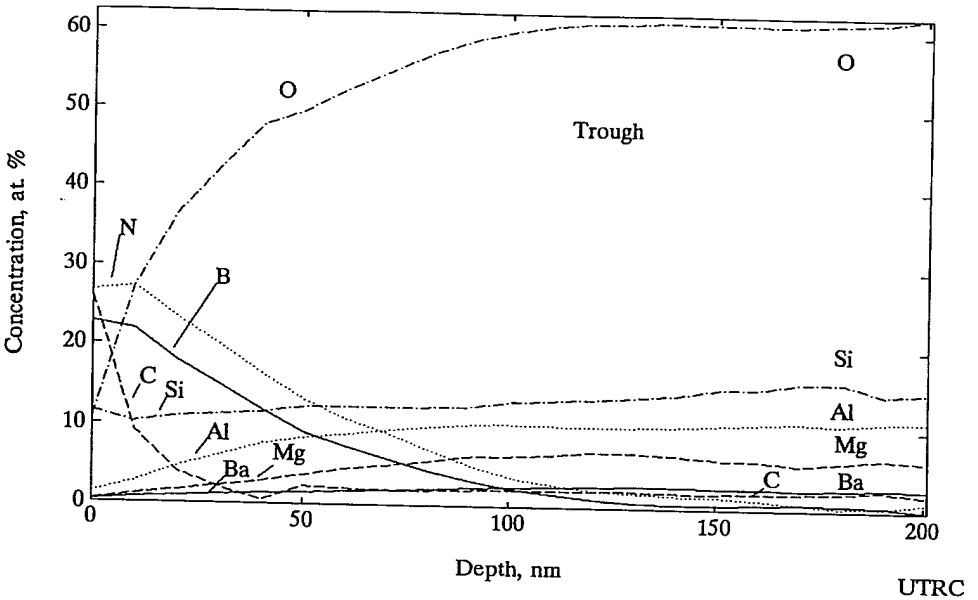

UTRC

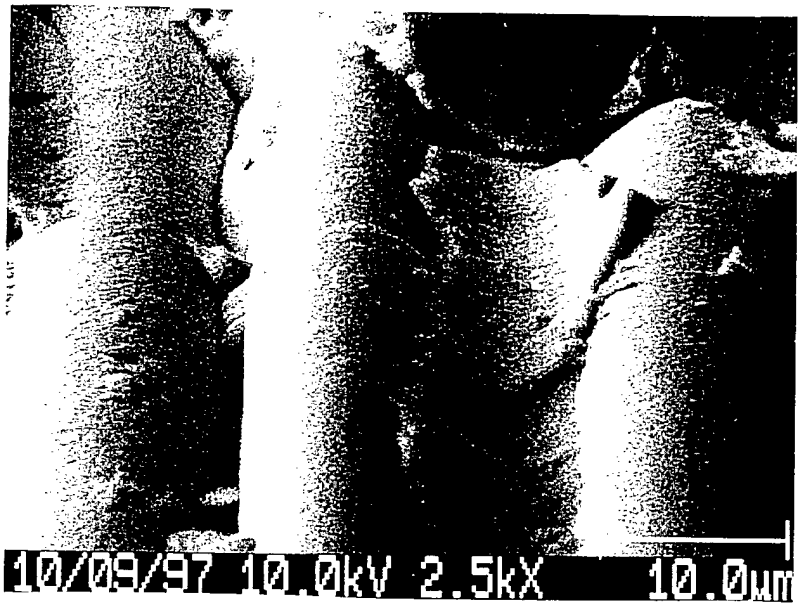

Fig. 49

OPTICAL/TEM CHARACTERIZATION OF BMAS/3M SiC/BN-COATED/NEXTEL 720 FIBER COMPOSITE - #146-94-3 (Ceramed)

1000X

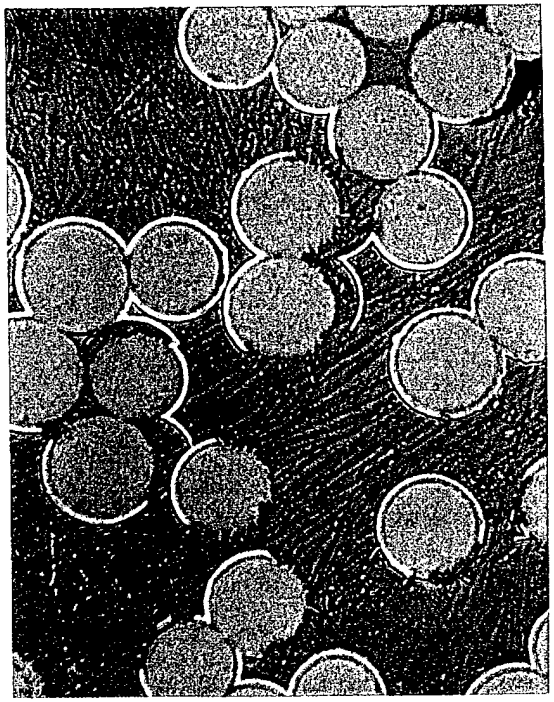

5400X

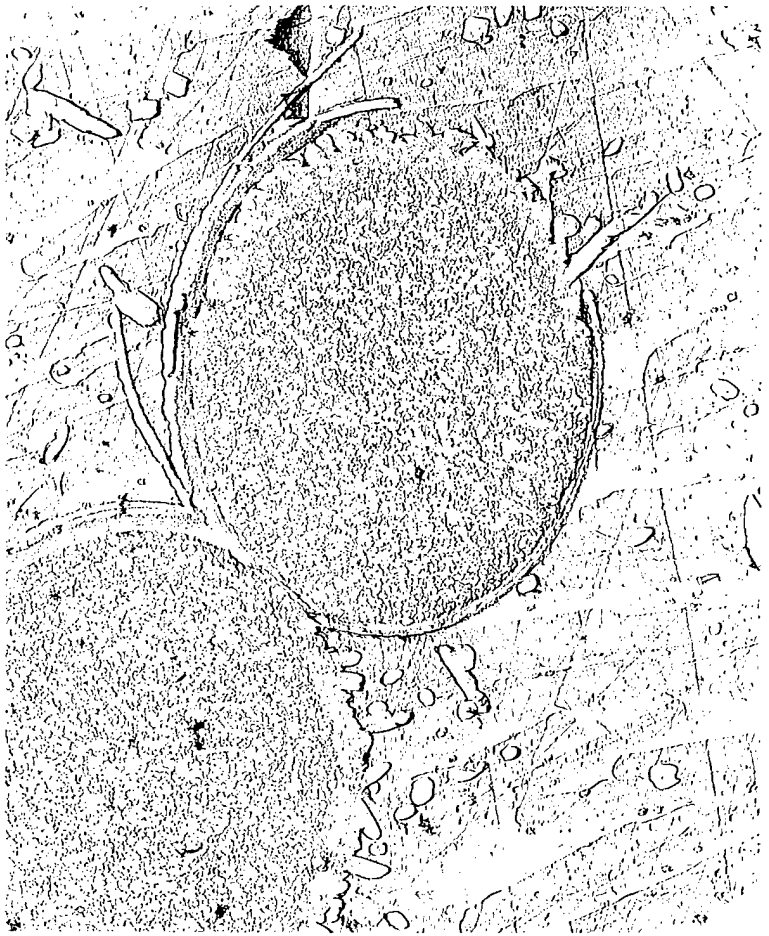

Fiber/matrix reactions were observed frequently and were always associated with SiC/BN coating debonds.

3.0μ

UNITED TECHNOLOGIES RESEARCH CENTER

TRANSMISSION ELECTRON MICROSCOPE LABORATORY

MML 34405

Fig. 50

TEM CHARACTERIZATION OF BMAS/3M BN-COATED/NEXTEL 720 FIBER COMPOSITE - #145-94-3 (Ceramed)

5400X

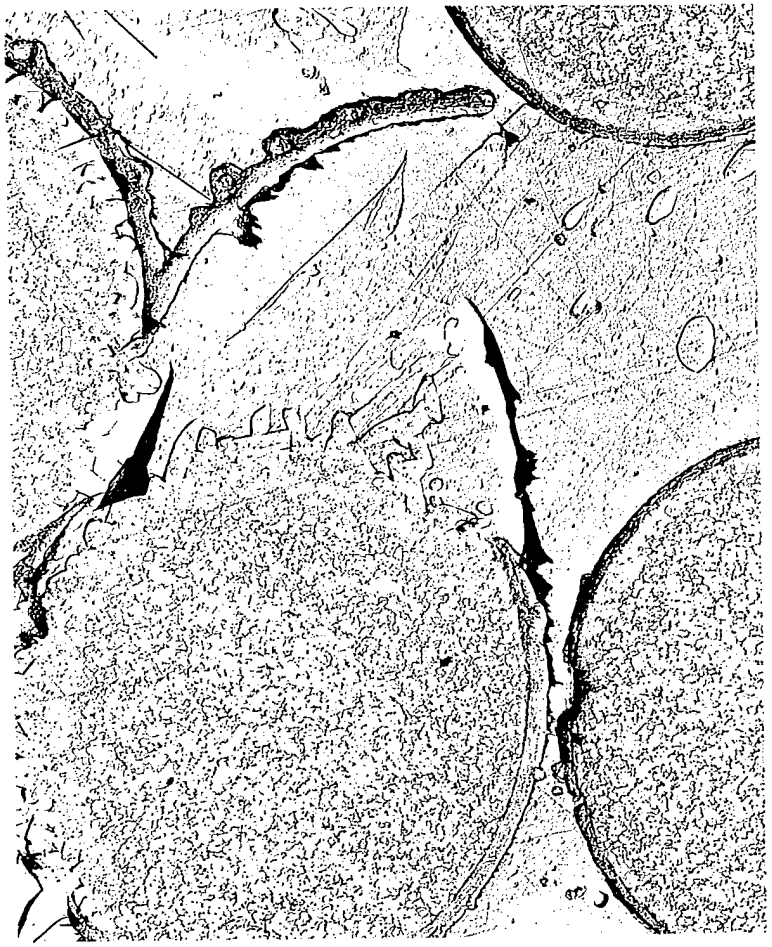

Fiber/matrix reactions were observed infrequently, but were always associated with BN-coating debonds

3.0μ

15000X

BN Coating intact, no fiber/matrix reaction

1.0μ

MML 34405

UNITED TECHNOLOGIES RESEARCH CENTER

TRANSMISSION ELECTRON MICROSCOPE LABORATORY

Fig. 51

COMPOSITE #31-96-2 (RT 3ptσ = 36 ksi, Ef = 0.10%)

Edge of tow

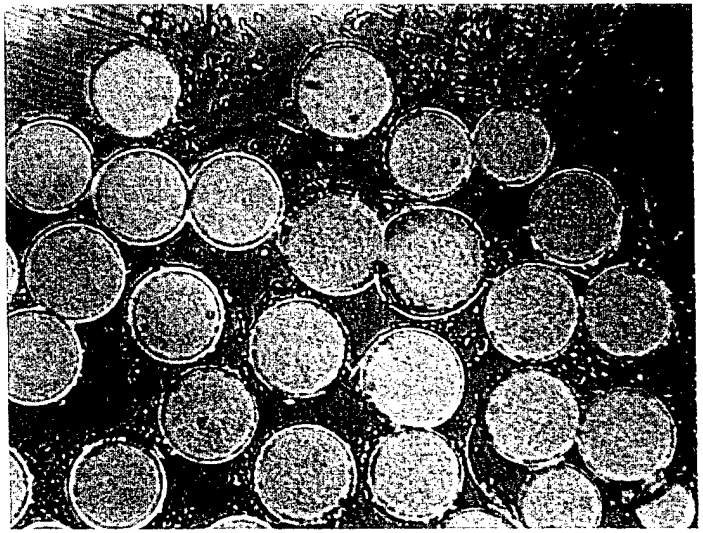

Fiber/matrix reaction (arrow)

1000X

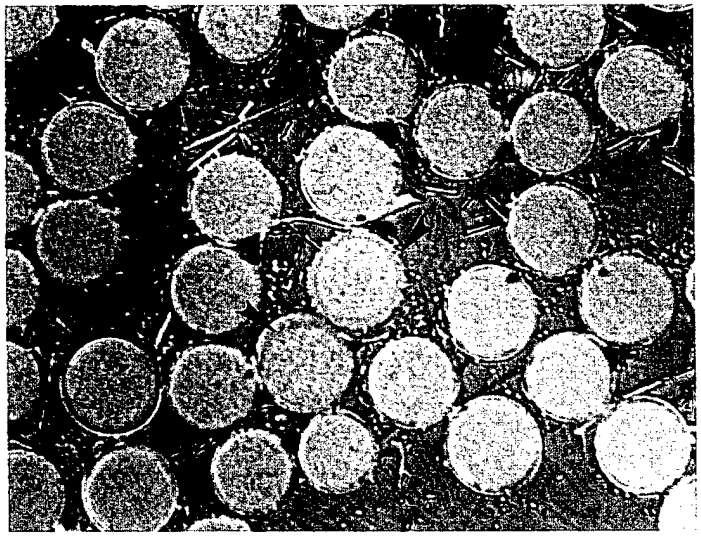

Middle of tow

5400X

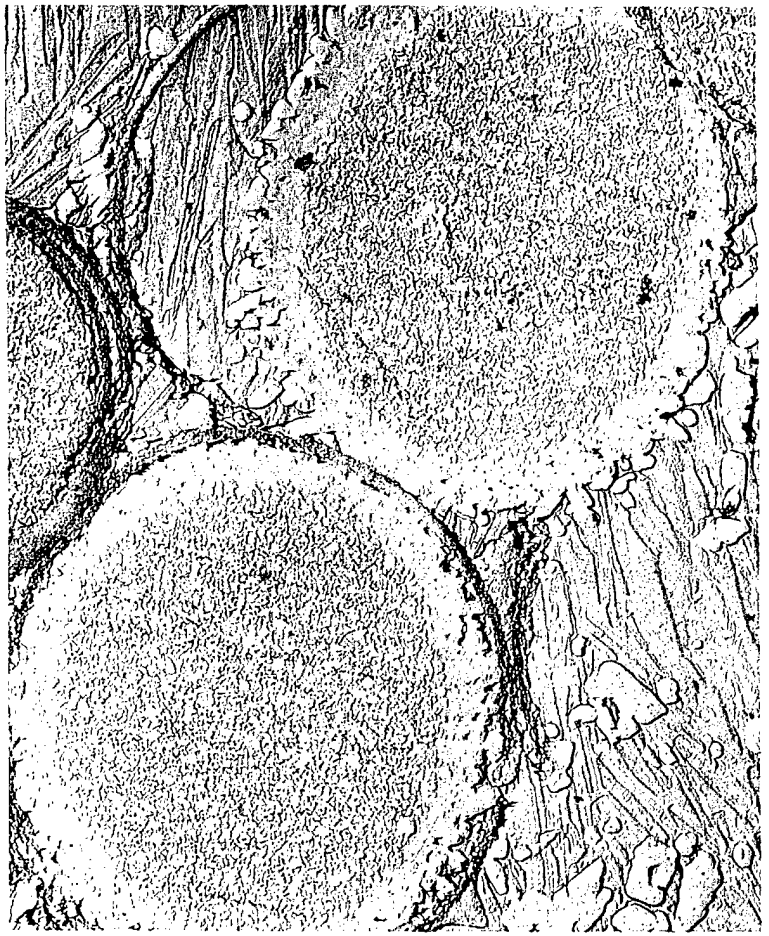

Note carbon coating debond and reaction zone encircling fiber

3.0μ

MML 34571

UNITED TECHNOLOGIES RESEARCH CENTER

TRANSMISSION ELECTRON MICROSCOPE LABORATORY

Fig. 52

BMAS MATRIX/THICK CARBON COATED NEXTEL 720 FIBER (0°/90°) CERAMED COMPOSITE #31-96-2 (RT 3ptσ = 36 ksi, Ef = 0.10%

9000X

2.0μ

15000X

1.0μ

Note layered structure of carbon coating

MML 34571

UNITED TECHNOLOGIES RESEARCH CENTER

TRANSMISSION ELECTRON MICROSCOPE LABORATORY

Fig. 53

BMAS MATRIX/THICK CARBON COATED NEXTEL 720 FIBER (0°/90°) CERAMED
+ 550°C, 100 hrs, O2 - COMPOSITE #31-96-7 (RT 3ptσ = 26 ksi, Ef = 0.15%)

9000X

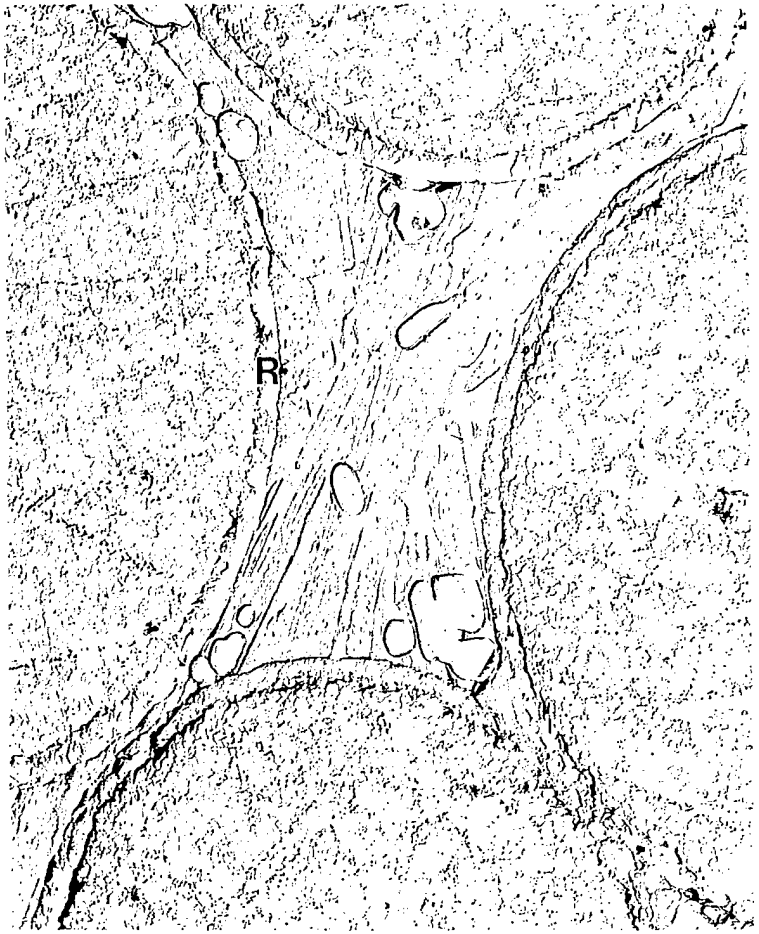

Resin = R

2.0μ

15000X

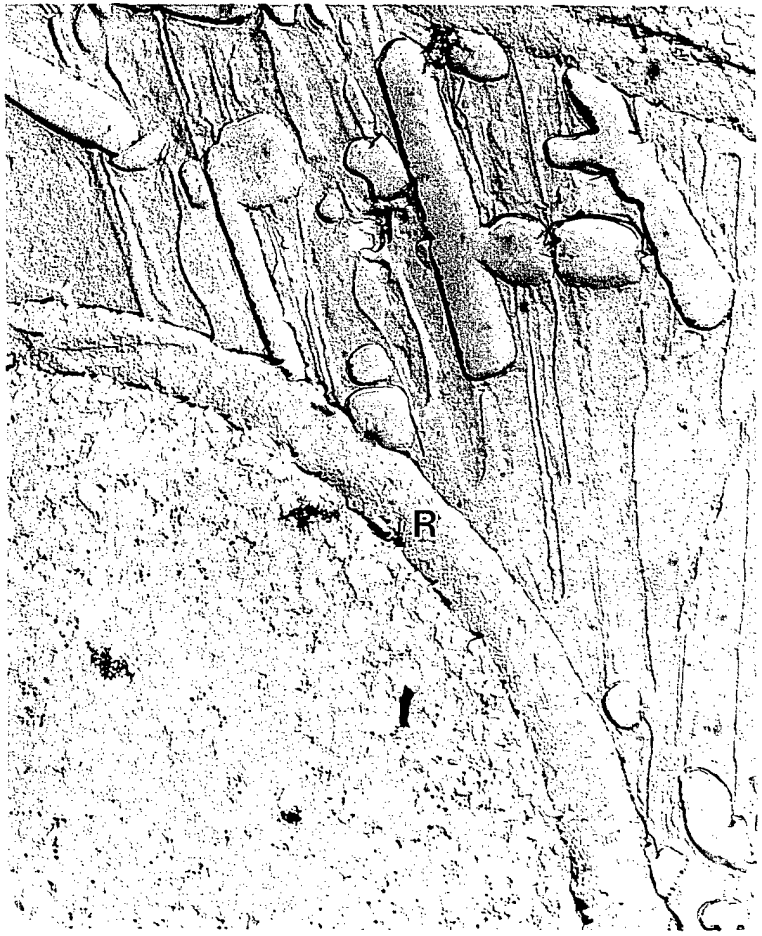

Note fiber/matrix interface entirely depleted of carbon coating, interface infiltrated with resin

1.0μ

MML 34571

UNITED TECHNOLOGIES RESEARCH CENTER

TRANSMISSION ELECTRON MICROSCOPE LABORATORY

Fig. 54

+ 550°C, 100 hrs, O2 - COMPOSITE #31-96-7 (RT 3ptσ = 26 ksi, Ef = 0.15%)

Edge of tow

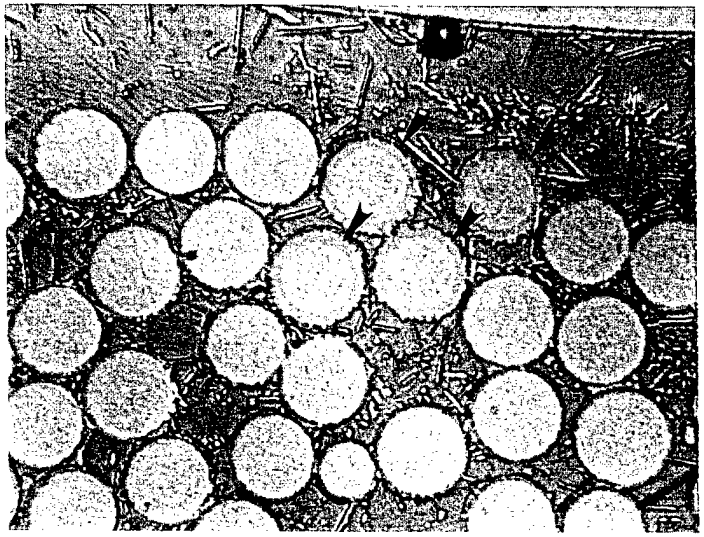

Fiber/matrix reaction (arrow) 1000X

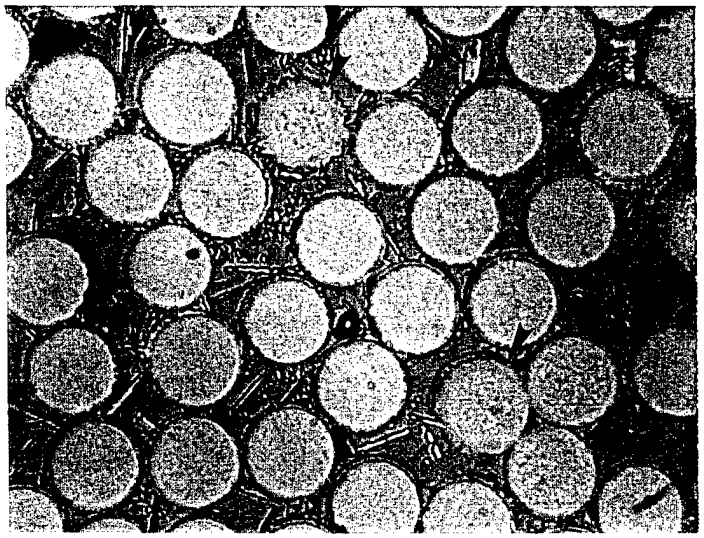

Middle of tow

5400X

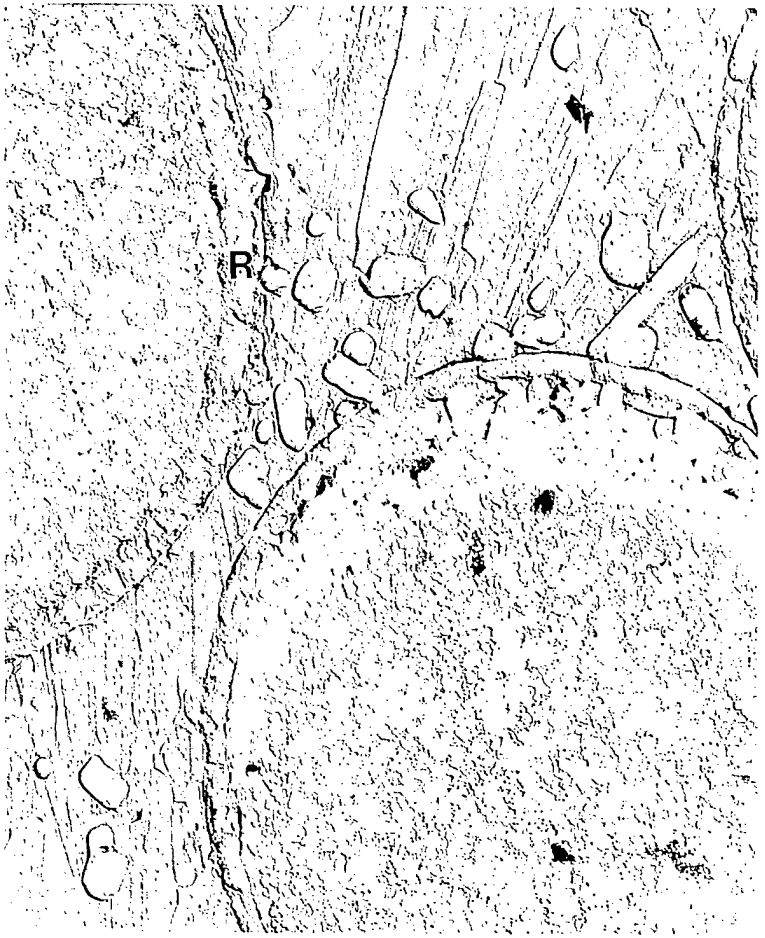

Resin = R

Note fiber/matrix interface entirely depleted of carbon coating, interface infiltrated with resin

3.0μ

MML 34571

UNITED TECHNOLOGIES RESEARCH CENTER

TRANSMISSION ELECTRON MICROSCOPE LABORATORY

Fig. 55

Scanning Auger Analysis of AFML Monazite (LaPO4) Coated Nextel 720 Fibers

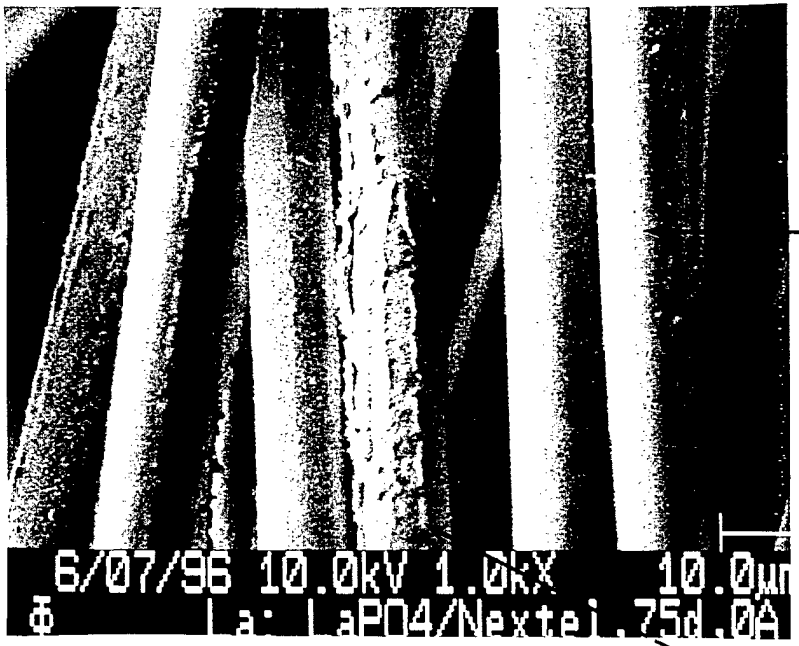

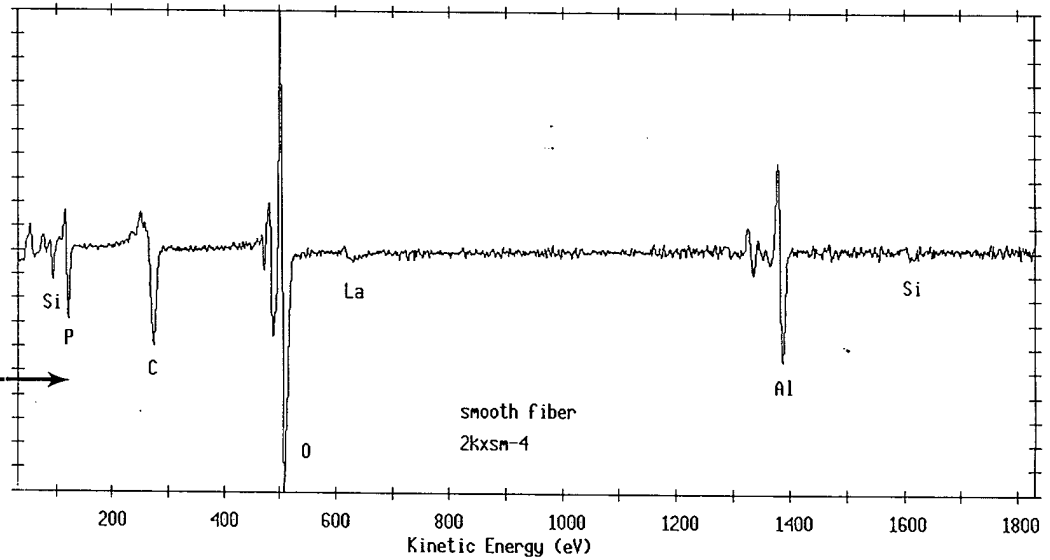

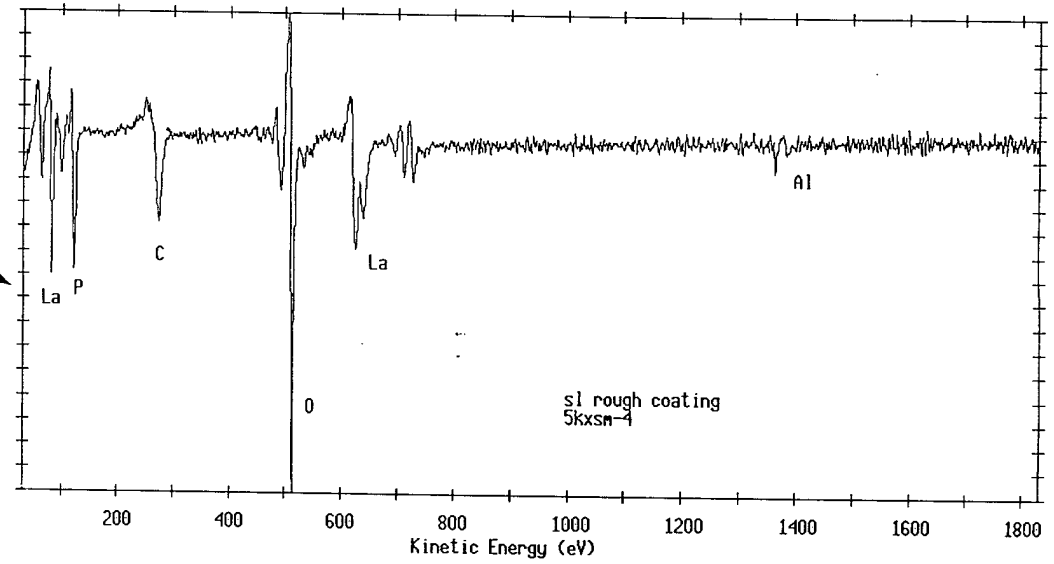

Fig. 56

BMAS/AFML MONAZITE (2 Layer) COATED NEXTEL 720 (0/90°) COMPOSITE #34-96

400X

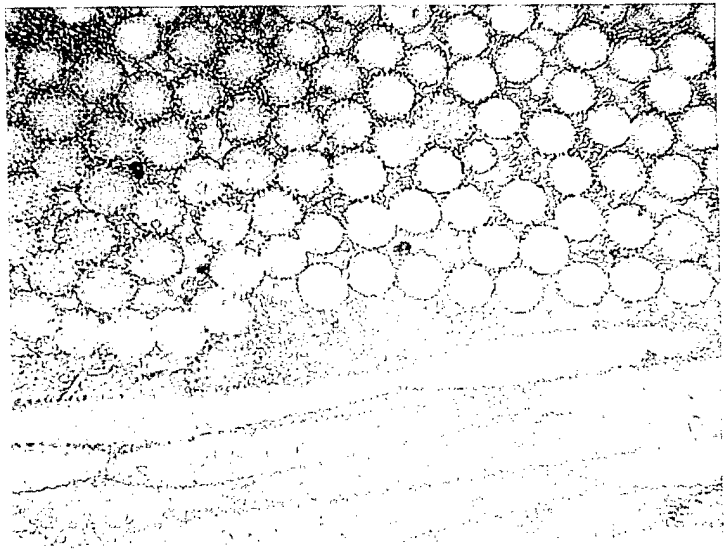

5400X

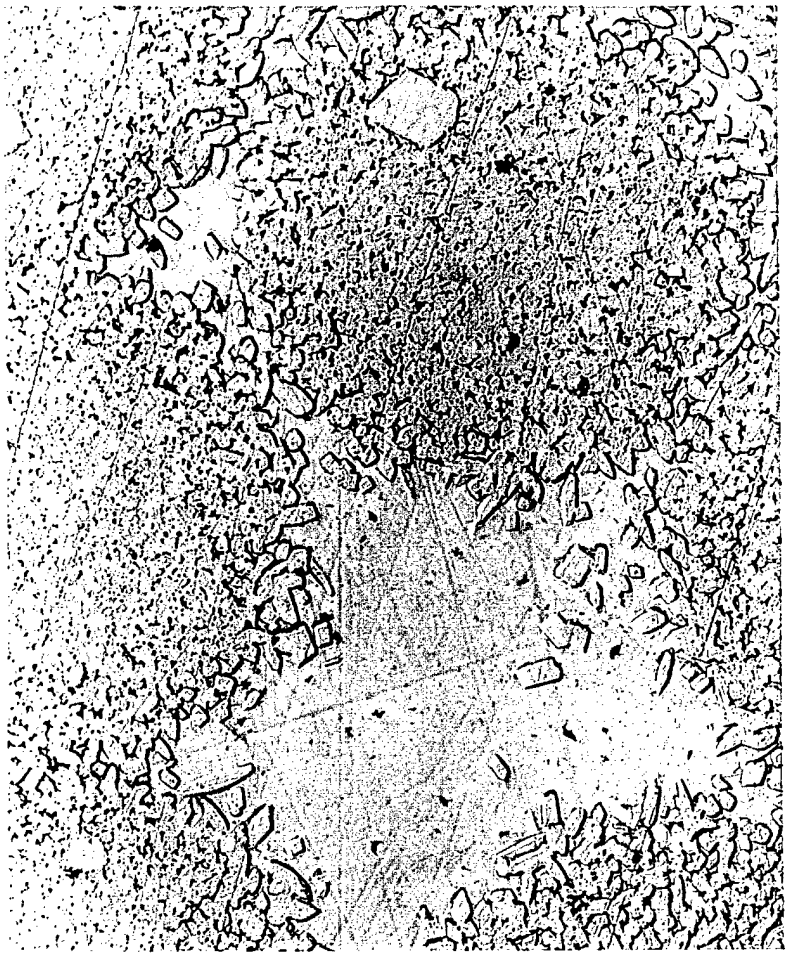

3.0μ

UNITED TECHNOLOGIES RESEARCH CENTER

TRANSMISSION ELECTRON MICROSCOPE LABORATORY

Fig. 57

Scanning Auger Depth Profile

University of Florida SiC Fiber (UF-294)

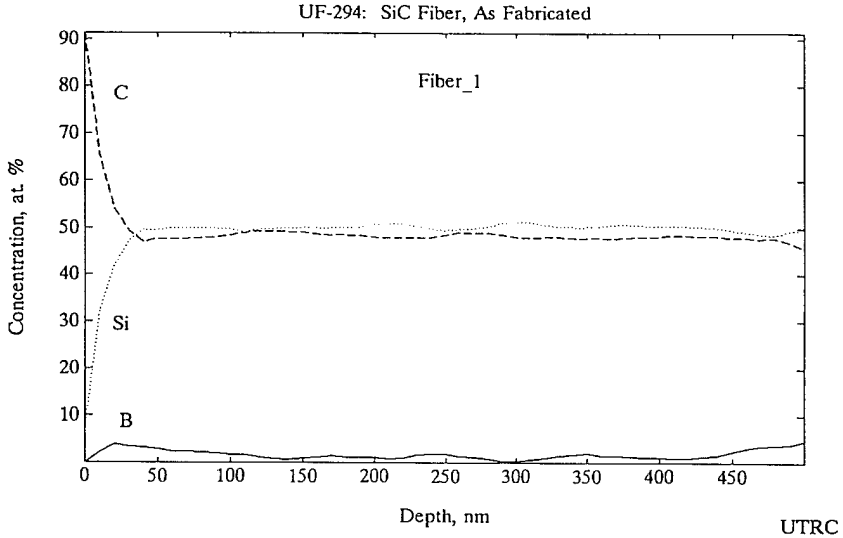

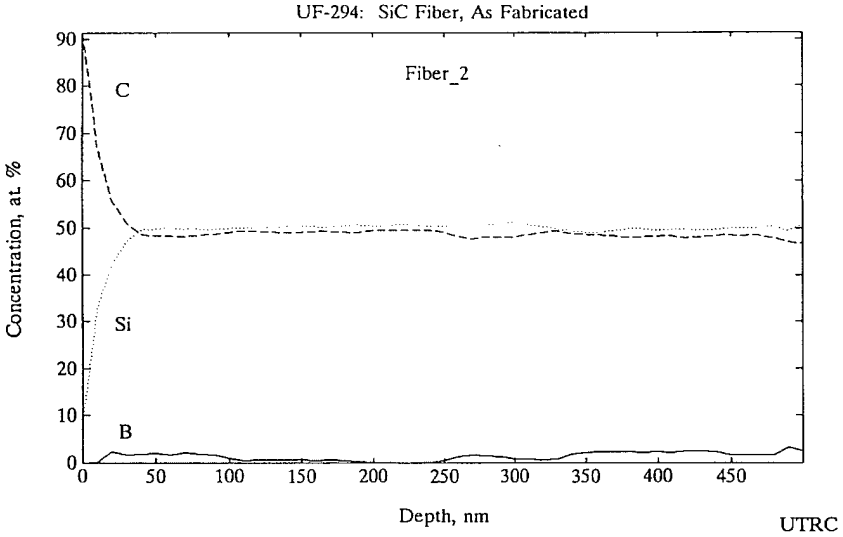

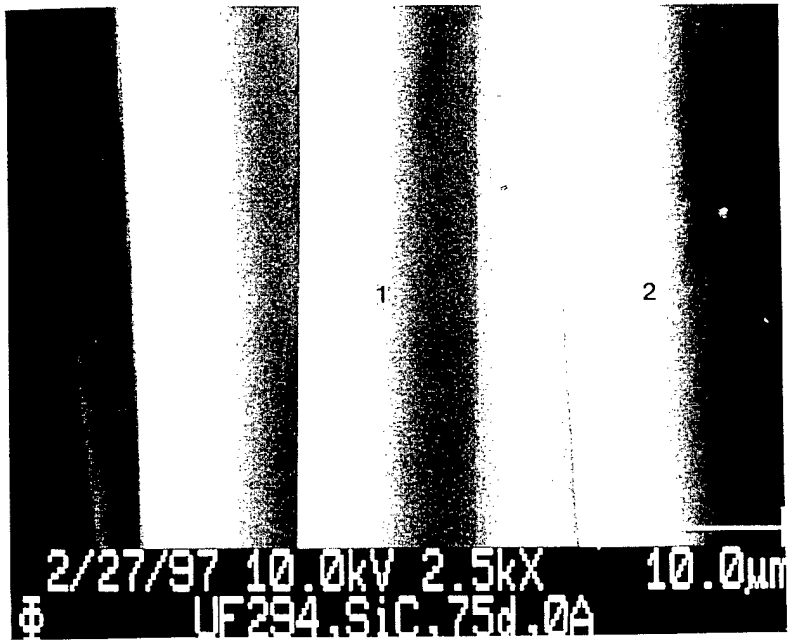

Fig. 58

UNIVERSITY OF FLORIDA SiC FIBER

#UF-294

A. Edge of Fiber

200 nm

B. Center of Fiber

200 nm

Fig. 59

Scanning Auger Depth Profile

University of Florida BN Coated SiC Fiber-Black Color (UF-294-BN)

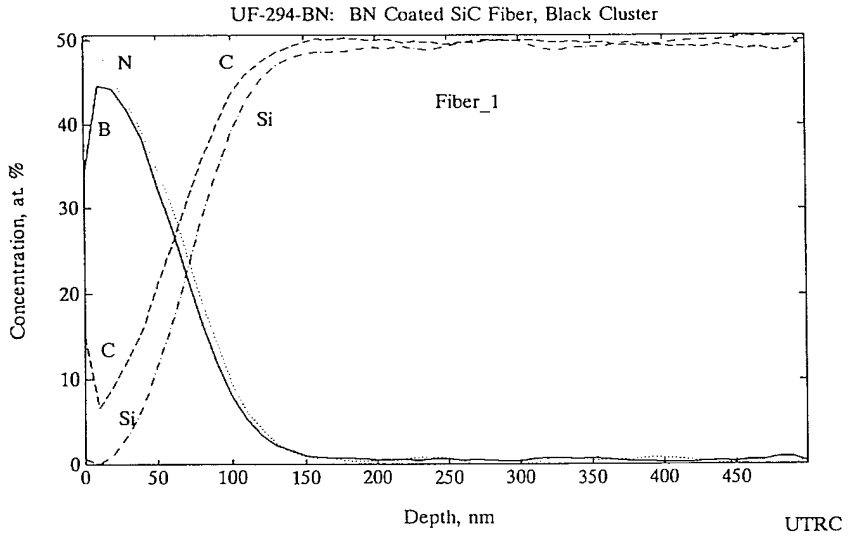

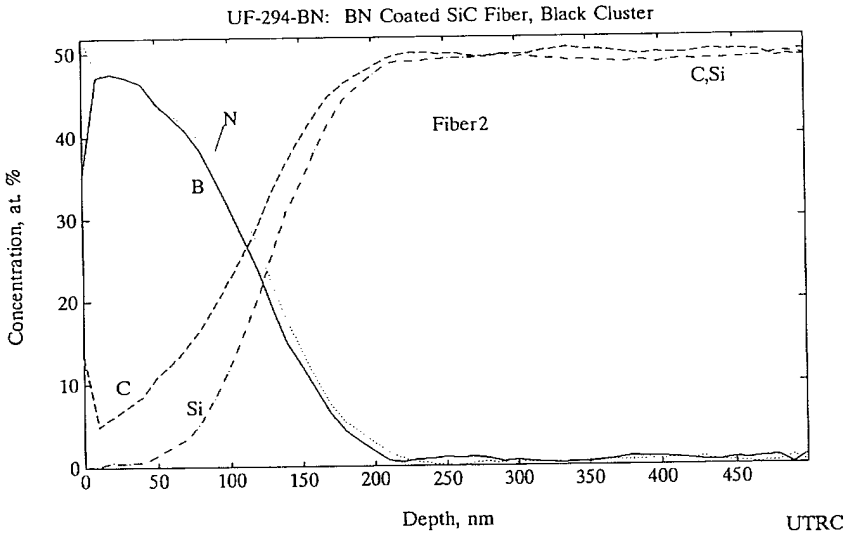

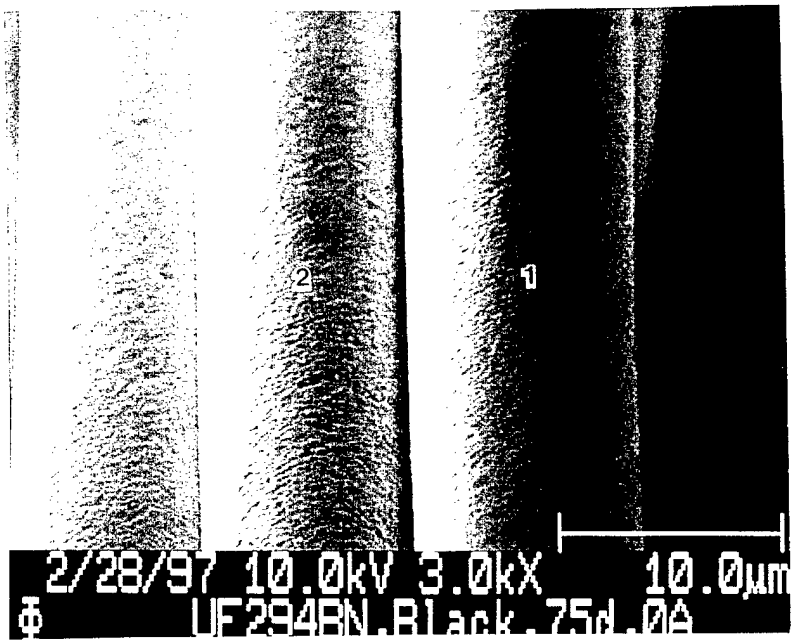

Fig. 60

Scanning Auger Depth Profile

University of Florida BN Coated SiC Fiber (UF - 364-4)

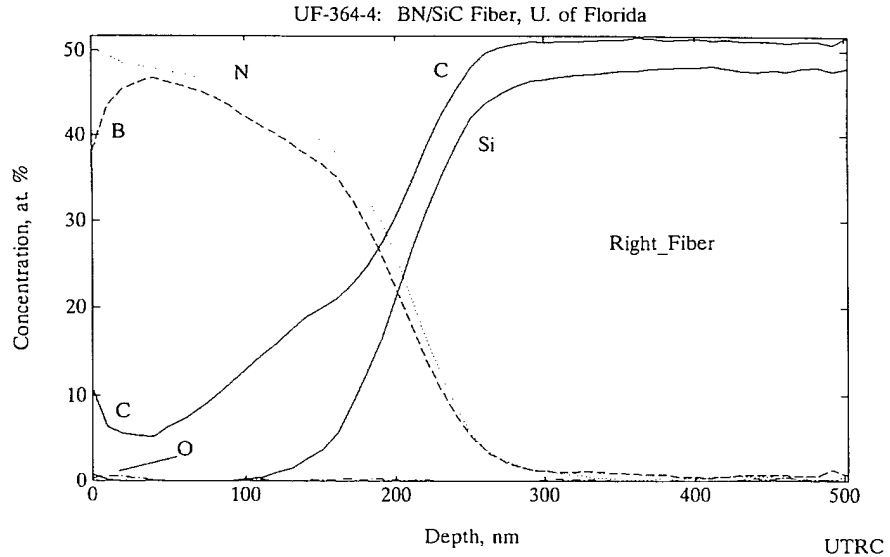

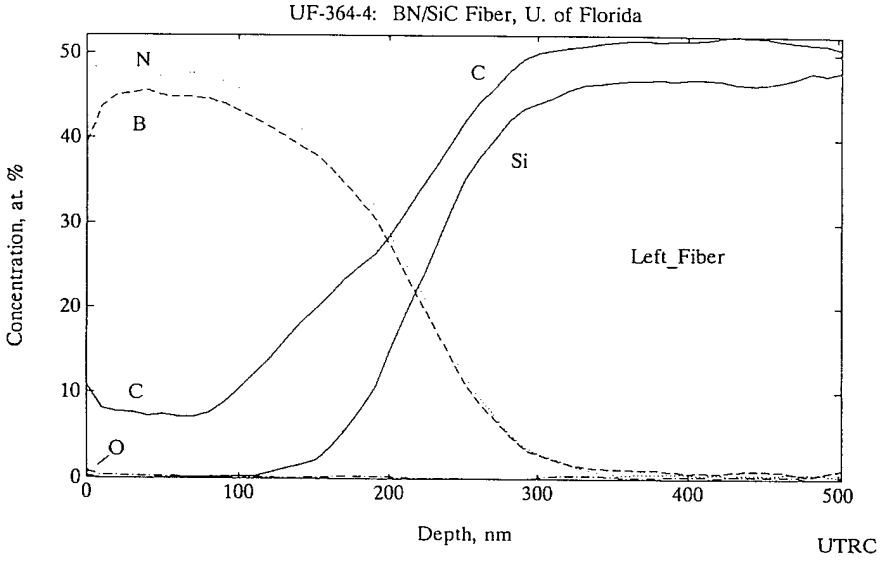

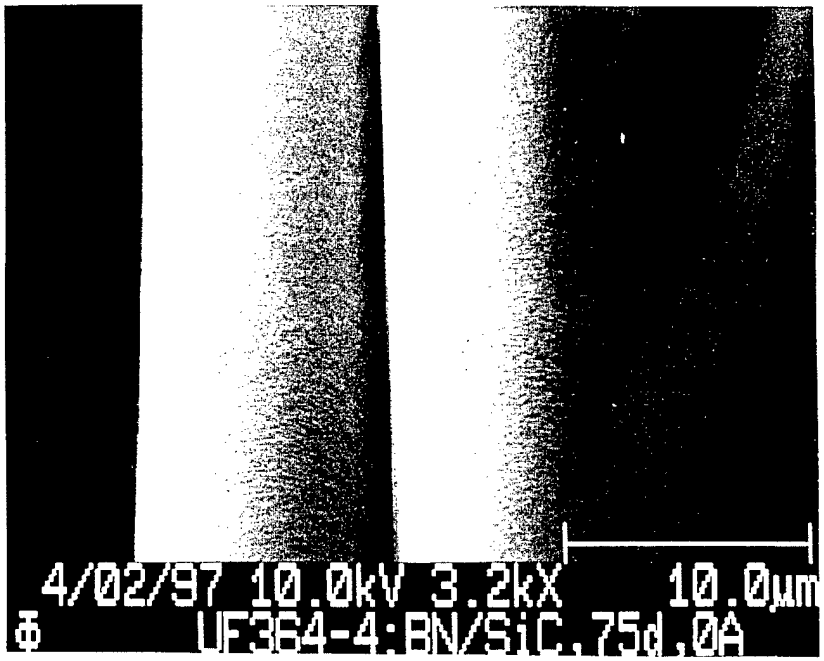

Fig. 61

University of Florida BN-coated SiC Fiber
UF 364-4

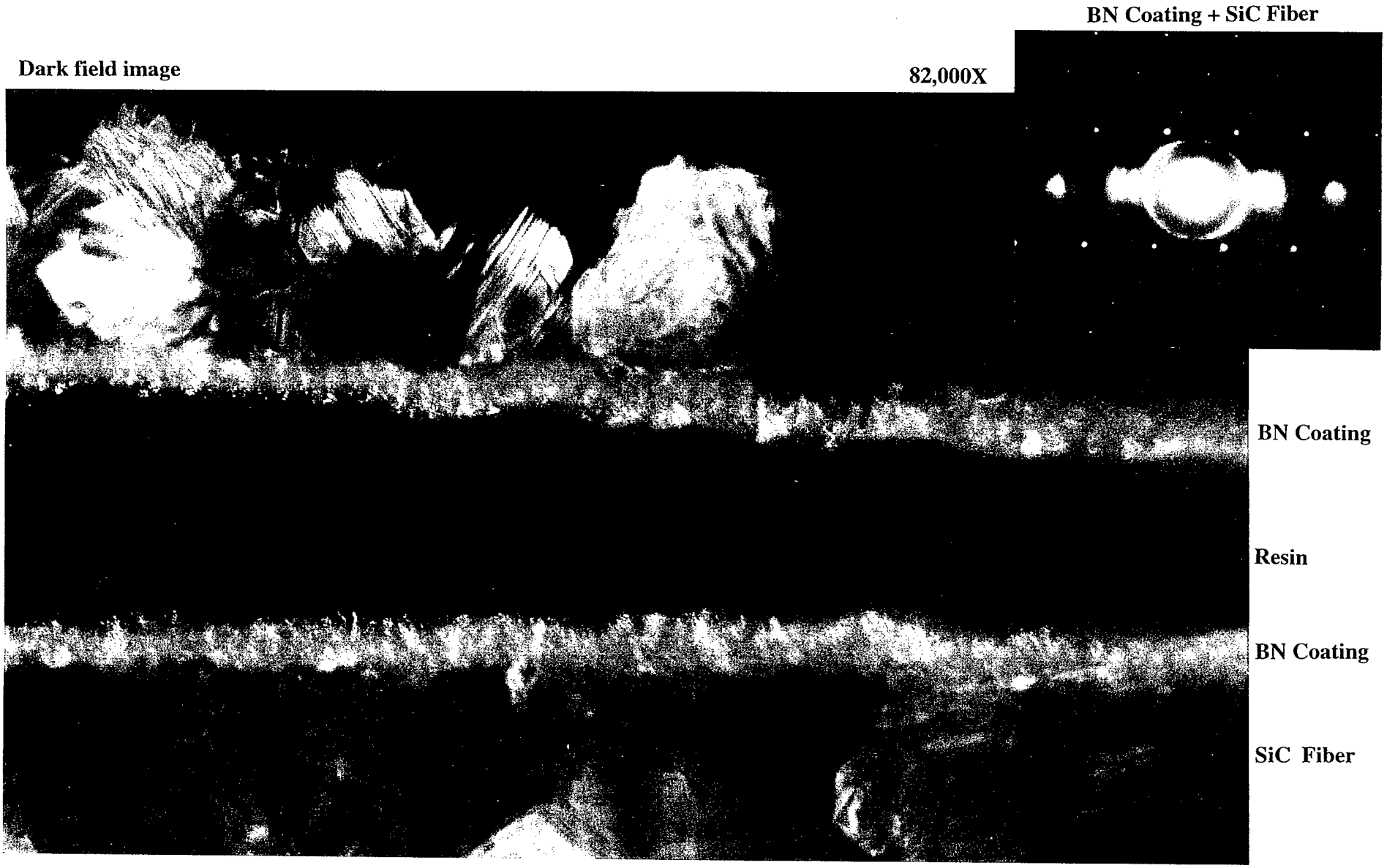

MML 34635

United Technologies Research Center Transmission Electron Microscope Laboratory

Fig. 62

UNIVERSITY OF FLORIDA BN-COATED SiC FIBER
UF-364-4

BN-coating

55,000X

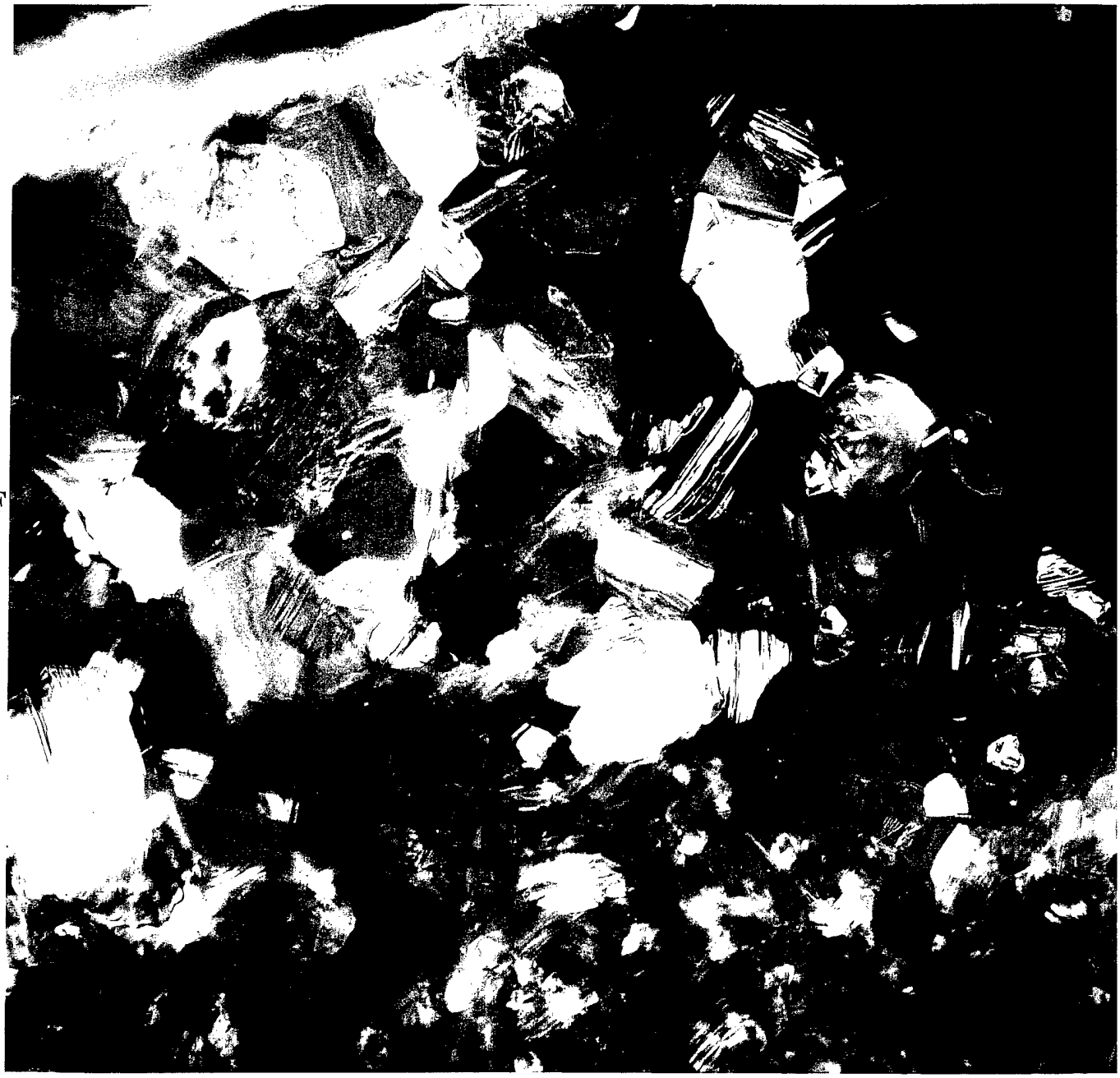

DF

Fiber grain size:

Surface = 150 - 600nm (Avg. 300nm)
Core = 50 - 300nm (Avg. 120nm)

0.5μ

UNIVERSITY OF FLORIDA BN-COATED SiC FIBER
UF-364-4

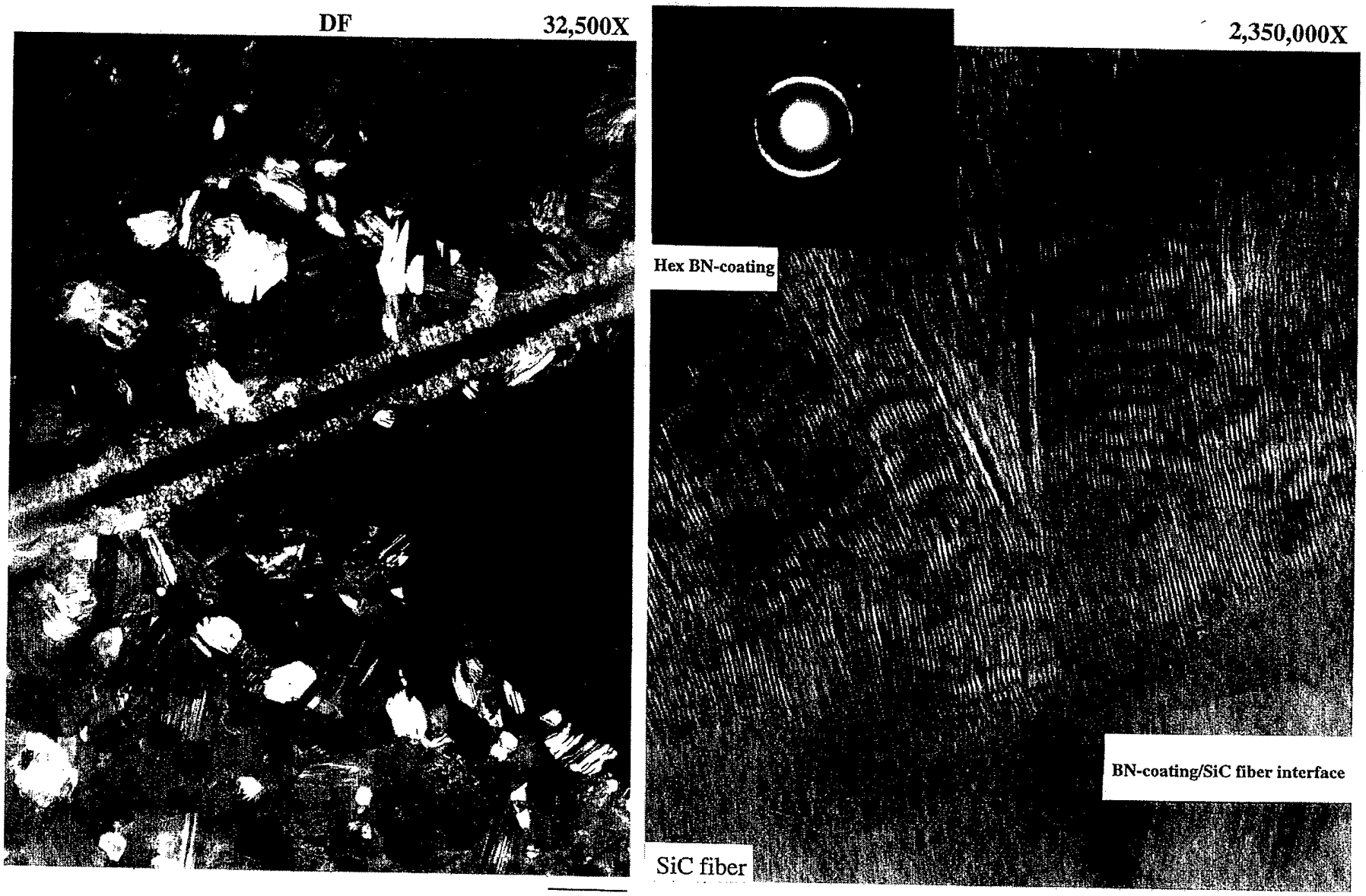

MML 34635

United Technologies Research Center

Transmission Electron Microscope Laboratory

Fig. 64

APPENDIX

Tensile and Fatigue Testing at the University of S. California (Contributed by Dr. Stephen Nutt and Mr. Chanman Park)

Mechanical properties of a cross-ply glass-ceramic composite were investigated by conducting tensile and fatigue experiments at high temperatures (700°C and 1100°C). The composite consisted of a barium magnesium aluminosilicate (BMAS) glass-ceramic matrix reinforced with 0/90 SiC fibers with a SiC/BN coating (specimen 14-97). Testing was conducted in air and in argon and all samples were oriented such that the 0° plies aligned with the maximum principal stress.

The testing machine used was an INSTRON 8562 closed chamber servomechanical system. The maximum bending was less than 5% of the applied stress. In these experiments the grips held the 25 mm gauge section dogbone coupons outside the 40 mm long hot zone. The load was applied using a constant crosshead speed. Displacement was measured using a low-force, side-contact capacitive extensometer. Uniaxial tensile experiments were performed at 700°C and 1100°C in air. The procedure was as follows:

1. Specimens were heated to the test temperature in 30-40 min.

2. The load was steadily increased using a cross-head speed of 0.6 mm/min($0.024s^{-1}$) until fracture occurred.

Fractured specimens were cooled to room temperature in 15-20 min. Tension-tension fatigue testing was also performed at 700°C and 1100°C in air and in argon. For argon environment testing, a gettering furnace was used to purify the argon (oxygen content of ~$0.8x10^{-11}$). The loading frequency was 2 Hz, which resulted in 10^5 load cycles in 9-10 h. At 700°C, the maximum stress was 110 MPa and minimum stress was 32 MPa. At 1100°C, the maximum and minimum stresses were 111 MPa and 39 MPa respectively.

a) Tensile Behavior in Air

The composite showed ultimate tensile strengths (UTS) of 162 MPa at 700°C and 178 MPa at 1100°C. Fig.1 shows tensile stress-strain curves for tests conducted at these temperatures. Table I lists the corresponding property values. In both cases, the composites showed elastic deformation upon initial loading. Deviation from elastic behavior often comes from the initiation of matrix microcracking. After this point, the stress was increased, finally reaching the UTS at which the composites failed. The UTS and strain-to-failure of the composites increased slightly with increasing temperature, possibly an indication of increased damage tolerance or softening in the matrix.

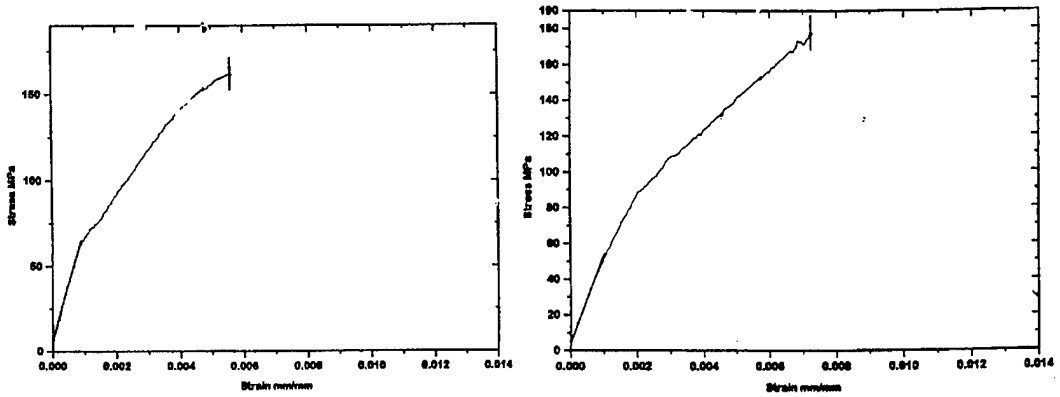

(a) At 700°C (b) At 1100°C

Fig.1 - Tensile stress versus strain at 700°C and 1100°C (strain rate=0.024s^{-1})

Table I. Tensile Properties of BMAS/SiC/BN/SiC fiber Composites

Temperature (°C)	E (GPa)	UTS (MPa)	strain-at-break (%)
700°C	64	162	0.56
1100°C	50	178	0.72

b) Tensile Fatigue Behavior in Air and in Argon

All samples survived 10^5 cycles without failure at a maximum stress of 111 MPa. The change in the stiffness of the composites during fatigue experiments is shown by measuring the elastic modulus after 1, 10, 100, 1000, 10000, and 100000 cycles (see Fig.2). Experiments were performed at 700°C and 1100°C in air and in argon.

At 700°C in air, the elastic modulus remained relatively constant until 1000 cycles, and then increased 35% from the 10^3 to 10^5 cycles. However, in argon at 700°C, the elastic modulus remained almost constant until 1000 cycles, then decreased by 5% over the next 99,000 cycles. The results show that the elastic modulus of the sample decreased 5% from the first to the 10th cycle, and remained relatively constant through the additional cycles when tested in air at 1100°C. However, at 1100°C in argon, the elastic modulus of the sample decreased 10% between the first and the 100th cycle, remaining constant until 10^4 cycles. Then the elastic modulus began to increase, rising 17% between 10^4 and 10^5 cycles.

The initial decreases in modulus shown in Fig. 2 can be attributed to an accumulation of microcracking and fiber/matrix debonding. These damage processes apparently saturated after a relatively small number of cycles (about 45). Also, Fig.2 shows that the elastic modulus increased between 10^3 and 10^5 loading cycles at 700°C in air. At 1100°C, the elastic modulus increased between the 10^4 and 10^5 cycles in argon.

Recovery of the elastic modulus during cyclic loading has often been reported in other fiber-reinforced glass or glass-ceramic-matrix composites. Shuler and co-workers suggested that several mechanisms might be responsible such as realignment of the fibers,

and an increase in the frictional sliding coefficient caused by generation of wear debris at interfaces, resulting in crack closure [1].

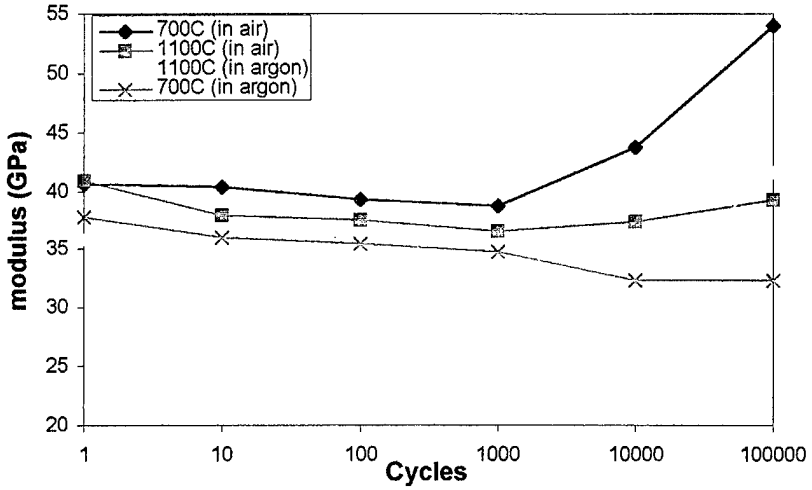

Fig.2 - Elastic modulus at different cycle points.

Reference:

[1] S.F. Shuler, J.W. Holmes, X. Wu, and D. Roach, "Influence of Loading Frequency on the Room-Temperature Fatigue of a Carbon-Fiber/SiC-Matrix Composite," *J. Am. Ceram. Soc.*, 76 [9] 2327-36 (1993)